Effects of Non-Steroidal Anti-Inflammatory Drugs on Cellular Structure and Adhesion Proteins in Human Colorectal Cancer

A Dissertation Presented for the

Doctor of Philosophy

Degree

The University of Tennessee, Knoxville

Jason Lee Liggett

December 2013

ACKNOWLEDGEMENTS

I would like to thank my mentor Dr. Seung Joon Baek and my committee: Dr. Michael M. Fry, Dr. Karla J. Matteson, and Dr. Jay Whelan. The help and support of all of our lab members both past and present has been a huge benefit. Special thanks to the former post doctorial fellows Dr. Seong-Ho Lee, Dr. Kioshi Yamaguchi, and Dr. Maria Cekanova and all of the others who helped me on my way: Dr. Chang Kyoung (CK) Choi, Dr. Robert L. Donnell, Dr. Chuck Margraves, Dr. Anthony E. English, Dr. Kenneth D. Kihm, Dr. Angelika A. NoegelDr. Michael F. McEntee, Misty Baily, Kim Rutherford, Dr. Jae Hoon Bahn, Dr. Kyu-Nam Cho, Dr. Yong-Chang Lim, Dr. Chul-Ho Kim, Dr. Jung-Ho Kim, Dr. Kyubo Kim, Dr. Chutwadee (Pum) Krisanapun, Kyung Won Min, Dr. Thararat (Gib) Nualsanit, Hataichanok (May) Pandith, Raphael Leon Richardson, Dr. Piyanuch (Nui) Rojsanga, Dmitriy Smolensky, Dr. Mee-Hyun Song, Dr. Mugdha (Chicka) Sukhthankar, Dr. Nichelle (Squeaky) Whitlock, Xiaobo Zhang (Ben), and Dr. Yi Zhong. I would also like to thank my wife Cristi and my kids Charlotte and Grant for putting up with my odd work hours and vague time frames.

ABSTRACT

This dissertation explores the effects of non-steroidal anti-inflammatory drugs (NSAIDs) on human colorectal cancer (CRC) cell proteins related to cellular structure and adhesion. NSAIDs are extensively used not only to treat inflammatory diseases but also to prevent cancer among high-risk groups. Their mechanisms are not fully understood, but both cyclooxygenase (COX) dependent and independent pathways play a role in NSAID-induced anti-tumorigenesis. Our lab previously reported that NSAIDs induce other anti-tumorigenic genes in a COX-independent manner (Chapter 1). Human CRC cells treated with the NSAID sulindac sulfide (SS) showed dramatic morphological changes under differential interference contrast and fluorescent microscopy, as well as weakened cellular adhesion and loss of membrane permeability as measured by micro-impedance. To elucidate a molecular mechanisms involved, two independent microarray analysis were performed using HCT-116 cells, and the gene Nesprin-2 was selected for further study based on its novelty in relation to cancer and its role in cell organization and structure (Chapter 2). SS-treated cells diminished Nesprin-2 mRNA expression compared to vehicle-treated cells. Other NSAIDs were also tested and demonstrated that inhibition of Nesprin-2 was not unique to SS. Additionally, immunohistochemistry showed higher levels of Nesprin-2 in the tumors of many tissue types in comparison with normal tissue. Further micro-impedance experiments on cells with reduced Nesprin-2 expression showed a proportional decrease in cellular adhesion. Next, we examined the effects of SS on another potentially oncogenic protein, epithelial cell adhesion molecule (EpCAM), which is over-

expressed in many cancers including CRC, breast, pancreas, and prostate. We found EpCAM to be regulated by SS in a manner that is independent of: COX activity, transcription, de novo protein synthesis, and proteasomal degradation. Our findings demonstrate that SS drives an uncharacterized cleavage of EpCAM between arginine residues at positions 80 and 81 which is blocked by mutation to alanine residues as well as deletions (Chapter 3). Findings presented in this dissertation (1) our data suggests that Nesprin-2 maybe a potential novel cancer-associated protein and NSAIDs decrease its expression (2) SS facilitates proteolysis of EpCAM at amino acids 80/81 and provides a novel COX-independent mechanism of NSAID anti-tumorigenesis at the post-translational level.

TABLE OF CONTENTS

Introduction 1
Chapter 1 Non-Steroidal Anti-Inflammatory Drugs and Colorectal Cancer 4
1.1 Introduction 5
1.2 Transcription Factors 6
1.2.1 Egr-1 6
1.2.2 ATF3 8
1.2.3 CHOP 10
1.2.4 Sp Proteins 12
1.2.5 SMAD proteins 14
1.3 Cell Membrane Proteins 15
1.3.1 EGFR 16
1.3.2 E-cadherin 17
1.4 Cytoskeletal Proteins 18
1.4.1 Thymosin β-4 19
1.4.2 Actin Stress Fibers 19
1.5 Cytokines 20
1.5.1 TGF-β1 20
1.5.2 NAG-1 23
1.6 Summary Conclusion 24
Chapter 2 Nonsteroidal Anti-Inflammatory Drug Sulindac Sulfide Suppresses Structural Protein Nesprin-2 Expression in Colorectal Cancer Cells 25
2.1 Abstract 26
2.2 Introduction 28
2.3 Materials and Methods 30
2.3.1 Reagents 30
2.3.2 Cell Culture 30
2.3.3 Microscopic Measurement 30
2.3.4 Electrical Impedance Measurements 31
2.3.5 Microarrays 32
2.3.6 Reverse Transcriptase PCR and Real Time PCR 33
2.3.7 Immunohistochemistry 34
2.3.8 Transfection of Nesprin-2 siRNA 34
2.3.9 Western Blot 35
2.3.10 Statistics 36
2.4 Results 36
2.4.1 SS Treatment Alters Cell Morphology and Interferes with Cell Adhesion in HCT-116 cells 36
2.4.2 Cell Organization and Biogenesis Genes Pathways are Down-Regulated by SS 39
2.4.3 Confirmation of Sulindac Sulfide Microarray Data 40
2.4.4 Time- and Dose-Dependent Down-Regulation of Nesprin-2 by several NSAIDs 44
2.4.5 Normal and Tumor Tissue Protein Expression of Nesprin-2 47
2.4.6 Cellular Impedance is Reduced by siRNA & shRNA Knock-down of Nesprin-2 50
2.5 Discussion 58

2.6 Conclusions 62
Chapter 3 CHAPTER III A Novel COX-Independent Mechanism of Sulindac Sulfide Facilitates Cleavage of Epithelial Cell Adhesion Molecule Protein 63
3.1 Abstract 64
3.2 Introduction 65
3.3 Materials and Methods 67
3.3.1 Reagents 67
3.3.2 Cell Culture 67
3.3.3 Reverse Transcriptase PCR and Real Time PCR 68
3.3.4 Expression Vectors 69
3.3.5 Immunofluorescence 70
3.3.6 Western Blot 70
3.3.7 3-D Spheroid Cell Invasion Assay 71
3.3.8 Statistics 72
3.4 Results 72
3.4.1 NSAIDs alter EpCAM expression. 72
3.4.2 SS affects EpCAM expression independent of transcriptional regulation, kinase activity, or proteasomal degradation pathway. 75
3.4.3 SS facilitates a specific cleavage of EpCAM at the N-terminal region. 77
3.4.4 Determination of SS cleavage site in the EpCAM protein 81
3.4.5 Mutation of the suspected EpCAM cleavage site influenced by SS. 81
3.4.6 Biological activity of EpCAM-iFLAG/V5-His (WT) and EpMUT-A80A81 under SS treatment. 84
3.5 Discussion 86
3.6 Conclusion 90
Conclusion 92
References 94
Vita 107

LIST OF TABLES

Table 2.1 Cell organization and biogenesis genes down-regulated by sulindac sufide . 40
Table 2.2 Normal tumor tissue array staining intensity. 53

LIST OF FIGURES

Figure 1.1 NSAID and transcription factor interactions. 11
Figure 1.2 NSAIDs' effect on the EGFR pathway. 17
Figure 1.3 NSAIDs' effect on the TGF-β/SMAD pathway. 22
Figure 2.1 HCT-116 cell adhesion and morphology during SS treatment. 38
Figure 2.2 Microarray conformation of genes down-regulated by SS. 43
Figure 2.3. Nesprin-2 mRNA expression in a time and dose dependent manner. 46
Figure 2.4 Nesprin-2 normal tumor tissue array. 49
Figure 2.5 The effect of Nesprin-2 mRNA knock-down of HCT-116 on micro-impedance. 51
Figure 2.6. The effect of Nesprin-2 mRNA knock-down of HCT-116 on micro-impedance. 57
Figure 3.1 NSAIDs effect EpCAM protein expression. 74
Figure 3.2 SS effects EpCAM protein expression in a manor independent of transcriptional regulation, kinase activity, or proteasomal degradation. 76
Figure 3.3 Exploring SS/EpCAM interaction through generation of a multi-tagged expression vector. 80
Figure 3.4 Deletions to explore potential SS related cleavage sites on EpCAM. 82
Figure 3.5 Mutation of the suspected EpCAM cleavage site influenced by SS. 83
Figure 3.6 Biological activity of EpMUT-A80A81 stable cell line. 85

LIST OF ABBREVIATIONS

AA	arachidonic acid
ATF3	activating transcription factor 3
COX	cyclooxygenase
CRC	colorectal cancer
CHOP	C/EBP-homologous protein
DADS	diallyl disulfide
DFU	5,5-dimethyl-3-(3-fluorophenyl)-4-(4-ethylsulfonyl)phenyl-2(5H)-furanone
DICM	differential interference contrast microscopy
EFM	epi-fluorescence microscopy
EGFR	Epidermal growth factor receptor
Egr-1	early growth respose-1
EMT	epithelial-to-mesenchymal transition
EpCAM	epithelial cell adhesion molecule
EpEX	EpCAM extracellular domain
EpICD	EpCAM's intracellular domain
ER	endoplasmic reticulum
Ese-1	epithelium-specific ETS transcription factor-1
ETS	E26 transformation-specific
FAP	familial adenomatous polyposis
FHL2	four and a half limb domain 2
IDH2	isocitrate dehydrogenase 2
IRCM	interference reflection contrast microscopy
KLF4	Kruppel-like factor 4
LPS	lipopolysaccharide
PERK	protein kinase-like endoplasmic reticulum kinase
PMA	phorbol myristate acetate
NAG-1	NSAID activated gene 1
NSAID	non-steroidal anti-inflammatory drug
SC-560	[5-(4-chlorophenyl)-1-(4-methoxyphenyl)-3-(trifluoromethyl)-1H-pyrazole]
Sp	Specificity
SS	sulindac sulfide
TA	tolfenamic acid
TGZ	troglitazone
VEGFR-1	vascular endothelial growth factor receptor-1

INTRODUCTION

This dissertation explores the effects of non-steroidal anti-inflammatory drugs (NSAIDs) on human colorectal cancer (CRC) cell proteins related to cellular structure and adhesion. NSAIDs are extensively used over the counter to treat headaches and inflammation as well as clinically to prevent cancer among high-risk groups. Their mechanisms are not fully understood, but both cyclooxygenase (COX) dependent and independent pathways play a role in NSAID-induced anti-tumorigenesis. Our lab previously reported that NSAIDs induce other anti-tumorigenic genes including NSAID activated gene one (NAG-1) and activating transcription factor 3 (ATF3) (Chapter 1).

Our goal was to shed further light on COX-independent activity by identifying, confirming, and characterizing novel NSAID targets related to cell structure and biogenesis in colorectal cancer cells. Human CRC cells treated with the NSAID sulindac sulfide (SS) showed dramatic morphological changes under differential interference contrast and fluorescent microscopy, as well as weakened cellular adhesion and loss of membrane permeability as measured by micro-impedance. To elucidate molecular mechanisms involved, two independent microarray analyses were performed using HCT-116 cells and Nesprin-2 was selected for further study based on its novelty in relation to cancer and its role in cell organization and structure (Chapter 2). SS diminished Nesprin-2 mRNA expression to one third of the level observed in vehicle-treated cells, as assessed by real-time PCR. Various other NSAIDs were also tested and demonstrated that inhibition of Nesprin-2 was not unique to SS. Additionally, immunohistochemistry showed higher levels of Nesprin-2 in the tumors of many tissue types in comparison with normal tissue. Further micro-impedance experiments on cells

with reduced Nesprin-2 expression showed a proportional decrease in cellular adhesion. Thus, our data suggest that Nesprin-2 may be a potential novel cancer-associated protein and NSAIDs decrease its expression.

Next, we examined the effects of SS on another potentially oncogenic protein, epithelial cell adhesion molecule (EpCAM), which is over-expressed in many cancers including CRC, breast, pancreas, and prostate. EpCAM is a type I transmembrane glycoprotein involved in adhesion. We found EpCAM to be down-regulated by SS in a manner that is independent of: COX activity, transcription, de novo protein synthesis, and proteasomal degradation. Our findings demonstrate that SS drives an uncharacterized cleavage of EpCAM between arginine residues at positions 80 and 81 which is blocked by mutation to alanine residues as well as deletions (Chapter 3). Proteolysis of EpCAM by NSAIDs may provide a novel mechanism by which NSAIDs affect anti-tumorigenesis at the post-translational level.

Findings presented in this dissertation suggest that Nesprin-2 is a potential novel oncogene and NSAIDs decrease its expression, and that SS facilitates proteolysis of EpCAM at amino acids 80/81 and provides a novel COX-independent mechanism of NSAID anti-tumorigensis at the post-translational level.

CHAPTER 1

NON-STEROIDAL ANTI-INFLAMMATORY DRUGS AND COLORECTAL CANCER

1.1 Introduction

Despite advancements in modern medicine, cancer is a major cause of death worldwide with a death toll of 7.6 million or about 13% of all deaths per year [1]. Colorectal cancer is the third most common cancer for both men and women [2]. Given this and the increasing life expectancies in the developed world, there are more chances of acquiring cancer, making research into mechanisms of colorectal cancer prevention a high priority.

Non-steroidal anti-inflammatory drugs (NSAIDs) are a class of drugs which have been utilized for their analgesic and antipyretic effects since ancient times. In more recent history NSAIDs have also been widely used and studied for their anti-tumorigenic and chemopreventive properties. The classical pathway of action for NSAIDs is by blocking the generation of prostaglandins from arachidonic acid (AA) via inhibiting cyclooxygenase-1 and -2 (COX-1 and -2) activity. COX-1 is present and expressed constitutively in most tissues [3]. COX-2 expression is usually transient and can be quickly induced by: cytokines including TNF-α, IL-1, and IL-2, bacterial endotoxin lipopolysaccharide (LPS), tumor promoter phorbol myristate acetate (PMA), and growth factors [4-6]. NSAIDs, however, suffer from side effects including gastrointestinal tract bleeding and kidney failure which may be attributable to COX-1 inhibition [7, 8]. In addition, a recent clinical trial of familial adenomatous polyposis (FAP) patients observed a three-fold increase in the risk of cardio-toxicity from the COX-2 inhibitor celecoxib [9, 10]. These adverse side effects of COX inhibition are strong motivation

driving research into the many COX-independent mechanisms of NSAIDs. There is still much work to be done elucidating the pathways of COX-independent activity of NSAIDs and this area will be the primary subject of this chapter.

1.2 Transcription Factors

Transcription factors bind to specific DNA sequences in order to regulate gene expression either as activators or repressors and have a wide range of functions including development, response to environmental or intracellular signals, cell cycle control, and pathogenesis. NSAIDs have been shown to affect a wide variety of transcription factors including Egr-1, ATF3, CHOP, and Sp proteins. This section will summarize how these transcription factors are regulated by NSAIDs.

1.2.1 Egr-1

The zinc-finger DNA binding protein early growth respose-1 (Egr-1) is involved in many roles including differentiation and mitogenesis [11, 12]. In most tissue types, Egr-1 is only expressed at low levels without stimulation. Egr-1 can be quickly induced by a number of signals including growth factors, mitogens, cytokines, stress, tissue damage, and differentiation factors [12]. Egr-1 has been demonstrated to act as a tumor suppressor in mouse two-step skin carcinogenesis studies using Egr-1 knock-out mice and has been shown to bind to the p53 promoter region both in vitro and in vivo [13]. Egr-1-dependent apoptosis is mediated by p53 in human melanoma cells [14].

Egr-1 is involved in apoptosis through a number of different pathways and apoptotic agents. Egr-1 plays an important role in up-regulating the anti-tumorigenic and pro-apoptotic protein NSAID activated gene-1 (NAG-1) protein expression in colorectal cancer cells during SS or other NSAID treatment [15]. NSAIDs also up-regulate Egr-1 which translocates to the nucleus and binds to the promoter region of NAG-1 [16]. This observation has been confirmed in vivo using a Sprague-Dawley rat model for early colorectal tumorigenesis which utilizes the colon-specific pro-carcinogen 1,2-dimethylhydrazine dihydrochloride (DMH) [17]. In this system Egr-1 and NAG-1 proteins where induced in rats treated with sulindac or celecoxib and DMH compared to rats only given DMH [17].

Another conventional NSAID, tolfenamic acid (TA), induces Egr-1 at the transcription level via enhancement of epithelium-specific ETS transcription factor-1 (ESE-1) nuclear translocation, which plays a role in activation of apoptosis in colorectal cancer cells [18]. Ultraviolet light-induced apoptosis in a mouse model is also dependent upon EGR-1 binding to the tumor suppressor PTEN's 5' un-translated region, and loss of EGR-1 in some cancers can result in radiation resistance [19].

EGR-1 can also induce apoptosis and effect cell differentiation through the endoplasmic reticulum (ER) stress pathway via the ER stress agent thapsigargin, in a protein kinase-like endoplasmic reticulum kinase (PERK) expression dependent manor [20]. Egr-1 is also involved in neuronal apoptosis through transactivation of pro-apoptotic BH3-only protein Bim gene expression [21]. In this rat model, Egr-1 has been shown to be both necessary and sufficient to mediate apoptosis of rat cerebellar granule

neurons [21]. In addition to NSAIDs, natural compounds such as resveratrol can also induce apoptosis via Egr-1, KLF4, and ATF3 [22].

In contrast, depending on the cell type and conditions, Egr-1 can also play a negative role in tumorigenesis. In androgen-independent prostate cancer Egr-1 is required for mediating CXCL5/ENA78's oncogenic activity on cell growth, migration, and epithelial-to-mesenchymal transition (EMT) via Snail stimulation, Cdk4 up-regulation, and inhibition of p27 [23]. Also, in human breast cancer cells EGR-1 mediated proliferation and survival is dependent on p300-dependent ATF5 acetylation [24].

Thus, Egr-1 plays a complex role in tumorigenesis and progression acting though many pathways including both natural compounds and NSAIDs. Therefore, although NSAIDs have been shown to increase Egr-1 expression, further characterization of the details of NSAID-induced Egr-1 and its role in tumorigenesis is required.

1.2.2 ATF3

ATF-3 is a cyclic adenosine monophosphate (cAMP) dependent transcription factor that is a member of the bZIP family [25]. ATF3 is induced by the COX non-selective NSAID SS, the COX-1 selective NSAID SC-560, the PPAR ɣ ligand troglitazone (TGZ), and the garlic derived diallyl disulfide (DADS) among others [26]. SS induces ATF3, C/EBP-homologous protein (CHOP), and NAG-1 [27]. Dominate negative protein kinase-like endoplasmic reticulum kinase (PERK) can inhibit SS induced NAG-1 [27]. However, dominant negative CHOP does not affect SS induced ATF3 protein expression, but does reduce SS induced NAG-1 expression [27]. Also,

anti-sense ATF3 blocks SS induced CHOP and NAG-1 protein expression [27]. Thus, it appears that CHOP is down-stream of ATF3 (Fig. 1.1). Phosphorlation of ATF2 also involved in NSAID up-regulation of ATF3 by increasing ATF3 promoter activity contributining to increased apoptosis in an ATF3-dependent manor in CRC cells treated with NSAIDs including TA [28].

Besides NSAIDs, 3,3′-Diindolylmethane (DIM), an indole-3-carbinol derivative from cruciferous vegetables, has shown promising *in vivo* anti-tumorigenic and pro-apoptotic activity. DIM treatment induced apoptosis in CRC cells while inducing ATF3 transcription and translation as well as increasing ATF3 promoter activity via over-expression of ATF4 and binding of ATF4 to the ATF3 promoter region [29]. The natural compound resveratrol also induced apoptosis through the ATF3 pathway [22].

Over-expression of ATF3 in several cancer cell lines leads to induction of cell cycle arrest and inhibition of proliferation [30]. Also, ATF3 expression is reduced in human cancer tissue compared to adjacent normal tissue [31]. There are many studies showing a relationship between ATF3 and apoptosis. The PI3K inhibitor LY294002 induces ATF3 and EGR-1 phosphorylation in a PI3K-independent manor in various CRC cell lines [32]. A nude mouse xenograft model using Ras transformed fibroblastes, either ATF3 -/- or ATF3 +/+, shows that ATF3 promotes cell death, arrests cell growth, and suppresses Ras-mediated tumorigenesis [33]. In prostate cancer cells Kruppel-like factor 6 (KLF6) has been demonstrated to bind to and activate the ATF3 promoter leading to apoptosis [34]. Both ATF3 over-expression and SS treatment down regulate metastasis-associated protein (MTA1) and β-catenin by real-time PCR in HCT-116

cells. ATF3 over-expression and SS treatment decreased invasion *in vivo,* and ATF3 over-expression resulted in smaller tumors in a mouse HCT-116 xenograft model [26]. ATF3 has thus been implemented in several anti-tumorigenic pathways and represents one explanation for some of NSAIDs COX-independent activity.

1.2.3 CHOP

C/EBP-homologous protein (CHOP) is an ER stress response protein and member of the bZIP transcription factor family which inhibits CCAAT/enhancer-binding protein (C/EBP) and liver-enriched transcriptional activator protein's (LAP) DNA-binding activity through the generation of heterodimers unable to bind DNA [35]. CHOP mRNA and protein levels are both elevated by SS treatment in colorectal cancer cells [27]. Celecoxib induces CHOP protein expression in malignant glioma cells, whereas SS requires carbonyl cyanide 4-(trifluoromethoxy)- phenylhydrazone (FCCP) co-treatment [36] to produce the same effect. FCCP is a protonophore which uncouples oxidative phosphorylation, causing the loss of mitochondrial membrane potential. FCCP also does not induce CHOP protein by itself in malignant glioma cells [36, 37]. This suggests that mitochondrial disruption accompanied by endoplasmic reticulum stress response is needed to induce CHOP expression in malignant glioma cells.

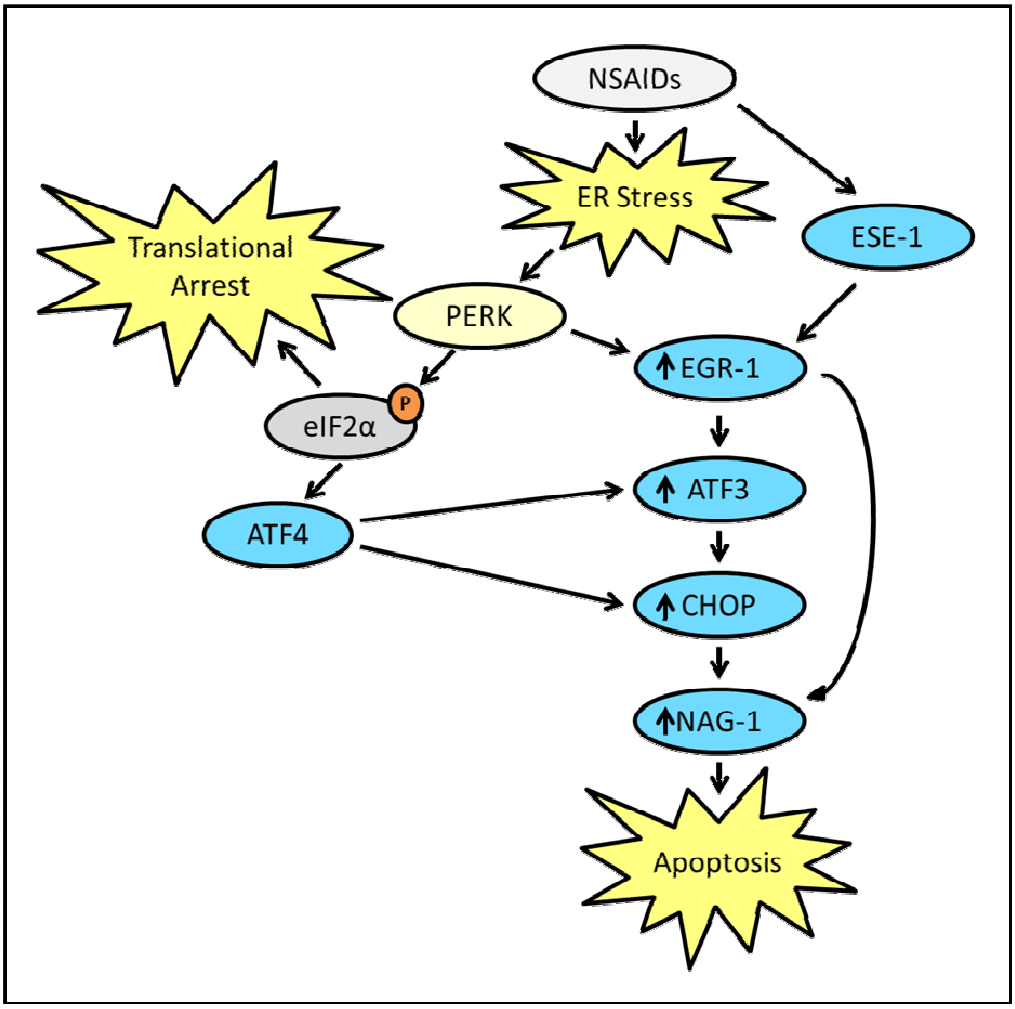

Figure 1.1 NSAID and transcription factor interactions.

NSAIDs cause ER stress which activates the ER membrane protein PERK. This results in PERK activating eIF2α through phosphorylation. P-eIF2α cause general translational arrest while at the same time stimulating ATF4 to translocate to the nucleus where ATF4 binds the promoter regions of ATF3 and CHOP. EGR-1 is up-regulated through both the PERK/ER stress pathway and by ESE-1 binding to EGR-1's promoter region. EGR-1 in turn stimulates ATF3 up-regulation and EGR-1 binds to NAG-1's promoter region. Dominate negative (DN) PERK will block NSAID activation of NAG-1. DN CHOP will not affect NSAID induced ATF3, but will reduce NSAID up-regulated NAG-1. Anti-sense ATF3 will inhibit both NSAID up-regulated CHOP and NAG-1.

1.2.4 Sp Proteins

Specificity (Sp) proteins are zinc-finger transcription factors that are members of the Sp/KLF sub-family which also includes Kruppel-like factors [38]. Sp proteins bind to the GC and/or GT boxes of many promoter genes. There are several Sp proteins including: Sp1, Sp2, Sp3, Sp4, Sp5 [39], Sp6/KLF14 [39], Sp7 [40], and Sp8 [41]. This section will focus on Sp1, Sp3, and Sp4 which are phylogenetically more similar to one another than to the other Sp proteins [39, 42] and have been associated with changes in regulation of tumorigenesis in several studies.

Sp1 is normally responsible for controlling various housekeeping genes; however, Sp1 has also been linked to the regulation of tumorigenesis [43]. Sp proteins contribute to the proliferation of metastatic tumor phenotypes and thus overexpression of these transcription factors is a negative survival prognostic factor in many human cancers [43].

TA has been shown to decrease Sp1, Sp3, and Sp4 protein expression as well as vascular endothelial growth factor receptor-1 (VEGFR-1) protein expression in pancreatic cancer cells [44]. Interestingly, small interfering RNA (siRNA) for Sp1, Sp3, and Sp4 also led to decreased VEGFR-1 [44]. Thus, TA decreases this important angiogenic factor via regulation of Sp proteins. This observation is supported by nude mouse data which shows that TA reduces Sp1, Sp3, and Sp4 protein expression in vivo as well. Also, vascular endothelial growth factor (VEGF) was demonstrated to be reduced by TA both in vitro and in vivo in this study [45]. TA has also been shown to

decrease Sp1, Sp3, and Sp4 in rhabdomyosarcoma (RMS) cells and in lung cancer cells both in vitro as well as in mouse models [46, 47].

COX-2 preferential NSAIDs including celecoxib also down-regulate Sp1 and Sp4 activity in human colorectal cancer cells; however, Sp3 protein expression was unchanged in this case [48]. This action was shown to be through COX-2 independent activation of Sp1 and Sp4 proteasomal degradation [48]. Recently Dr. Safe's group has shown that TA, and the novel nitric oxide (NO) chimera containing NSAID ethyl 2-((2,3-bis(nitrooxy)propyl)disulfanyl)benzoate (GT-094), down-regulate Sp1, Sp3, and Sp4 in human CRC cells both *in vitro* and in a mouse xenograft model leading to decreased expression of multiple proteins including: angiogenic VEGF and VEGFR-1, proliferation promoting cyclin D1 and hepatocyte growth factor receptor, cell survival proteins survivin and Bcl-2, and the pro-inflammatory gene products NFκBp65/p50 [49, 50]. The suggested mechanism for TA's action on Sp proteins was through caspase activation. Thus, the COX-2 preferential NSAID celecoxib only decreased Sp1 and Sp4 in CRC cells while the conventional NSAID TA appeared to down-regulated Sp1, Sp4, and Sp3. Aspirin and its major sodium salicylate have also recently been shown to decrease Sp1, Sp4, and Sp3 in a caspase-dependent manor in human CRC *in vitro* as well as in a mouse model [51]. The addition of zinc sulfate inhibited aspirin-mediated apoptosis and Sp protein suppression, which suggests that aspirin's cleavage of Sp proteins is dependent upon sequestration of zinc ions [51]. Taken together this data shows that a wide variety of NSAIDs of varying COX specificity all down-regulate Sp proteins in several different cancers including pancreatic, lung, rhabdomyosarcoma, and colon.

The consistency of these results across these experiments makes NSAID action through Sp protein regulation a promising pathway.

1.2.5 SMAD proteins

Human SMAD proteins are homologs of both the *Caenorhaditis elegans* small body size (SMA) protein and the *Drosophila melanogaster* mothers against decapentaplegic (MAD) protein which is regulated by maternal effect enhancement of weak decapentaplegic alleles [52]. Thus, the nomenclature SMAD is a portmanteau of SMA and MAD. SMAD transcription factors are key regulators of the TGF-β signaling pathway and normally form heteromeric complexes of SMAD members which translocate to the nucleus and regulate gene expression through binding with other transcription factors, co-repressors, or co-activators [53]. SMAD is another example of the tissue specificity and the complex effects of specific micro-environments on the outcome of expression of a given protein. In early stages of tumorigenesis, SMAD signaling can have tumor suppressive effects, while helping to drive metastasis in late stage cancers [54]. A vast array of proteins are effected by the SMAD pathway and many of these are linked to cell migration and invasion of cancer cells [55]. Thus, SMAD signaling in advanced stage tumorigenesis is a promising target for cancer treatment.

The salicylic acid derivative 5-aminosalicylic acid (5-ASA) has been demonstrated to inhibit TGF-β-mediated SMAD2/3 phosphorylation and subsequently suppress nuclear translocation of SMAD2/3 in human colorectal cancer cell [56]. A recent large case-control study of colon and rectal cancer patients observed genetic

variation of TGFβ/SMAD pathway genes; this study suggests that the use of aspirin/NSAIDs modulates cancer risk associated with SMAD genes [57]. A recent finding from our lab demonstrates that TA inhibits TGF-β-induced SMAD phosphorylation through the ERK MAP kinase pathway, Fig. 1.3, in various cancer cells [58]. TA showed the strongest reduction of phosphorylated SMAD2 in a screen of NSAIDs including several examples of conventional, COX-1 preferential, and COX-2 preferential NSAIDs [58]. The interference of SMAD signaling by NSAIDs represents a promising mechanism of anti-tumor action.

1.3 Cell Membrane Proteins

Cell membrane proteins are a diverse group of proteins that perform a wide variety of functions. Some are adhesion modules responsible for cell-cell binding, while others are responsible for anchoring the plasma membrane to the actin cytoskeleton. Cell surface proteins can act as receptors for paracrine and autocrine cell signaling and are responsible for signal transduction into the cytoplasm and even translocation into the nucleus to effect transcription. Lipid rafts provide the scaffolding for many different protein-protein interactions in, on, and under the plasma membrane. Over-expressed membrane proteins are a highly studied area due to their potential prognostic value cancer markers and chemotherapy promise of more cancer cell specific drug delivery.

1.3.1 EGFR

Epidermal growth factor receptor (EGFR) is a single pass receptor tyrosine kinase which is mutated and/or over-active in a high percentage of cancers. EGFR signaling is down-stream of the cyclooxygenase pathway and production of PGE2. EGFR signaling can lead to cell proliferation through the Erk1/2 pathway and/or cell survival, invasion, and angiogenesis through the AKT pathway. EGFR is the target of approved CRC treatments including the EGFR soluble decoy receptor fusion protein Ziv-Aflibercept and the mouse/human chimeric monoclonal antibody Cetuximab which can bind to and shut-off mutated EGFR that is functioning with or without growth factor signaling. Sulindac metabolites, sulindac sulfide and sulindac sulfone, down-regulate EGFR signaling through inhibiting activation and expression of EGFR in CRC cell lines [59]. The dual NSAID Licofelone, inhibits both COX and 5-lipoxygenase (5-LOX), has been shown to decrease CRC membrane fluidity leading to the inhibition of EGFR signaling which contributes to apoptosis [60]. NSAIDs could be another attractive method to target EGFR and the negative side-effects of COX inhibition could be minimized by co-treatment with other EGFR target treatments.

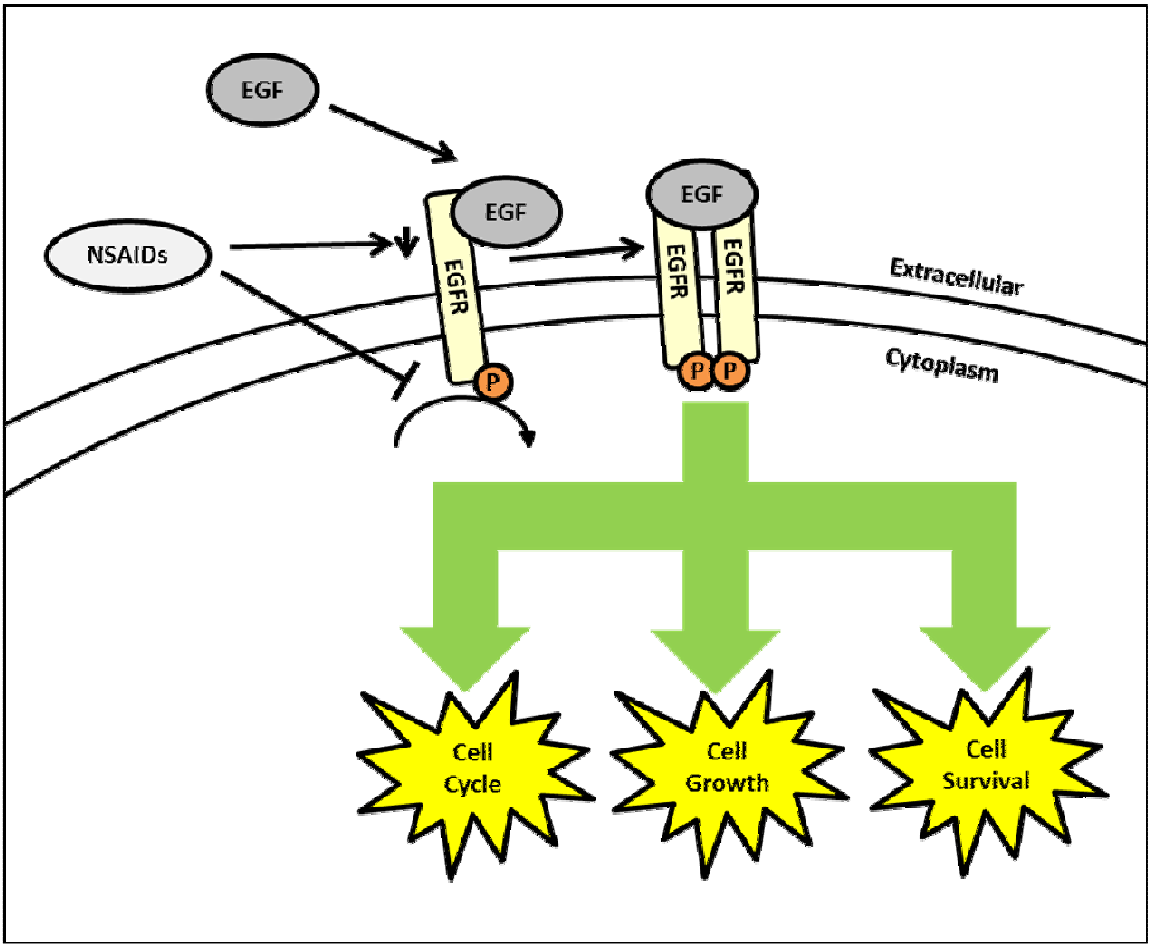

Figure 1.2 NSAIDs' effect on the EGFR pathway.

NSAIDs such as sulindac sulfide down-regulate EGFR protein expression. Also, NSAIDs block phosphorylation of EGFR necessary for activation of down-stream EGFR signaling. EGFR pathways include cell cycle progression, increased cellular growth, and increased cell survival and resistance to apoptosis.

1.3.2 E-cadherin

E-cadherin is a calcium-dependent type-1 transmembrane protein. It is important for tight cell-cell junctions and anchors to the cytoskeleton. E-cadherin can play an important role in tumor progression through its sequestration of β-catenin to the plasma

membrane which prevents β-catenin from acting in the Wnt signaling pathway and for its job function as a cell adhesion molecule. Loss of E-cadherin function and/or expression is an important step in EMT leading to invasion and migration. Soluble E-cadherin (sEcad) may have oncogenic activity in cutaneous squamous cell carcinomas via association with the HER/IGF-1R-family receptors and activation of MAPK and PI3K/mTOR pathways [61]. In an animal model study, sulindac treatment protected $APC^{Min/+}$ mice from E-cadherin loss and accumulation of nuclear β-catenin in colon tumors [62]. The non-selective NSAID indomethacin reduced protein levels of E-cadherin and collagen IV while increasing the activity of matrix metalloprotease-9 (MMP-9) leading to enhanced motility *in vitro* in lung cancer cell lines [63]. This may be an example where cancer type and stage is critical to treatment outcome. Through the course of invasion and metastasis cancer cells first need to lose their tight cell-cell adhesion to allow the cells to travel through the vascular and/or lymphatic system; then in order to establish a new colonies, the cancer cells will need to re-establish tight junctions at the metastasis sites. This creates a complex situation when targeting dysregulated cell adhesion molecules.

1.4 Cytoskeletal Proteins

Cytoskeletal proteins are critical for maintaining normal cell form and function. They represent the highways for vesicle trafficking which is a key element of autocrine and paracrine cellular signaling. Cytoskeletal protein rearrangement is also critical part

of cell migration. All of these aspects are areas which would need to be dysregulated to allow a pre-cancerous cell to go through EMT and metastasize to a new disease site.

1.4.1 Thymosin β-4

Thymosin β-4 is a member of the β-thymosins family of highly conserved 5 kDa peptides which are involved in actin sequestration and normal cell migration as well as aberrant tumor metastasis [64]. Thymosin β-4 over-expression in SW480 CRC cells has also been shown to assist immune evasion and resistance to anticancer therapy; this process involves FasL-bearing T cells and to the topoisomerase II inhibitors doxorubicin and etoposide which down-regulate Fas and up-regulate Survivin expression [65]. COX-1 preferential NSAIDs such as indomethacin and SC-560 induce thymosin β-4 while the conventional NSAID SS does not induce thymosin β-4 [66]. Induction of oncogenes such as thymosin β-4 by some but not all NSAIDs could be one explanation for the varied outcomes of treatment with different NSAIDs.

1.4.2 Actin Stress Fibers

Actin stress fibers are the prominent contractile structures in most tissue cultures and consist of bundles of actin filaments, crosslinking proteins, and myosin II motors [67]. They are key factors in contractility and cell motility which are needed for morphogenesis and cellular adhesion [67]. Non-motile cells tend to have thick and fairly stable stress fibers, whereas motile cells usually have thinner and fewer actin stress fibers which are very dynamic [68]. Many developmental and physiological processes

depend on the proper regulation of actin cytoskeleton, and dysregulation can lead to pathological conditions such as myofibrillar myopathies, neurological disorders, and cancer [69].

SS, as well as the phenolic antioxidant caffeic acid phenethly ester (CAPE) at sub-apoptotic doses of each, causes cytoskeletal reorganization, loss of actin stress fibers, and loss of focal adhesion plaques in human colon carcinoma cells [70]. The COX-1 specific NSAID indomethacin and the COX-2 specific NSAID NS-398 reduced actin stress fibers in wounded gastric epithelial cells [71]. Indomethacin also causes dramatic morphological changes including time and dose dependent loss of stress fibers in lung cancer cell lines [63]. The COX-1 preferential NSAIDs indomethacin and SC-560 cause cytoskeletal reorganization in HCT-116 CRC cells [66]. It appears that NSAIDs affect actin stress fibers in a range of cancer types regardless of cyclooxygenase preference for COX-1, COX-2, or a lack of preference. This is one explanation for NSAID induced apoptosis through anchorage loss, anoikis.

1.5 Cytokines

1.5.1 TGF-β1

Transforming growth factor β 1 is a TGF-β superfamily member that is a secreted soluble polypeptide involved in many cellular processes such as cell growth and proliferation as well as apoptosis. Complexes are formed by TGF-β family members binding to type I and type II receptors [72]. TGF-β uses endothelial specific ALK1 and

ALK5 type I receptors, the type II receptor TGFBR2, and the co-receptors β-glycan and endoglin [73].

The conventional NSAID naproxen sodium lowered serum TGF-β1 levels and interfered with healing in rats with fractured tibias. However, rats co-treated with naproxen sodium and granulocyte colony stimulating factor (G-CSF) did not have lowered TGF-β1 levels and did not impede fracture healing [74]. This suggests that TGF-β1 may be responsible for the inhibition of fracture healing that many NSAIDs cause. In a swine model for thoracic surgery the COX-2 preferential NSAID diclofenac reduced the amount of TGF-β in the pleural effusion caused by mechanical pleural abrasion, and the diclofenac group also had reduced pleural effusion volume, white cell count, and protein content [75]. However, the non-selective NSAID ketorolac and the COX-1 favoring NSAID indomethacin had no effect on TGF-β expression and bioactivity in rat osteoblast-enriched cultures [76]. It is very common for cancers to have TGF-β receptors which are mutated and always active regardless of the presence or absence of ligand; in these cases regulating TGF-β ligands would be not be effective and the TGF-β pathway would need to pursued down-stream in order to change the signaling outcome.

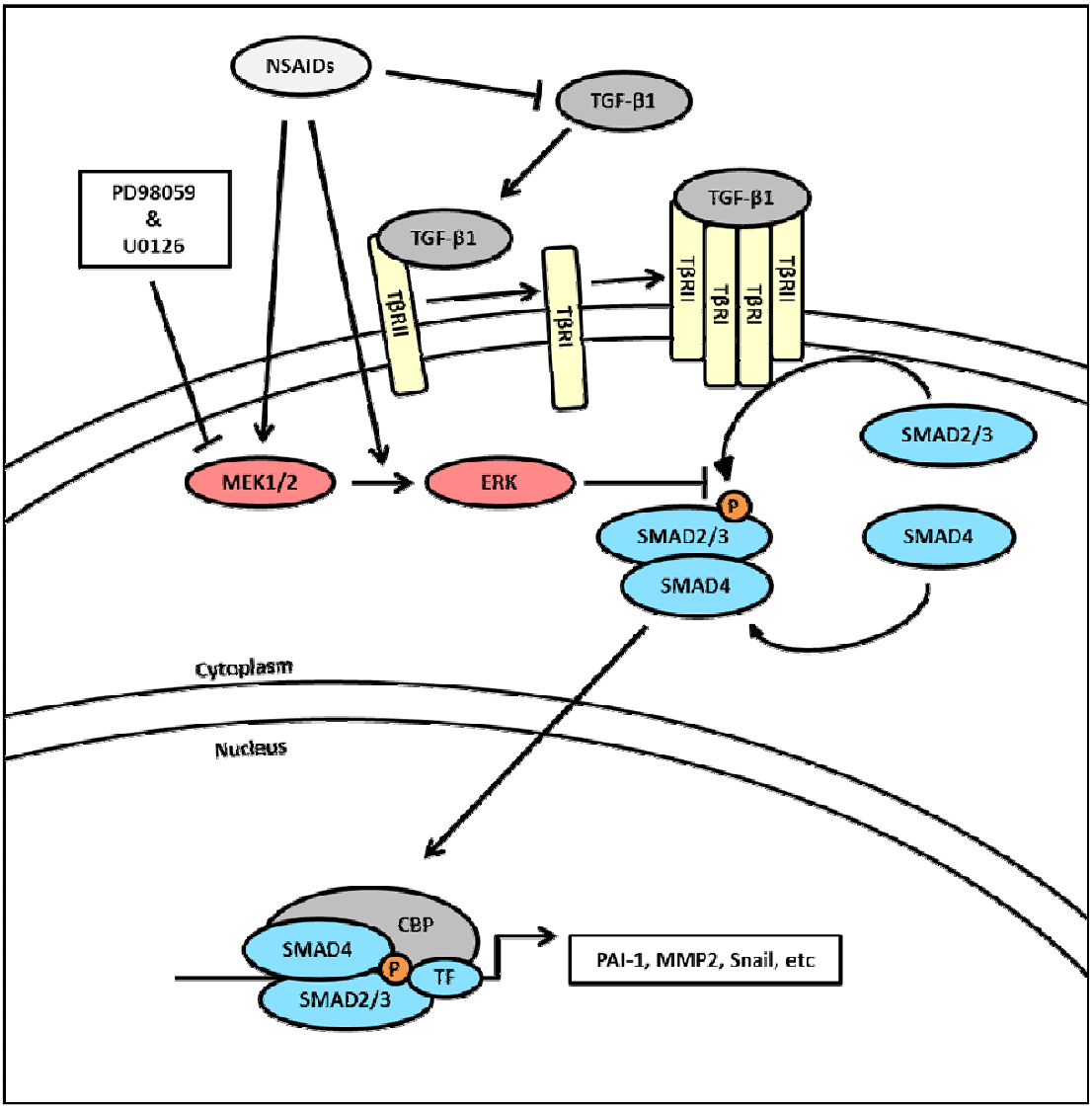

Figure 1.3 NSAIDs' effect on the TGF-β/SMAD pathway.

TGF-β ligand binds to a type II receptor (TβRII) dimer then recruits a type I receptor (TβRI) dimer and forms a heterotetrameric complex with the ligand. This complex phosphorylates SMAD2/3 and the SMAD complex translocates to the nucleus to initiate down-stream targets. NSAIDs reduce TGF-β1 serum levels *in vivo*. NSAIDs, especially tolfenamic acid, stimulate the MEK-ERK pathway which inhibits C-terminal phosphorylation of SMAD2/3, thus blocking nuclear translocation of SMAD2/3. The MEK1/2 inhibitors PD98059 and U0126 partially restore SMAD2/3 phosphorylation in the presents of NSAIDs. This suggests that NSAIDs also stimulate the MEK-ERK pathway down-stream of MEK1/2.

1.5.2 NAG-1

Non-steroidal anti-inflammatory gene 1 (NAG-1 also known as GDF-15) is a divergent member of the TGF-β superfamily. The pro form of NAG-1 is cleaved at the RXXR amino acid site to free the 112 amino acid mature form from the C-terminal region [72]. Mature secreted NAG-1 forms a homodimer utilizing the seventh cysteine residue to form a disulfide bridge while the first six cysteine residues may form a cysteine knot which is common in the TGF-β superfamily [72]. NAG-1 is one of the few TGF-β proteins whose receptors remain unknown.

NAG-1 is the downstream target of three major tumor suppressor pathways including p53, Egr-1, and GSK-3β [77, 78]. NSAIDs such as SS induce NAG-1 protein expression at the transcriptional level via Egr-1 transcription factors [15, 79]. NSAIDs up-regulate Egr-1 *in vitro* and *in vivo,* which translocates to the nucleus and binds to the promoter region of NAG-1 [16, 17]. This Egr-1 stimulation appears to be a down-stream result of increased protein expression of ESE-1 [18]. SS induced NAG-1 can be blocked by dominate negative PERK and by dominant negative CHOP, though dominant negative CHOP does not block ATF3 induction [27]. Interestingly anti-sense ATF3 inhibits SS induced CHOP and NAG-1 protein expression [27]. This suggests that NAG-1 is down-stream of CHOP which is down-stream of ATF3 which is down-stream of PERK which is down-stream of SS. NAG-1 is involved in many pro-apoptotic pathways and its regulation is quite complex.

1.6 Summary Conclusion

NSAIDs interact with many pathways in human colorectal cancer. There are many promising cyclooxygenase-independent mechanisms utilized by NSAIDs which provide potential avenues for developing new and better drugs that minimize or eliminate the undesirable side effects of cyclooxygenase inhibition such as gastric bleeding and cardiovascular risks.

NSAIDs up-regulate a number of transcription factors such as the tumor suppressors Egr-1, ESE-1, ATF3, CHOP, and p53. Tumorigenic cell growth and survival stimulating transcription factors such as Sp1, Sp3, and Sp4 are also down-regulated by NSAIDs. The often oncogenic cell membrane protein EGFR is down-regulated by NSAID treatment in CRC cell lines. The cell adhesion protein E-cadherin is protected in $APC^{Min/+}$ mice from loss expression by NSAID treatment. NSAIDs cause cytoskeletal reorganization, loss of actin stress fibers, and up-regulate the actin sequestration protein thymosin β-4. The secreted protein TGF-β1 is decreased by NAIDS *in vitro* and *in vivo*. NSAIDs also impact the TFG-β pathway down-stream of TFG-β1 by inhibiting phosphorylation of SMAD2. This could be useful for situations where TFG-β receptors' activity is no longer ligand dependent due to mutation. The secreted tumor suppressor protein NAG-1 is induced by NSAIDs both *in vitro* and *in vivo* via p53, Egr-1, and GSK-3β and other pathways. NSAIDs and improved derivatives of NSAIDs have great potential as both chemotherapeutic and chemopreventive agents.

CHAPTER 2
NONSTEROIDAL ANTI-INFLAMMATORY DRUG SULINDAC SULFIDE SUPPRESSES STRUCTURAL PROTEIN NESPRIN-2 EXPRESSION IN COLORECTAL CANCER CELLS

The results discussed in this chapter have been published in *Biochimica et Biophysica Acta (BBA) - General Subjects*, Volume 1840, Issue 1, January 2014, Pages 322-331.

2.1 Abstract

Aims:

Nonsteroidal anti-inflammatory drugs (NSAIDs) are well known for treating inflammatory disease and have been reported to have anti-tumorigenic effects. Their mechanisms are not fully understood, but both cyclooxygenase (COX) dependent and independent pathways are involved. Our goal was to shed further light on COX-independent activity.

Main methods:

Human colorectal cancer cells were observed under differential interference contrast microscopy (DICM), fluorescent microscopy, and micro-impedance measurement. Microarray analysis was performed using HCT-116 cells treated with sulindac sulfide (SS). PCR and western blots were performed to confirm the microarray data and immunohistochemistry was performed to screen for Nesprin-2 expression. The micro-impedance experiment was repeated including Nesprin-2 knock-down by siRNA.

Key findings:

HCT-116 cells treated with SS showed dramatic morphological changes under DICM and fluorescent microscopy, as well as weakened cellular adhesion as measured by micro-impedance. Nesprin-2 was selected from two independent microarrays, based on its novelty in relation to cancer and its role in cell organization. SS diminished Nesprin-2

mRNA expression as assessed by reverse transcriptase and real time PCR. Various other NSAIDs were also tested and demonstrated that inhibition of Nesprin-2 mRNA was not unique to SS. Additionally, immunohistochemistry showed higher levels of Nesprin-2 in many tumors in comparison with normal tissues. Further micro-impedance experiments on cells with reduced Nesprin-2 expression showed a proportional loss of cellular adhesion.

Significance:

Our data suggest that Nesprin-2 may be a potential novel human cancer-associated protein and NSAIDs decrease its expression.

2.2 Introduction

Non-steroidal anti-inflammatory drugs (NSAIDs) are widely used in the treatment of inflammatory disease through inhibition of prostaglandin production by cyclooxygenase-2 (COX-2). Interestingly, COX-2 expression is up-regulated in human colorectal tumors and regulates tumor growth in animal models [80-82]. NSAIDs have been shown to inhibit incidence and mortality of colorectal cancer in a broad range of studies [83, 84]. Although the chemopreventive and anti-tumorigenic activity of NSAIDs in cancer is well established, the molecular mechanisms responsible have not been completely elucidated.

The NSAID sulindac sulfide (SS) inhibits growth of tumors in azoxymethane-induced rat colon models [85], suppresses intestinal polyp formation in APC/Min mice [86, 87], down-regulates β-catenin protein apoptosis [88], and induces apoptosis under a number of experimental conditions [89-91]. SS has been shown to change colorectal cancer cell morphology [92], alter cytoskeletal organization, and cause loss of actin stress fibers [93, 94]. This is probably due to a dose-dependent reduction of tyrosine phosphorylation of focal adhesion kinase [94]. It has also been demonstrated that SS reduces cell migration and invasion in mouse models and human colorectal cell lines [95, 96].

We speculated that SS alters gene expression related to cell organization, and subsequently we found the structural gene Nesprin-2 (NUANCE/Syne-2) was down-regulated in two independent microarrays using two different doses of SS-treated human colorectal cancer cells. Nesprin-2 is a giant protein with an α-actin-like actin

binding domain [97]. To date, together with the closely related Enaptin/Nesprin-1, Nesprin-2 is the largest of the α-actin superfamily, and it encodes a 796 kDa protein containing an N-terminal actin-binding domain, central coiled-coil rod domain, and a C-terminal transmembrane domain [97, 98]. Nesprin-2 also has many truncated alternate splicing forms [99, 100]. The majority of Nesprin-2 is localized to the nuclear envelope, while a very small fraction can be found in the cytoplasm; the tissue distribution of Nesprin-2 mRNA is fairly ubiquitous with most tissues, showing at least trace amounts [97]. Recently Nesprin-2 has been shown to affect nuclear size and to be involved in regulating genes during wound healing [101, 102]. This colossal protein contains multiple binding sites and serves as a framework for protein complexes on the nuclear envelope [103, 104].

In this study, we found that human colorectal cancer HCT-116 cells dramatically changed their morphology and cell adhesion by treatment with SS, as assessed using biological, chemical, optical, and electrical methods. Subsequently, Nesprin-2 was identified and confirmed as being down-regulated by SS. Finally, we showed that Nesprin-2 is more highly expressed in tumor tissues, compared to normal tissues, suggesting that Nesprin-2 may be a novel cancer-associated protein.

2.3 Materials and Methods

2.3.1 Reagents

The NSAIDs used in this study were purchased as follows: SS, TA, and SC-560 from Cayman Chemical Company (Ann Arbor, Michigan); diclofenac from Sigma-Aldrich (St. Louis, MO); 5,5-dimethyl-3-(3-fluorophenyl)-4-(4-ethylsulfonyl)phenyl-2(5*H*)-furanone (DFU) was as a gift from Merck (Rahway, NJ). All other chemicals were purchased from Fisher Scientific, unless otherwise specified.

2.3.2 Cell Culture

All cells were purchased from ATCC and grown at 37°C with 5% CO_2. HCT-116 and HT-29 cells were cultured with McCoy's 5A modified. HCT-116 cells were kept to fewer than 20 passages to maintain the expected cellular mutations. SW480 cells were cultured with RPMI-1640. All culture media was supplemented with 10% fetal bovine serum, 100 µg/ml streptomycin, and 100 UI penicillin. Serum free media was used for all SS and vehicle treatments unless stated otherwise.

2.3.3 Microscopic Measurement

Three microscopic techniques were employed, differential interference contrast microscopy (DICM) and epi-fluorescence microscopy (EFM) for imaging the whole cell

including dorsal surface, as well as interference reflection contrast microscopy (IRCM) for imaging the ventral surface of cells.

The microscopic imaging system consisted of an Olympus IX-71 inverted microscope, a plan apochromat 100 x oil immersion objective with adjustable numerical aperture, 14-bit electron multiplier charge coupled device from Hammamatsu, and an incubation chamber that kept the temperature (37°C), humidity, and CO_2 (5%) levels constant. In order to examine the entire cellular morphology response to SS using DICM and EFM, HCT-116 cells were plated at a concentration of $1x10^5$ cells/ml. After 24 hr, cells were stained with LavaCell™ solution (Active Motif, Carlsbad, CA) to a concentration of 0.6 μM for 6 hr. Next, the media was changed to serum-free media containing 30 μM SS, and the cells were monitored microscopically for the next 6 hr. IRCM was used to examine the bottom morphology changes of HCT-116 cells exposed to 10 μM and 30 μM SS.

2.3.4 Electrical Impedance Measurements

A data acquisition and analysis system was implemented using LabVIEW (National Instruments, Austin, TX). Preliminary naked scans were performed to optimize sensitivity and to check for any electrode debris or defects. The electrodes were then inoculated with 400 μL media containing HCT-116 cells at a concentration of $2.4x10^4$ cells/ml under a range of SS concentrations. During the cellular micro-impedance scans, data was acquired at a rate of 32 Hz for 16 sec using a 30 ms filter time constant and 12 dB/decade roll off for approximately 96 hr. Averages and standard deviation

estimates were obtained from 512 sampled data points over the 16 sec time intervals. During the experiments cell-inoculated electrodes were kept in a cell culture incubator.

2.3.5 Microarrays

Two independent microarray experiments were performed: Human Array-Illumina HEEBO oligo microarray and Agilent oligo microarray. The 48.5K Human Array-Illumina HEEBO oligo microarray was purchased from Microarrays Inc (Nashville, TN). RNA was isolated from DMSO or 5 µM treated HCT-116 cells after 24 hr. One microgram of total RNA was used to synthesize cDNA. The arrays were hybridized at 42°C for 12-16 hr in a humidified hybridization chamber (GenomicTree, Korea). After washing microarrays were immediately dried using the microarray centrifuge (GenomicTree, Korea). The hybridization images were analyzed by GenePix Pro 6.0 (Axon Instruments, Sunnyvale, CA).

Another microarray analysis was conducted using Agilent human oligo 1A arrays (Agilent Technologies, Palo Alto, CA). HCT-116 cells were treated with DMSO or 10 µM SS for 24 hr. Total RNA was amplified using the Agilent Low RNA Input Fluorescent Linear Amplification Kit protocol. Starting with 500 ng of total RNA, Cy3- or Cy5-labeled cRNA was produced according to manufacturer's protocol. For each two color comparison, 750 ng of each Cy3 and Cy5 labeled cRNAs were mixed and fragmented using the Agilent *In Situ* Hybridization Kit protocol. Hybridizations were performed using the Agilent 60-mer oligo microarray processing protocol. Data was obtained using Agilent Feature Extraction software v7.5. Intensity plots were generated for each ratio

experiment, and genes were considered “signature genes” if the p value was less than 0.001. Functional annotation of genes was performed according to the Gene Ontology Consortium (http://www.geneontology.org/index.shtml) by GeneSpring v7.3.

2.3.6 Reverse Transcriptase PCR and Real Time PCR

RNA was isolated from cell cultures using Qiagen’s RNeasy Mini Kit following the manufacturer’s protocol. One microgram of RNA was used to generate cDNA using BIORAD’s iScript™ cDNA Synthesis Kit following the manufacturer’s protocol. PCR was performed with the following primers:: Nesprin-2 Giant forward 5’-CAGTCCTTACAACTCCTGGGACAC-3’, Nesprin-2 Giant reverse 5’-GACTGATTCTCCTACCCACAGACTC-3’; Nesprin-2 all isoforms forward 5’-TCACAGAGCAGCAGTCAGGT-3’, Nesprin-2 all isoforms reverse 5’-GCTCACGTTGACAGAGACCA-3’; Nesprin-2 α_1 forward 5’-GGAAGACCCCAGAGAAATCC-3’, Nesprin-2 α_1 reverse 5’-CCTGTCACCTTCCATTTGCT-3’; Nesprin-1 forward 5’-GGCTGAAAATCGAAGAGACG-3’, Nesprin-1 reverse 5’-CATCTC TGTGAGCCAGACCA-3’; GAPDH forward, 5’-GGGCTGCTTTTAACTCTGGT-3’, GAPDH reverse 5’-TGGCAGGTTTTTCTAGACGG-3’; IDH2 forward 5’-GACGGAGATGTGCAGTCAGA-3’, IDH2 reverse 5’-GTCCGTGGTGTTCAGGAAGT-3’; NAG-1 forward 5’-CTCCAGATTCCGAGAGTTGC-3’, and NAG-1 reverse 5’-AGAGATACGCAGGTGCAGGT-3’. Densitometric analysis of reverse transcriptase PCR was performed using Scion Image software (Frederick, MD). Real Time PCR was

performed using Thermo Scientific's Absolute qPCR SYBR Green Mix (Waltham, MA) on a Bio-Rad MyiQ iCycler thermal cycler using Bio-Rad iQ5 version 2.1 software following the manufacture's protocol (Hercules, CA). Measurements were standardized using GAPDH, and each set of three or more trials was averaged.

2.3.7 Immunohistochemistry

Immunostaining on a Biochain Tissue Array Human Tumor Tissue II (Lot# A711214) slide was performed using standard immunohistochemistry procedures (T8235713-2; Newark, CA). The slide was incubated overnight at 4°C with undiluted mAB K20-478 hybridoma antibody against Nesprin-2 [97] and secondary antibody treatment was performed using biotinylated anti-mouse immunoglobulins from BioGenex (HK-335-9M; San Ramon, CA). Nesprin-2 protein was stained brown with Chromogen-DAB solution and cells were counterstained with Hematoxylin (Richard Allen Scientific, Kalamazoo, MI). Tissues were rated for stain intensity by microscopic examination of three observers. An Olympus BX41 microscope with an Olympus DP70 digital camera employing integrated software was used for image capture/scaling.

2.3.8 Transfection of Nesprin-2 siRNA

HCT-116 cells were transfected with siRNA using PepMute reagent for 24 hours (SignaGen, Rockville, MD) following the manufacturer's protocol. The final concentration of siRNA was 10 nM for both the Control siRNA-A, sc-37007, and Syne-2

siRNA, sc-61630 (Santa Cruz Biology, Inc., Santa Cruz, LA). After 24 hours the media was changed with fresh complete media and allowed to grow for 24 more hours. The cells were then suspended and diluted to $2.4x10^4$ cells/ml with McCoy's 5A modified media. Cells were then treated with either DMSO or 30 μM SS. These cells were used for impedance experiments and harvested to isolate RNA for real time PCR.
The cells were suspended and diluted to $2.4x10^4$ cells/ml with McCoy's 5A modified media. Cells were then treated with either DMSO or 30 μM SS. These cells were used for impedance experiments and harvested to isolate RNA for PCR.

2.3.9 Western Blot

Cells lysates were isolated in RIPA buffer (50 mM Tris-HCl pH 7.4, 150 mM NaCl, 1 mM EDTA, 1% Triton X-100, 1% sodium deoxycholate, 0.1% SDS) supplemented with protease inhibitors (1mM PMSF, 1 μg/mL aprotinin, 1 μg/mL leupeptin) and phosphatase inhibitors (10 mM NaF, 0.1 mM Na_3VO_4,). Protein concentration was determined by BCA protein assay (Pierce, Rockford, IL). The proteins were separated on SDS–PAGE and transferred to nitrocellulose membranes (Osmonics, Minnetonka, MN). The membranes were incubated with anti-Nesprin-2 (sc-51220, Santa Cruz Biotechnology, Inc., Santa Cruz, CA) in 1% bovine serum albumin at 4°C overnight. After three washes with tris buffered saline containing 0.05% Tween 20, the blots were incubated with peroxidase-conjugated IgG for one hour at room temperature and visualized using ECL (Amersham Biosciences, Piscataway, NJ) and a LAS-4000 mini (Fujifilm Life Sciences, Stamford, CT).

2.3.10 Statistics

Unless stated otherwise statistical significance was determined using single-tailed paired Student t tests. P-values are noted with asterisks as follows: *P < 0.05, **P < 0.01, and ***P < 0.001.

2.4 Results

2.4.1 SS Treatment Alters Cell Morphology and Interferes with Cell Adhesion in HCT-116 cells

Micro-impedance measurements were used to quantitatively examine relative changes in proliferation and morphology, due to the modulations in cell-cell adhesion, cell-substrate adhesion, and plasma membrane capacitance under different concentrations of SS. It is well known that NSAIDs alter cell morphology and adhesion in cell culture [94]. Resistance and reactance are both measured as functions of time and AC frequencies; Fig. 2.1A and B present results only at representative frequencies of 5.62 kHz and 100 kHz, respectively. These changes are represented as the induction of apoptosis [105, 106]. Higher concentrations of SS produced a reduction in the normalized impedance components reflecting changes in cell-cell adhesion, and cell-substrate adhesion (resistance, Fig. 2.1A), and the capacitance of the plasma membrane (Reactance, Fig. 2.1B). This data demonstrates the suppression of cell-cell and cell-substrate adhesion by SS in a dose and time dependent manner. To examine cellular morphology HCT-116 cells were treated with SS in the presence of LavaCell

staining solution, which stains only cytoplasm and the nuclear membrane and is not cytotoxic under these conditions. As shown in Fig. 2.1C, SS changes cell morphology causing cellular rounding and nuclear condensation. Interestingly the apoptotic feature, “blebbing”, can be clearly seen under SS treatment (Fig. 2.1C, arrows). IRCM imaging shows dynamic gap morphology responses of live cells under SS treatment; dark areas indicate tight focal adhesion points between cell and substrate while lighter areas show increased gap between cell and substrate (Fig. 2.1D). Higher concentrations of SS showed a more dramatic increase in cellular gap from substrate and most bottom contacts including the close contacts as well as the remaining brighter areas noticeably diminished in response to the cellular shrinkage and retraction caused by SS, while some of the tightest focal contacts remain along the periphery of cells (Fig. 2.1D). Thus, SS induces loose adhesion between cells and substrate which results in cellular apoptosis.

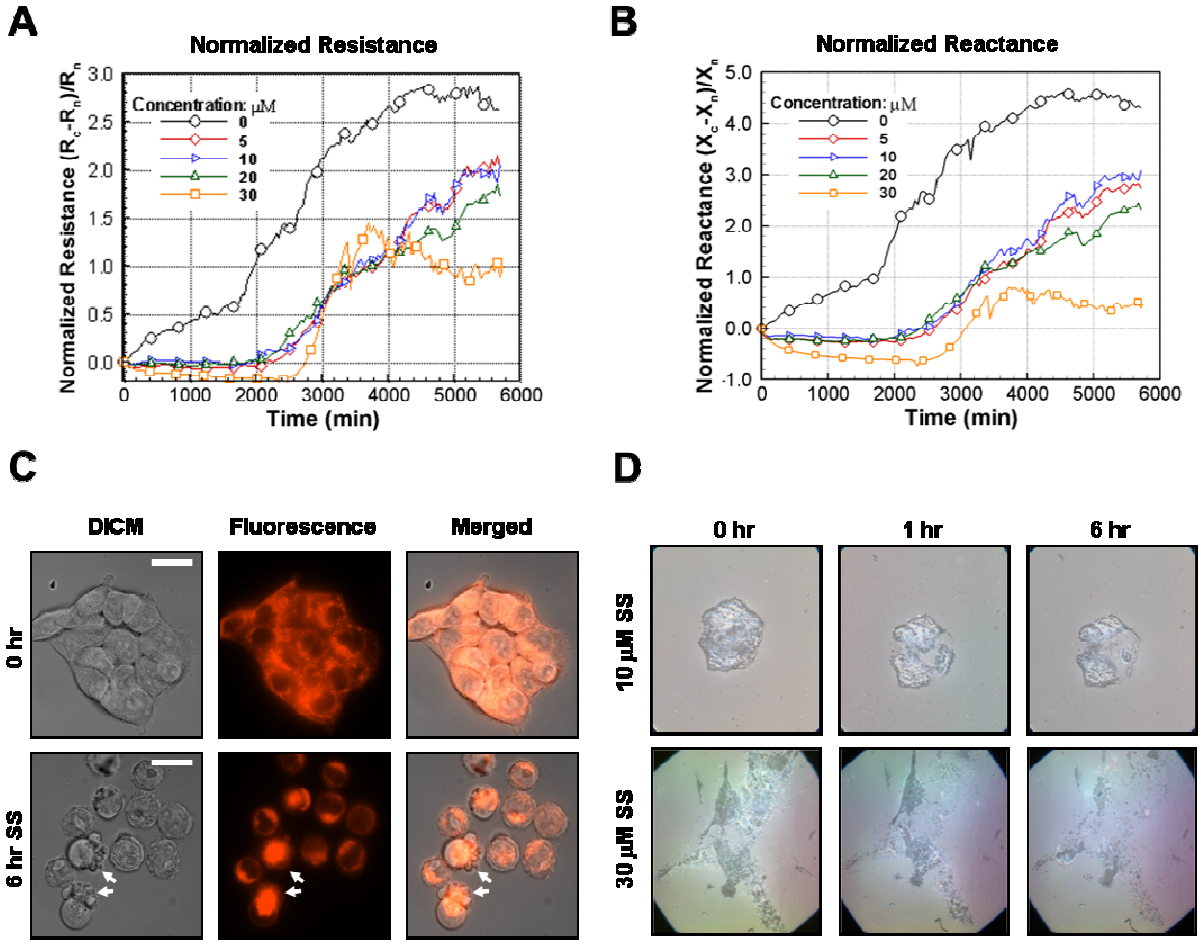

Figure 2.1 HCT-116 cell adhesion and morphology during SS treatment.

Biosensors were used to examine the dynamic attachment and spreading of colorectal cancer cells by monitoring micro-impedances. (A) The corresponding normalized resistance of HCT-116 cells. (B) The corresponding normalized reactance of HCT-116 measured for the same cells. The terms R and X represent the resistance and reactance, respectively, and the subscripts c and n indicate cell covered and naked scans, respectively. Symbols represent 20 data intervals. (C) Cellular morphology of HCT-116 cells was observed during 6 hr, 30 µM SS treatment in a real time manner. Observations were made using DICM and EFM. LavaCell (0.6 µM) was used for staining cytoplasm & membranes. The arrows indicate apoptotic blebbing. Scale bars represent 10 µm. (D) IRCM images to examine cellular gap morphology responses of HCT-116 cancer cells under SS treatment.

2.4.2 Cell Organization and Biogenesis Genes Pathways are Down-Regulated by SS

To elucidate molecular mechanisms by which SS affects cell morphology two independent microarray experiments were performed and compared. The genes of interest using SS-treated HCT-116 cells were chosen for function in “cellular organization and biogenesis” using the Gene Ontology Consortium. Surprisingly, only two genes, isocitrate dehydrogenase 2 (IDH2) and Nesprin-2, were commonly down-regulated in the category of Cell Organization and Biogenesis and no genes were commonly up regulated between these two microarrays in this category (Table 2.1). These genes represent potential targets of SS. IDH2 is a mitochondrial isozyme and Nesprin-2 is a large structural protein. Nesprin-2 was selected for further study based on its higher fold reduction compared to IDH2 and its unique role as a link between the actin cytoskeleton and the nuclear envelope as well as its novelty in relation to cancer.

Table 2.1 Cell organization and biogenesis genes down-regulated by sulindac sufide

Two independent oligo microarray experiments were performed on HCT-116 cells, treated by either 5 µM or 10 µM of sulindac sulfide (SS). Functional annotation of genes was performed according to Gene Ontology Consortium by GeneSpring 7.3. The two microarrays were compared for commonly up- and down-regulated genes in the categories of cell organization and biogenesis. The only two common genes with a cut off of a 1.5 fold change were IDH2, a mitochondrial isozyme, and Nesprin-2, a large structural protein.

Gene Name	Other Names	GeneBank Acc.No.	Gene Description	5 µM SS	10 µM SS
IDH2	IDH, IDP, IDHM, ICD-M,	NM_002168	isocitrate dehydrogenase 2 (NADP+), mitochondria	-1.37	-1.52
Nesprin-2	NUA, SYNE-2, Nesprin-2	NM_015180	nucleus and actin connecting element	-1.99	-1.75

2.4.3 Confirmation of Sulindac Sulfide Microarray Data

Down-regulation of Nesprin-2 and IDH2 mRNA by SS was confirmed by PCR in three replicates, standardized to GAPDH as a positive control (Fig. 2.2A). The fold reductions in these two genes correlates with the microarray data in that Nesprin-2 is more strongly down-regulated than IDH2 in both cases. We also examined NAG-1 (positive control) and Nesprin-1 expression. NAG-1 has been known to be induced by SS [107] whereas Nesprin-1 is another form of Nesprin family proteins.

Interestingly Nesprin-1 did not show any alterations in the presence of SS (Fig. 2.1A) indicating that NSAIDs affect Nesprin-2 in a specific manner. As shown in Fig. 2.1A Nesprin-2 repression was significant at $p < 0.001$ and IDH2 was reduced at $p <$

0.05. Protein expression of truncated Nesprin-2 forms was checked by western blot to verify that the mRNA reduction actually translates into a loss of protein expression in HCT-116 and SW480 cells after an initial screen of many cell lines for detectable levels of Nesprin-2 isotypes (Fig. 2.1B and data not shown). There are two Nesprin-2 alternate splicing variants that are very close to the observed Nesprin-2 protein size, Nesprin-2α_1 and Nesprin-2α_2 (Fig. 2.1C). To help differentiate between the two variants, two sets of PCR primers were designed; one that targets both isoforms and another which does not recognize Nesprin-2α_2. Reverse transcriptase PCR was performed on HCT-116 cells treated with vehicle or 30 µM SS for 24 hours and showed down-regulation in both sets (Fig. 2.1C).

Figure 2.2 Microarray conformation of genes down-regulated by SS.

(A) HCT-116 cells were treated with 30 µM SS for 24 h, and three replicates of reverse transcriptase PCR were performed. Representative gel electrophoresis images are shown with NAG-1 as a positive control for SS treatment and GAPDH as a loading control. Averages of densitometer analysis of mRNA expression levels from the three replicates were normalized to GAPDH and compared to the vehicle. The data represent mean ± S.E. P-values of **, $P < 0.01$, and ***, $P < 0.001$. (B) Schematic showing Nesprin-2 isoforms: Giant, α1, and α2. Locations of PCR primers, siRNA targets, and shRNA targets are shown. Reverse-transcriptase PCR data shows the effect of 30 µM SS for 24 hr using primers specific for Nesprin-2 α1, specific for Nesprin-2 α2, and primers which amplifiy most isoforms of Nesprin-2 including: Giant, α1, and α2. Nesprin-2 Giant specific primers are shown in (A). (C) Western blot analysis of cells treated with vehicle or 30 µM SS for 24 hr using anti-Nesprin-2 targeting the C-terminal region. The arrow indicates the correct size for Nesprin-2 α2.

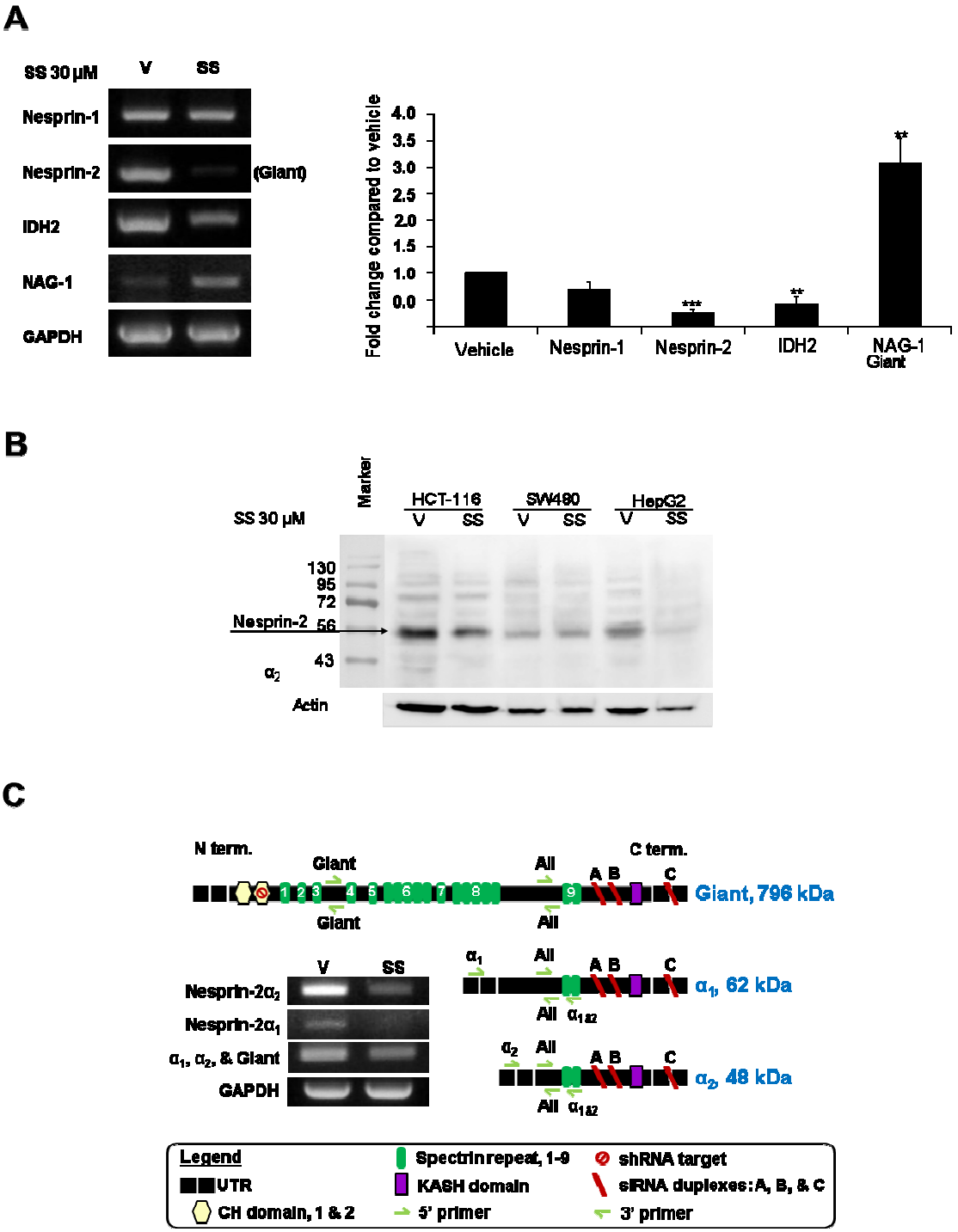

Figure 2.2 Continued.

2.4.4 Time- and Dose-Dependent Down-Regulation of Nesprin-2 by several NSAIDs

Nesprin-2 has previously been reported in the leading edge of migrating cells in wound-healing assays [97]. Due to this and its structural role, Nesprin-2 is an excellent candidate for investigation of the effects of SS on cell morphology and adhesion. Nesprin-2 mRNA was suppressed in a time dependent manner with significant reductions beginning at 6 h of treatment, $p < 0.01$ (Fig. 2.3A). Nesprin-2 down-regulation by SS was also dose dependent, starting with 1 μM up to 30 μM (Fig. 2.3B). Next, a range of other NSAIDs was tested to see if Nesprin-2 reduction is unique to SS or common among NSAIDs. A wide range of NSAIDs were used including conventional NSAIDs, which inhibit both COX-1 and COX-2 (SS, TA, and diclofenac) as well as the COX-1 specific inhibitor SC-560 and the COX-2 specific inhibitor DFU. All NSAIDs significantly reduced Nesprin-2 mRNA expression at $p < 0.05$, with the most dramatic repression by SS (Fig. 2.3C). Interestingly, SS repression of Nesprin-2 is not limited to HCT-116 cells; however, this does not occur in all colorectal cancer cell lines tested. Sulindac sulfide treatment for 24 hours significantly reduced Nesprin-2 in HT-29 cells; however, SW480 cells showed a reduction in Nesprin-2 with no statistical significance (Fig. 2.3D).

Figure 2.3. Nesprin-2 mRNA expression in a time and dose dependent manner.

(A) Nesprin-2 down-regulation by SS was shown by real time PCR to be time-dependent over a 24 h time course for HCT-116 cells treated with 30 µM SS. (B) HCT-116 cells also showed a dose dependant response by real time PCR to SS over a 24 h treatment. (C) A variety of NSAIDs (SS 30 µM, tolfenamic acid 20 µM, diclofenac 100 µM, SC-560 25 µM, and DFU 100 µM) were tested on HCT-116 cells for 24 hr (reverse transcriptase PCR). (D) Other colorectal cancer cell lines, HT-29 and SW480, were tested for Nesprin-2 suppression by reverse transcriptase PCR with SS after 24 hr treatments. (E) Reverse transcriptase PCR on HCT-116 cells pre-treated with 5 µM actinomycin D for 1 hr prior to a SS time course was performed and lines indicate a linear regression trend. Representative reverse transcriptase-PCR data and the densitometry results (bottom) as well as real time PCR data are shown from at least three independent experiments normalized to GAPDH and compared to 0 hr (A & E) or vehicle (B, C, & D). The data represent mean ± S.E. *P<0.05, ***P* < 0.01, and ****P* < 0.001.

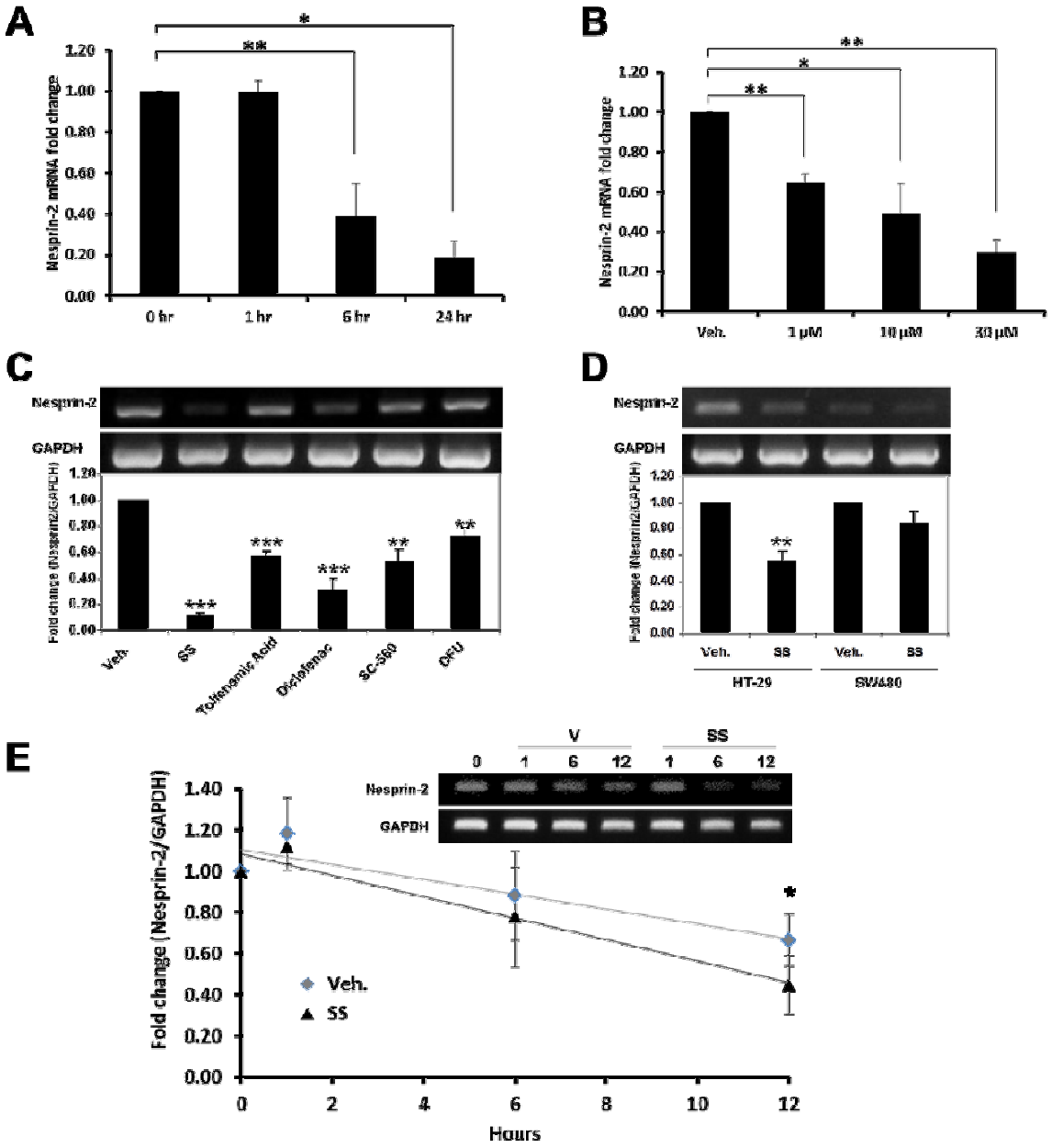

Figure 2.3. Continued.

2.4.5 Normal and Tumor Tissue Protein Expression of Nesprin-2

A tissue array slide containing a range of normal and neoplastic tissues was used to study Nesprin-2 protein expression on the microscopic level. The majority of the normal and neoplastic tissues in the array did not have detectable levels of positive staining, although the antibody detects all isotypes. Increased immunohistochemical staining of Nesprin-2 protein was observed in the neoplastic epithelial cells in tissues of breast, duodenum, rectum, and thyroid, compared to normal tissue (Fig. 2.4, Table 2.2). Focal to diffuse, mild to moderate positive staining was present within the cytoplasm of neoplastic cells. Discernible cytoplasmic staining of normal cells was limited to rare foci of crypt cells in the rectum. Although Nesprin-2 has been primarily detected in the nuclear membrane [97], our data suggest Nesprin-2 expression mostly in cytoplasm. This cytoplasmic localization in multiple neoplastic epithelial cells as well as the proliferative crypt cells of the rectum supports Nesprin-2's potential role as an oncogene.

Figure 2.4 Nesprin-2 normal tumor tissue array.

Immunohistochemical staining of Nesprin-2 in human normal and tumor tissue array. Slides were stained with Nesprin-2 antibody, seen as brown coloring, and counter stained with Hematoxylin. Three independent observers note stain intensity for 47 normal tissues and 47 tumor tissues (Table 2). Representative images from the tissues with the highest expression are shown. The large frames were taken with a 40X objective lens (50 µm scale bars), and the small frames in the upper left corners are at 100X (10 µm scale bars).

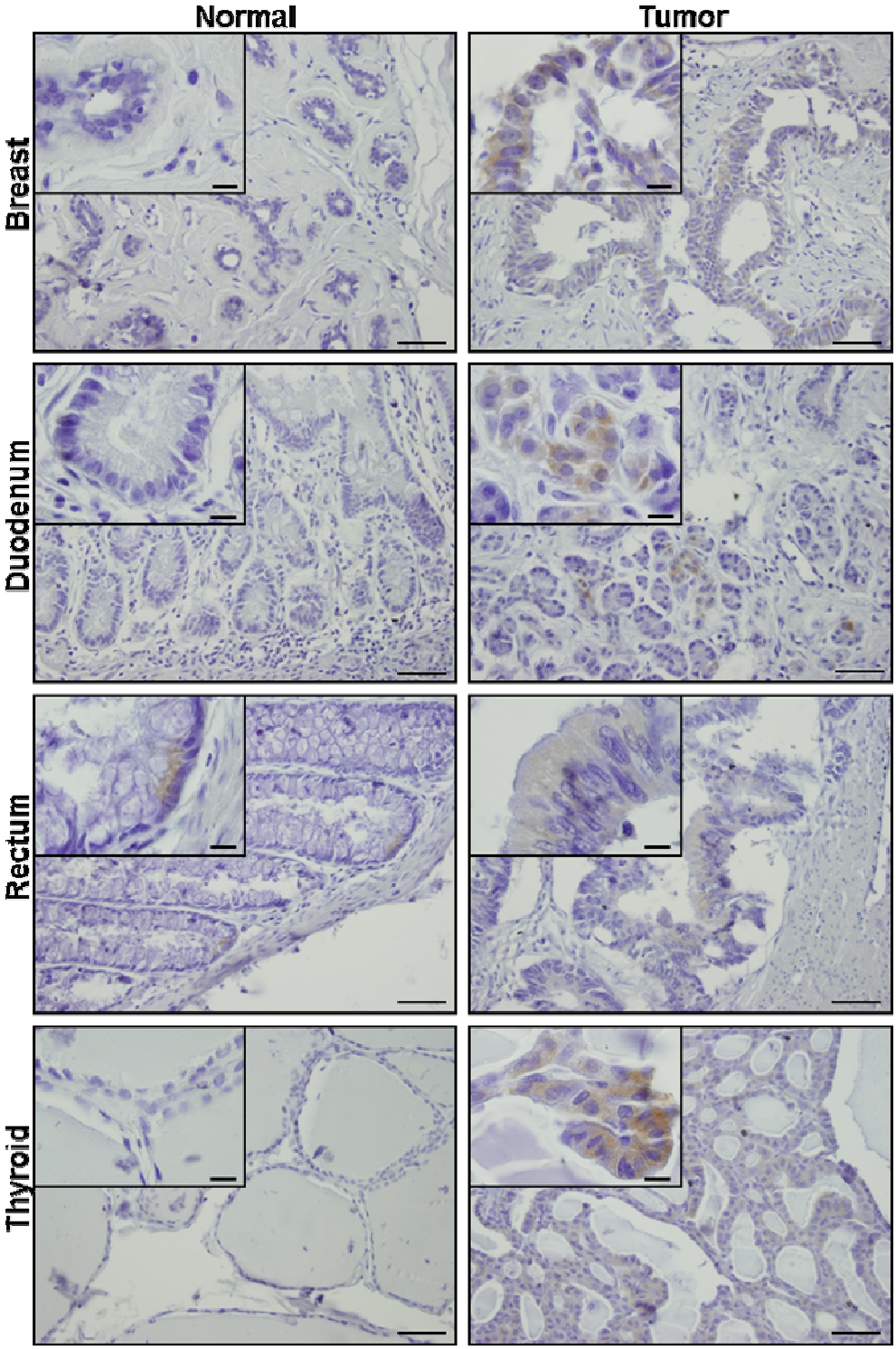

Figure 2.4 Continued.

2.4.6 Cellular Impedance is Reduced by siRNA & shRNA Knock-down of Nesprin-2

The micro-impedance experiment was performed on HCT-116 cells either transfected with siRNA against Nesprin-2 or non-targeting control siRNA, then treated with vehicle or SS. In the case of the SS-treated cells, initial adhesion was similar at first for both Nesprin-2 knock-down and non-targeting control cells. After approximately a day and a half the Nesprin-2 knock-down cells showed reduced adhesion compared to the non-targeting control cells (Fig. 2.5B and C). The average reduction in Nesprin-2 mRNA when adjusted by GAPDH was a knock-down of 53% (Fig. 2.5A). Normalized resistance is representative of cell-cell and cell-substrate adhesion while normalized reactance reflects the plasma membrane capacitance. Both normalized resistance and reactance in the Nesprin-2 knock-down cells showed a reduction ranging from 50% after two days when the cells were most actively growing to 20% at completion of the three and a half day experiment as compared with the control siRNA transfected cells treated with vehicle (Fig. 2.5B and C). Similar impedance results were generated with shRNA targeted against Nesprin-2, though the knock-down was less (Fig. 2.6). This suggests that reduction in Nesprin-2 by SS treatment could be contributing to the loss of adhesion in colorectal cancer cells.

Figure 2.5 The effect of Nesprin-2 mRNA knock-down of HCT-116 on micro-impedance.

(A) Nesprin-2 expression knock-downed by siRNA. Nesprin-2 siRNA was transfected, and subsequently real time PCR was performed in triplicate to validate the siRNA in our system. GAPDH was used to amplify for RNA control. The graph shown represents a relative fold change, as the control siRNA set is 1.0 from three independent experiments. *$P < 0.01$. (B) Micro-impedance measurement of HCT-116 cells with knocked-down Nesprin-2 expression. HCT-116 cells were transfected with non-targeting control siRNA or siRNA Nesprin-2 and treated with vehicle or 30 µM SS. (C) The corresponding normalized reactance of these same cells was measured at the same time during this period. The terms R and X represent the resistance and reactance, respectively, and the subscripts c and n indicate cell covered and naked scans, respectively. Symbols represent 26 data intervals.

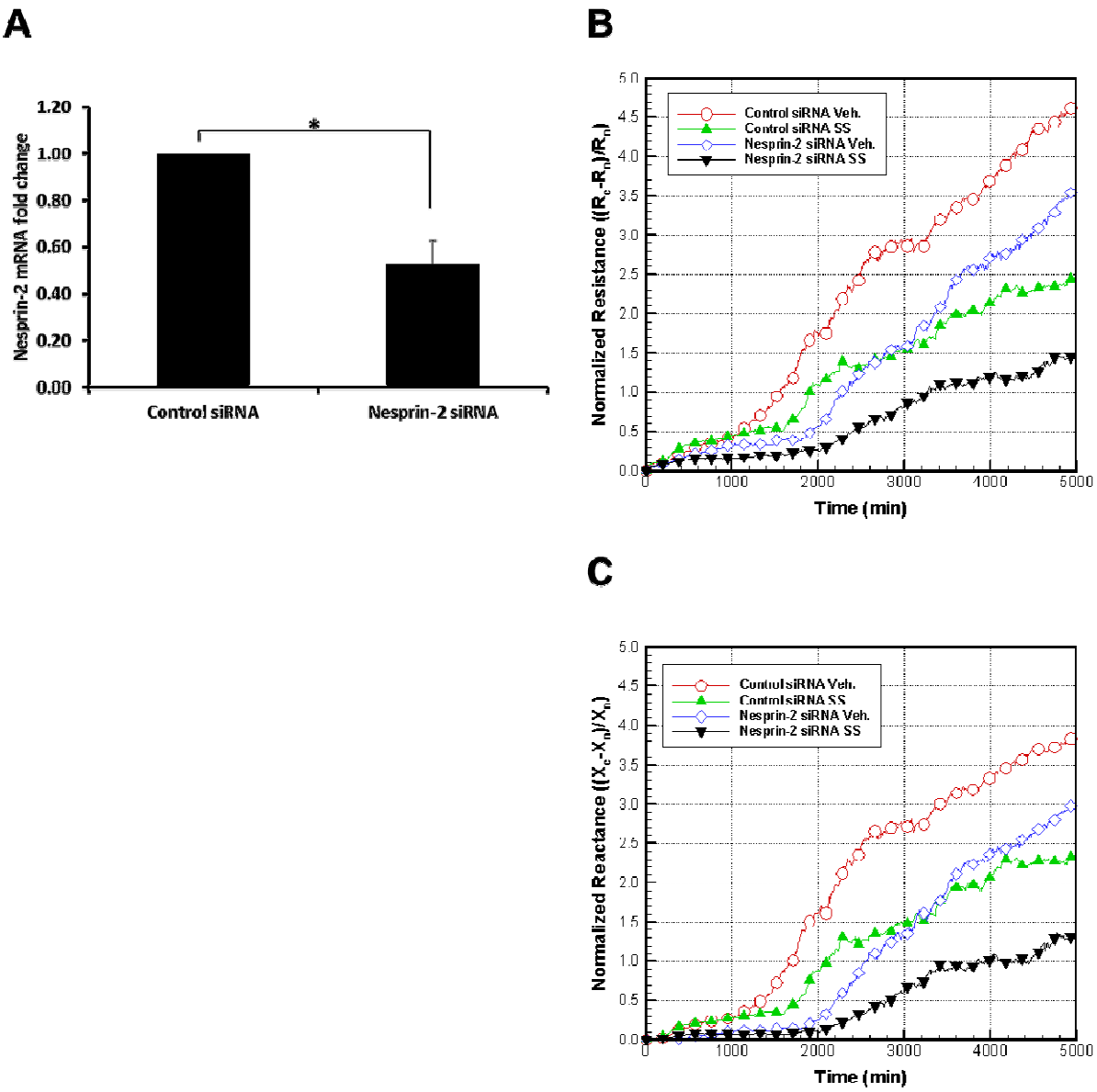

Figure 2.5 Continued.

Table 2.2 Normal tumor tissue array staining intensity.

Immunohistochemical Staining of Nesprin-2 in Normal and Tumor Tissue. Immunostaining was performed on a Biochain Tissue Array Human Tumor Tissue II (Lot# A711214) using mAB K20-478 antibody against Nesprin-2 and counterstained with hematoxylin. Each of the 96 positions was evaluated for staining intensity, localization of staining, and the distribution of staining. The staining intensity was scored from 0 to 3+. The type of cell stained was also noted where applicable.

Position	Organ	Staining	Localization	Cell Type	Distribution
A1	Positive Control	0	0	N/A	N/A
A2	Negative Control	0	0	N/A	N/A
A3	Adrenal Tumor	0	0	N/A	N/A
A4	Adrenal	2+	cytoplasm	cortical epithelium	diffuse
A5	Adipose Tumor	0	0	N/A	N/A
A6	Adipose	0	0	N/A	N/A
A7	Bladder Tumor	1+	cytoplasm	epithelium	rare, scattered
A8	Bladder	1-2+	cytoplasm	epithelium	occasional disseminated
A9	Bladder Tumor	0-1+	cytoplasm	epithelium	rare, scattered
A10	Bladder	1+	cytoplasm	epithelium	diffuse
A11	Brain Tumor	1+	cytoplasm	glial tumor cells	rare, scattered
A12	Brain	0	0	N/A	N/A
B1	Breast Tumor	0	0	N/A	N/A
B2	Breast	1-2+	cytoplasm	epithelium	diffuse
B3	Breast Tumor	0	0	N/A	N/A
B4	Breast	0	0	N/A	N/A
B5	Colon Tumor	0	0	N/A	N/A
B6	Colon	0	0	N/A	N/A
B7	Colon Tumor	0	0	N/A	N/A
B8	Colon	0	0	N/A	N/A
B9	Duodenum Tumor	2+	cytoplasm	epithelium, glandular	rare, multifocal, global
B10	Duodenum	0	0	N/A	N/A
B11	Esophagus Tumor	1+	cytoplasm	epithelium	rare focal
B12	Esophagus	0		N/A	N/A
C1	Esophagus Tumor	0	0	N/A	N/A
C2	Esophagus	0	0	N/A	N/A
C3	Esophagus Tumor	0	0	N/A	N/A
C4	Esophagus	0	0	N/A	N/A

Table 2.2 Continued.

Position	Organ	Staining	Localization	Cell Type	Distribution
C5	Fallopian Tumor	0	0	N/A	N/A
C6	Fallopian Tube	0	0	N/A	N/A
C7	Gall Bladder Tumor	0	0	N/A	N/A
C8	Gall Bladder	0	0	N/A	N/A
C9	Kidney Tumor	0	0	N/A	N/A
C10	Kidney	0	0	N/A	N/A
C11	Kidney Tumor	0	0	N/A	N/A
C12	Kidney	1+	cytoplasm	epithelium	occasional disseminated
D1	Liver Tumor	0	0	N/A	N/A
D2	Liver	0	0	N/A	N/A
D3	Liver Tumor	0-1+	cytoplasm		diffuse
D4	Liver	1-2+	cytoplasm	epithelium	1+diffuse, 2+ scattered
D5	Lung Tumor	1+	cytoplasm	epithelium	diffuse
D6	Lung	0	0	N/A	N/A
D7	Lung Tumor	0	0	N/A	N/A
D8	Lung	0	0	N/A	N/A
D9	Lung Tumor	0	0	N/A	N/A
D10	Lung	0	0	N/A	N/A
D11	Lung Tumor	1+	cytoplasm	epithelium	rare scattered
D12	Lung	0	0	N/A	N/A
E1	Lung Tumor	1+	cytoplasm		rare scattered
E2	Lung	0	0	N/A	N/A
E3	Lymphoma	0	0	N/A	N/A
E4	Lymph Node	0	0	N/A	N/A
E5	Lymphoma	0	0	N/A	N/A
E6	Lymph Node	0	0	N/A	N/A
E7	Ovary Tumor	0	0	N/A	N/A
E8	Ovary	0	0	N/A	N/A
E9	Ovary Tumor	0	0	N/A	N/A
E10	Ovary	0	0	N/A	N/A
E11	Pancrease Tumor	1+	cytoplasm	epithelium	rare scattered
E12	Pancrease	0	0	N/A	N/A

Table 2.2 Continued.

Position	Organ	Staining	Localization	Cell Type	Distribution
F1	Parotid Tumor	2+	golgi?	plasma cells	disseminated
F2	Parotid	0	0	N/A	N/A
F3	Prostate Tumor	0	0	N/A	N/A
F4	Prostate	0	0	N/A	N/A
F5	Rectum Tumor	0	0	N/A	N/A
F6	Rectum	0	0	N/A	N/A
F7	Rectum Tumor	1+	cytoplasm	cytoplasm	locally diffuse
F8	Rectum	0	0	N/A	N/A
F9	Skin Tumor	0	0	N/A	N/A
F10	Skin	1+	cytoplasm	basal epithelium	locally diffuse
F11	Small Intestine Tumor	1+	cytoplasm	epithelium	rare scattered
F12	Small Intestine	0	0	N/A	N/A
G1	Soft Tissue Tumor	0	0	N/A	N/A
G2	Soft Tissue	0	0	N/A	N/A
G3	Stomach Tumor	0	0	N/A	N/A
G4	Stomach	1+	cytoplasm	glandular epithelium	disseminated
G5	Stomach Tumor	0	0	N/A	N/A
G6	Stomach	0	0	N/A	N/A
G7	Stomach Tumor	0	0	N/A	N/A
G8	Stomach	0	0	N/A	N/A
G9	Testis Tumor	0	0	N/A	N/A
G10	Testis	1+	cytoplasm	inerstitial cells	diffuse, may be an artifact
G11	Throat/Ph. Tumor	0	0	N/A	N/A
G12	Throat/Pharynx	0	0	N/A	N/A
H1	Throat/Ph. Tumor	1+	golgi?	plasma cells	
H2	Throat/Pharynx	0	0	N/A	N/A
H3	Thymus Tumor	0	0	N/A	N/A
H4	Thymus	0	0	N/A	N/A
H5	Thyroid Tumor	1+	cytoplasm	epithelium	diffuse
H6	Thyroid	0	0	N/A	N/A
H7	Thyroid Tumor	0	0	N/A	N/A
H8	Thyroid	0	0	N/A	N/A
H9	Uterus Tumor	0	0	N/A	N/A
H10	Uterus	0	0	N/A	N/A
H11	Uterus Tumor	0	0	N/A	N/A
H12	Uterus	0	0	N/A	N/A

Figure 2.6. The effect of Nesprin-2 mRNA knock-down of HCT-116 on micro-impedance.

(A) Nesprin-2 expression knock-downed by shRNA. Nesprin-2 shRNA was transfected, and subsequently RT-PCR was performed in triplicate for each of the three micro-impedance measurements, with the same cells used to inoculate the electrodes for the micro-impedance measurements. A representative RT-PCR gel from three independent experiments is shown. GAPDH was used to amplify for RNA control. The graph shown in the bottom represents a relative fold change, as the empty vector set is 1.0 from three independent experiments. P-values of **, $P < 0.01$. (B) Micro-impedance measurement of HCT-116 cells with knocked-down Nesprin-2 expression. HCT-116 cells were transfected with empty vector or shRNA Nesprin-2 and treated with vehicle or 30 µM SS. (C) The corresponding normalized reactance of these same cells was measured at the same time during this period. The terms R and X represent the resistance and reactance, respectively, and the subscripts c and n indicate cell covered and naked scans, respectively. Symbols represent 20 data intervals.

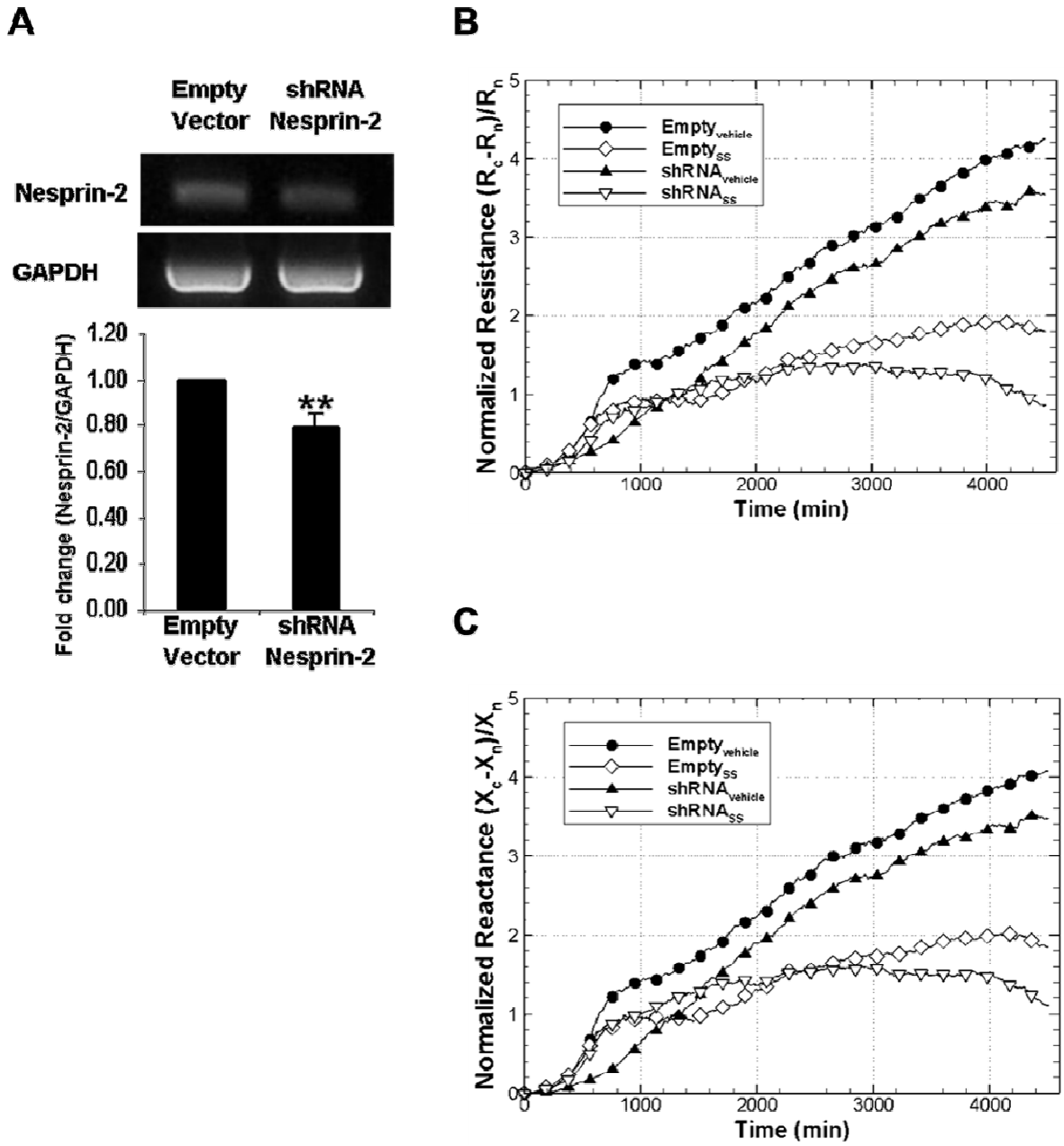

Figure 2.6. Continued.

2.5 Discussion

There are several well-known methods to examine cell proliferation and morphological changes under specific treatments including fluorescence microscopy, flow cytometry, and biochemical assays. While these methods are stationary and need fluorescent or radioactive probes, micro-impedance measurement is a bio-analytical technique that is capable of non-invasively and dynamically monitoring proliferation in real time without the use of chemical probes. The use of micro-electrodes to measure cellular impedance was pioneered by Giaever and Keese [108, 109]. Since then, this technique has been applied to a number of biological studies that deal with cellular barrier function, attachment, spreading, and adhesion [110-115]. In addition, frequency-dependent electrical impedance measurements have been used to evaluate the model parameters associated with cell-cell and cell-matrix junction formation [116-118]. In the present study, micro-impedance measurements were used to quantitatively examine proliferation and morphological changes such as cell-cell adhesion and cell-substrate adhesion under different concentrations of SS. Our data demonstrated the suppression of cell-cell and cell-substrate adhesion by SS in a dose-dependent manner. Subsequently, DICM was performed to observe cell morphology. Unlike phase contrast microscopy (PCM), DICM can visualize a wide variety of specimens such as very thin filaments, thick specimens, and sharp interfaces and can create realistic 3-dimensional shapes as an effective tool to qualitatively and quantitatively examine the effects of anti-tumorigenic compounds on cell adhesion. IRCM has been well known to provide a more comprehensive examination of cellular bottom morphology responses when exposed to

drugs. Early use of IRCM in cell biology goes back to Curtis' examination of how cells adhered to glass [119]. Subsequently, other groups improved this method by using a high numerical aperture objective lens, while a theoretical analysis attempted to quantify cell substrate separation distances [120, 121].

Microarrays were performed and two genes were identified as commonly down-regulated genes, based on biogenesis and cell organization pathways. The IDH2 and Nesprin-2 genes represent potential targets of SS since the IDH2 and Nesprin-2 mRNA seen in our microarray studies are confirmed by PCR. The fold reductions in these two genes observed through multiple replications of PCR correlates with the microarray data in that Nesprin-2 is more strongly down-regulated than IDH2 in both cases. Nesprin-2 was selected for this study based on its unique role as a link between the actin cytoskeleton and the nuclear envelope as well as its novelty in relation to cancer. Interestingly, Nesprin-1 did not show any alterations in the presence of SS (Fig. 2.4.6A), indicating that NSAIDs affect Nesprin-2 in a specific manner.

While the NSAID doses used in this study were much too high for serum relevancy, they were modest compared to other colorectal studies due to the higher concentrations obtainable in the colon. Sulindac is converted to the active metabolite SS in the liver and travels back to the gut through bile ducts where it is concentrated. Also, the natural colonic bacteria converts a large portion of sulindac to SS [122]. These two factors suggest that orally administered sulindac can lead to luminal SS concentrations in the colon that are higher concentrations than obtainable in serum [123]. Human familial adenomatous polyposis (FAP) patients can achieve 10-15 µM

plasma concentrations of SS at doses that regress polyps [124, 125]. Animal studies have demonstrated that SS concentration in the colon mucosa is many-fold higher than serum levels [126]. The cells of the colonic epithelium could be subject to SS concentrations as high as 20-fold above what can be observed in the serum [123]. Based on the tissue to plasma level ratio of SS in the colon of 10-20 [123, 126], other groups have justified using much higher SS concentrations, as high as 100-200 µM, as plausible in the human colon [127, 128]. Therefore, our doses used in this study could be in the range of clinical doses occurring in the gut.

Nesprin-2 has previously been reported to be present on the leading edge of migrating cells in wound-healing assays [97]. Due to this and its structural role, Nesprin-2 is an excellent candidate for investigation of the effects of SS on cell morphology and adhesion. Nesprin-2 mRNA expression is reduced by SS treatment in a time- and dose-dependent manner (Fig. 2.4.6). Other NSAIDs conventional as well as COX 1 and COX 2 specific all show reductions in Nesprin-2, with the most dramatic repression by SS. Interestingly, SS repression of Nesprin-2 is not limited to HCT-116 cells; however, this does not occur in all colorectal cancer cell lines tested. It has been reported that β-catenin participates in modulating cytoskeletal dynamics in association with the microfilament-bundling protein fascin [129]. SW480 cells (active β-catenin signaling) did not show a significant reduction of Nesprin-2 in the presence of SS (Fig. 2.4.6B and 2.4.7D), probably explained by the cell context, whereas HCT-116 and HT-29 cells possess a mutant β-catenin gene. Therefore, β-catenin signaling may inhibit SS-dependent Nesprin-2 down-regulation. However, further studies may be required to

elucidate the molecular mechanism by which SS down-regulates Nesprin-2 in a cell-specific manner.

In the present study, siRNA consistently reduced Nesprin-2 mRNA expression by an average of 53%. This reduction in Nesprin-2 mRNA expression correlated nicely with the reduction in cell-cell and cell-substrate adhesion seen in the normalized resistance and cell's plasma membrane capacitance seen in the normalized reactance of the Nesprin-2 knockdown cells, as compared with the control siRNA-transfected cells treated with vehicle. In the case of the SS-treated cells, initial adhesion was similar at first for both Nesprin-2 knockdown and control siRNA cells. The Nesprin-2 knockdown cells showed reduced adhesion compared to the control siRNA cells. This suggests that reduction in Nesprin-2 by SS treatment could contribute to the loss of adhesion in colorectal cancer cells.

Expression of Nesprin-2 in most tissues was too low to be routinely detected by immunohistochemistry using standard light microscopy, although the antibody used detects all isotypes. Notably increased staining for Nesprin-2 expression in tumor tissues over normal tissue can be seen in mammary, duodenal, rectal, and thyroid tissues. Although Nesprin-2 has been primarily detected in the nuclear membrane [97], our data suggest Nesprin-2 expression mostly in cytoplasm of tumor tissue. This cytoplasmic localization in multiple neoplastic epithelial cells as well as the proliferative crypt cells of the rectum supports Nesprin-2's potential role as an oncogene. To the best of our knowledge, this is the first report that Nesprin-2 is more highly expressed in tumor tissues than in normal tissues.

2.6 Conclusions

The present study suggests that Nesprin-2 could be involved in oncogenesis and that SS treatment reduces its expression. This is strengthened by the increased Nesprin-2 expression observed in several different tumor types compared to normal tissue. This is further supported by Nesprin-2 knock-down cells mimicking the cell-cell and cell-substrate adhesion patterns seen with SS treatment proportional to the amount of suppression. Nesprin-2's vast size and position on the nuclear envelope and cytoplasm mark it as potential scaffolding for many other protein-protein interactions. Further study of Nesprin-2 could lead to a novel target for cancer treatment.

CHAPTER 3 CHAPTER III
A NOVEL COX-INDEPENDENT MECHANISM OF SULINDAC SULFIDE FACILITATES CLEAVAGE OF EPITHELIAL CELL ADHESION MOLECULE PROTEIN

3.1 Abstract

Non-steroidal anti-inflammatory drugs (NSAIDs) are extensively used over the counter to treat headaches and inflammation as well as clinically to prevent cancer among high-risk groups. The inhibition of cyclooxygenase (COX) activity by NSAIDs plays a role in their anti-tumorigenic properties. NSAIDs also have COX-independent activity which is not fully understood. In this study, we report a novel COX-independent mechanism of sulindac sulfide (SS), a conventional NSAID, which facilitates a previously uncharacterized cleavage of epithelial cell adhesion molecule (EpCAM) protein. EpCAM is a type I transmembrane glycoprotein that has been implemented as an over-expressed oncogene in many cancers including colon, breast, pancreas, and prostate. We found EpCAM to be regulated by SS in a manner that is independent of COX activity. Our findings demonstrate that SS drives cleavage of the extracellular portion of EpCAM near the N-terminus. This SS driven cleavage is blocked by deleting amino acids 55-81, as well as by simply mutating arginine residues at positions 80 and 81 to alanine. Proteolysis of EpCAM by NSAIDs may provide a novel mechanism by which NSAIDs affect anti-tumorigenesis at the post-translational level.

3.2 Introduction

Non-steroidal anti-inflammatory drugs (NSAIDs) have been used for the treatment of inflammatory diseases, but a body of evidence suggests that NSAIDs exhibit anti-tumorigenic activity [130-133]. The mechanisms involve both cyclooxygenase (COX) dependent and independent pathways; much attention is paid to COX-independent manner. Our lab and others have reported several targets of NSAIDs in a COX-independent manner [134, 135]; however, more molecular targets of NSAIDS are needed to understand the nature of NSAIDs in anti-tumorigenesis.

Epithelial cell adhesion molecule (EpCAM) is a type I transmembrane glycoprotein. Initial studies focused on its role as a Ca^{+2} independent homophilic adhesion molecule [136]. The extracellular region of EpCAM contains two epidermal growth factor (EGF)-like domains which are involved in both reciprocal interactions between EpCAM molecules on adjacent cells, and lateral interactions between EpCAM molecules [136]. In addition, EpCAM can interfere with E-cadherin's interaction with the cytoskeleton [137]. As the protein expression of EpCAM increases it becomes the dominate adhesion molecule as it diminishes cadherin-mediated cell-cell adhesions [137]. Thus, this transition from cadherin to EpCAM mediated cell adhesion could be important to early tumor progression.

More recent focus has been on EpCAM's involvement in cancer progression and invasion. There are many reports showing EpCAM expressed at high levels in many cancer types including gastric, intestinal, colorectal, ovarian, and others [138-142].

Down-regulation of EpCAM in gastric cancer cells which overexpress EpCAM inhibits proliferation [139]. EpCAM is transcriptionally repressed by the tumor suppressor p53 in breast cancer [143]. Increased proliferation observed in conjunction with high EpCAM expression could be due in part to its regulation of cell cycle progression through Cyclin D1 expression [144]. Furthermore, EpCAM expression in EpCAM negative cells has been shown to be involved in epithelial to mesenchymal transition (EMT) [145, 146]. Interestingly, EpCAM may act as protagonist or antagonist depending upon the specific context within complex biological systems. EpCAM which is widely viewed as an oncogene due to its role in early tumor development may be beneficial as an adhesion molecule in later stages of cancer progression. For example, a few studies have suggested that loss of EpCAM expression is associated with poor patient prognosis and is favorable to metastasis [147-150]. Most of the research currently being done on EpCAM focuses on either using it as a cancer biomarker [151] or as a target for therapeutic antibodies [152, 153]. EpCAM's biological activity in cancer in the context of tumor stage and specific cellular micro-enviroment needs to be elucidated to understand EpCAM's potentially dynamic role in tumor progression.

One of the pathways that EpCAM affects in tumorigenesis is an alternate Wnt signaling pathway. It has been shown that EpCAM can bind to β-catenin through a complex with four and a half limb domain 2 (FHL2) [154]. This complex is released from the interior of the cell membrane and can translocate to the nucleus and initiate downstream TCF/LEF signaling, following proteolysis of EpCAM's extracellular domain (EpEX) then cleavage of EpCAM's intracellular domain (EpICD) [155]. Recently,

EpCAM has been shown through new detailed study of multiple antibodies, to express multiple proteolytic fragments [156]. Thus, EpCAM is not only a biomarker of cancer cells, but also exhibits multiple biological activities that needed to be elucidated.

Our group focused on NSAID-effects on anti-tumorigenesis. We found that the NSAID SS dramatically decreases EpCAM's expression via facilitating one of the cleavage sites on the extra-cellular region of EpCAM. In this study, we suggest that SS affects many pathways and one such novel mechanism is SS's cleavage of EpCAM.

3.3 Materials and Methods

3.3.1 Reagents

The NSAIDs used in this study were purchased as follows: SS, TA, and SC-560 from Cayman Chemical Company (Ann Arbor, Michigan); diclofenac from Sigma-Aldrich (St. Louis, MO); 5,5-dimethyl-3-(3-fluorophenyl)-4-(4-ethylsulfonyl)phenyl-2(5*H*)-furanone (DFU) was as a gift from Merck (Rahway, NJ). All other chemicals were purchased from Fisher Scientific, unless otherwise specified.

3.3.2 Cell Culture

All cells were purchased from ATCC and grown at 37°C with 5% CO_2. HCT-116 and HT-29 cells were cultured with McCoy's 5A modified. HCT-116 cells were kept to fewer than 20 passages to maintain the expected phenotype. SW480 cells were

cultured with RPMI-1640 medium. LoVo cells and A549 cells were cultured with Ham's F12 medium. HepG2 cells were cultured with DMEM medium. Each cell line used was not passaged for longer than three months before retrieving fresh cells from liquid nitrogen stock to preserve the expected phenotypes. All culture media was supplemented with 10% fetal bovine serum, 100 µg/ml streptomycin, and 100 UI penicillin. Serum free media was used for all SS and vehicle treatments unless stated otherwise.

3.3.3 Reverse Transcriptase PCR and Real Time PCR

RNA was isolated from cell cultures using Qiagen's RNeasy Mini Kit following the manufacturer's protocol. One microgram of RNA was used to generate cDNA using BIORAD's iScript™ cDNA Synthesis Kit following the manufacturer's protocol. PCR was performed with the following primers:: EpCAM forward 5'- CTG CCA AAT GTT TGG TGA TG -3'; EpCAM reverse 5'- ACG CGT TGT GAT CTC CTT CT -3'; GAPDH forward, 5'- GGG CTG CTT TTA ACT CTG GT -3', GAPDH reverse 5'- TGG CAG GTT TTT CTA GAC GG -3'; NAG-1 forward 5'-CTC CAG ATT CCG AGA GTT GC -3', and NAG-1 reverse 5'-AGA GAT ACG CAG GTG CAG GT -3'. Densitometric analysis of reverse transcriptase PCR was performed using Scion Image software (Frederick, MD). Real Time PCR was performed using Thermo Scientific's Absolute qPCR SYBR Green Mix (Waltham, MA) on a Bio-Rad MyiQ iCycler thermal cycler using Bio-Rad iQ5 version 2.1 software following the manufacture's protocol (Hercules, CA). Measurements were standardized using GAPDH and each set of three or more trials were averaged.

3.3.4 Expression Vectors

All expression vectors where generated from pcDNA3.1 V5/His TOPO TA (Invitrogen Life Technologies, Carlsbad, CA). Primers used include (deleted regions are marked [x]): EpCAM-full-F 5'- GCC ACC ATG GCG CCC CCG CAG GTC CTC -3', EpCAM-full-R 5'- TGC ATT GAG TTC CCT AT -3', EpCAM-Top-iFLAG-F 5'- T GCC GCA GCT GAT TAC AAG GAT GAC GAC GAT AAG CAG GAA GAA TGT GTC -3', EpCAM-Bot-iFLAG-R 5'- CA TTC TTC CTG CTT ATC GTC GTC ATC CTT GTA ATC AGC TGC GGC AAA AGT CG -3', EpCAM-53-77-F 5'- T GGT GCA CAA [x] GGC TCA AAA CTT GGG AGA AGA GCA AAA CC -3', EpCAM-53-77-R 5'- G TTT TGA GCC [x] TTG TGC ACC AAC TGA AGT ACA CTG GC -3', EpCAM-53-58-F 5'- T GGT GCA CAA [x] AAG CTG GCT GCC AAA TG -3', EpCAM-53-58-R 5'- C AGC CAG CTT [x] TTG TGC ACC AAC TGA AGT ACA C -3', EpCAM-59-65-F 5'- C ATT TGC TCA [x] GTG ATG AAG GCA GAA ATG AAT GGC TC -3', EpCAM-59-65-R 5'- C CTT CAT CAC [x] TGA GCA AAT GAC AGT ATT TTG TGC ACC -3', EpCAM-66-72-F 5'- C AAA TGT TTG [x] GGC TCA AAA CTT GGG AGA AGA GCA AAA CC -3', EpCAM-66-72-R 5'- G TTT TGA GCC [x] CAA ACA TTT GGC AGC CAG CTT TGA GC -3', EpMUT-RR-AA-F 5'- GGC TCA AAA CTT GGG GCA GCA GCA AAA CCT GAA GGG GC -3', EpMUT-RR-AA-R 5'- GCC CCT TCA GGT TTT GCT GCT GCC CCA AGT TTT GAG CC -3'.

3.3.5 Immunofluorescence

The cells were seeded on 35 mm glass bottom plates (MatTek Corp., P35G-1.5-10-C, Ashland, MA, USA) and grown in culture media for 48 hours. The cells were washed twice with PBS, fixed with ice-cold acetone for 15 min, and washed in PBS for five minutes three times. Non-specific binding of the antibodies was blocked by universal blocking solution (Biogenex, San Ramon, CA) for 30 min at room temperature and the cells were incubated with a mixture of specific antibodies for FLAG-tag (1:250) (Rockland, 600-401-383) and V5-tag (1:250) (AbD Serotech, MCA1360GA) overnight at 4°C. The cells were washed with PBS containing 0.1% Tween 20 (PBS-T) for five minutes three times and incubated with secondary antibodies goat anti-mouse TRITC conjugate (1:250) (Southern Biotech, 1032-03) and goat anti-rabbit Alexa Fluor 488 (1:300) (Invitrogen, A11008) for one hour covered at room temperature. The nucleuses were counter-stained with 0.5 mg/mL of DAPI for two minutes and then washed for five minutes with PBST three times. The slides were mounted with a few drops of an aqueous mounting medium after the excess PBST was decanted. A fluorescence microscope was used to detect protein expression of (Nikon, Eclipse E600, Melville, NY, USA). QCapure software version 2.66.4 was used to capture tif images at a 400x magnification.

3.3.6 Western Blot

Cells lysates were isolated in RIPA buffer (50 mM Tris-HCl pH 7.4, 150 mM NaCl, 1 mM EDTA, 1% Triton X-100, 1% sodium deoxycholate, 0.1% SDS)

supplemented with protease inhibitors (1mM PMSF, 1 µg/mL aprotinin, 1 µg/mL leupeptin) and phosphatase inhibitors (10 mM NaF, 0.1 mM Na_3VO_4,). Protein concentration was determined by BCA protein assay (Pierce, Rockford, IL). The proteins were separated on SDS–PAGE and transferred to nitrocellulose membranes (Osmonics, Minnetonka, MN). The membranes were incubated in primary antibody diluted in 5% milk made with TBS-T at 4°C overnight. The antibodies used in this study include: anti-EpCAM (CBL251, Chemicon International/Millipore, Billerica, MA); anti-Actin (sc-1615), anti-EpCAM (sc-51681), and anti-V5 from Santa Cruz Biotechnology Inc. (Santa Cruz, CA); anti-NAG-1 which was generated previously [134]; anti-β-catenin (BD Biosciences, San Jose, CA); anti-FLAG (600-401-383, Rockland Immunochemicals Inc., Gilbertsville, PA), anti-Cyclin D1(#2978S), anti-E-cadherin (#3195S) from Cell Signaling Technology (Danvers, MA). After three washes with tris buffered saline containing 0.05% Tween 20, the blots were incubated with peroxidase-conjugated IgG for one hour at room temperature and visualized using ECL (Amersham Biosciences, Piscataway, NJ) and a LAS-4000 mini (Fujifilm Life Sciences, Stamford, CT).

3.3.7 3-D Spheroid Cell Invasion Assay

HCT-116 stable cells, EpCAM wt and EpCAM mut, were seeded into round bottom 96 well plates at 3,000 cells per well in 50 µl of 1x spheroid formation ECM medium following the manufacture's protocol (Cultrex, 96 Well 3D Spheroid BME Cell Invasion ASsay, 3500-096-K). Two of the treatment samples had 30 µM SS added to the 1x spheroid formation ECM medium at the time of plating as well as after formation

of the invasion matrix and two treatment samples only had 30 µM SS treatment added to the growth medium beginning after setting up the invasion matrix. The cells were allowed 72 hours for spheroid formation, then the invasion matrix was formed according the Cultrex's protocol. Following invasion matrix formation, medium containing 5 µM EGF or vehicle and 30 µM SS or vehicle was added to the top and spheroids where observed for 10 days post-invasion matrix and treatment.

3.3.8 Statistics

Unless stated otherwise statistical significance was determined using single-tailed paired Student *t* tests. P-values are noted with asterisks as follows: *P < 0.05, **P < 0.01, and ***P < 0.005.

3.4 Results

3.4.1 NSAIDs alter EpCAM expression.

HCT-116 cells were screened for reduction of EpCAM protein by various NSAIDs including: SS, diclofenac (Diclo.), aspirin (Asp.), TA, and 5,5-dimethyl-3-(3-fluorophenyl)-4-(4-methylsulphonyl)phenyl-2(5H)-furanone) (DFU) (Fig. 3.1A). SS and TA both showed marked reduction in EpCAM protein expression (Fig. 3.1A). SS was selected for further study due to its more dramatic effect. HCT-116 cells showed both a time and dose dependent loss of EpCAM expression from SS treatment (Fig. 3.1B and

C). Several other cell lines including the human colorectal cancer cell lines HT-29, LoVo, and SW480, the human lung carcinoma cell line A549, and the human hepatocellular carcinoma cell line HepG2 were screened for EpCAM reduction by SS (Fig. 3.1D). All cell lines which had detectable EpCAM expression except A549 cells showed reduction of EpCAM by SS (Fig. 3.1D). Interestingly, SS treatment at the levels used here did not decrease EpCAM expression in SW480 cells, which we have observed to be more resistant to SS treatment and require higher concentrations of SS to produce a similar response (data not shown).

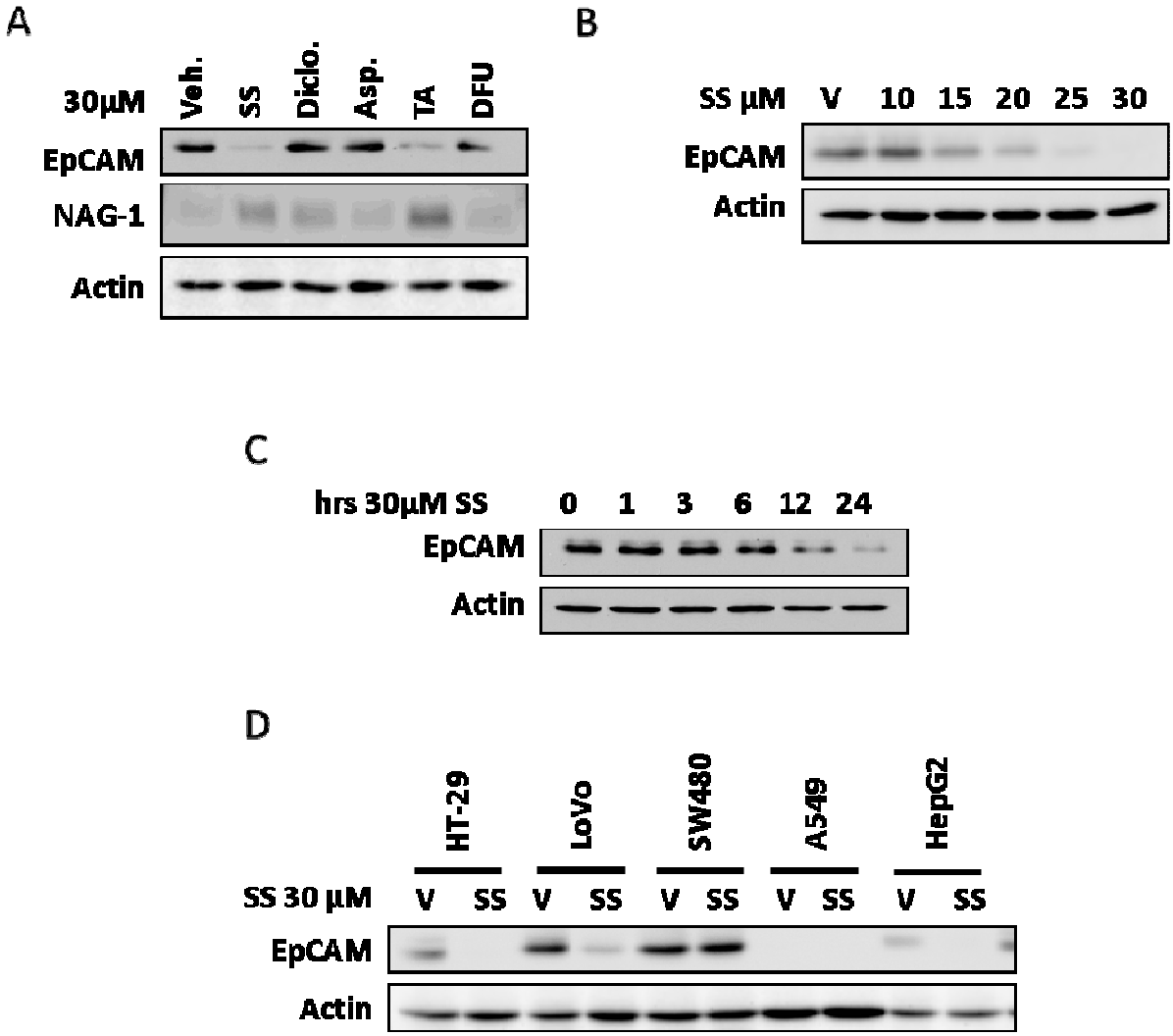

Figure 3.1 NSAIDs effect EpCAM protein expression.

(A) Western blot screen of HCT-116 cells with NSAIDs (30 µM: sulindac sulfide, diclofenac, aspirin, tolfenamic acid, and 5,5-dimethyl-3-(3-fluorophenyl)-4-(4-methylsulphonyl)phenyl-2(5H)-furanone) for effects on EpCAM protein expression. NAG-1 is shown as a positive control. (B) Western blot of EpCAM protein expression in HCT-116 cells treated with sulindac sulfide in incrementally increasing doses. (C) Western blot of EpCAM protein time course with 30 µM sulindac sulfide treatment. (D) Western blot of EpCAM protein expression under 30 µM sulindac sulfide treatment in various cell lines. Actin protein expression is shown as loading controls.

3.4.2 SS affects EpCAM expression independent of transcriptional regulation, kinase activity, or proteasomal degradation pathway.

EpCAM mRNA expression was measured by reverse-transcriptase PCR under various SS doses, all of which demonstrated no significant effect of SS treatment on EpCAM mRNA expression (Fig. 3.2A). Next, inhibitors for various kinase pathways including CKII, EGFR, JAK2, GSK-3, MEK/ERK, PI3K, JNK, PKC, p38 MAPK, and mTOR were screened for rescue of EpCAM expression in the presence of SS (Fig. 3.2B). None of these were able to restore EpCAM to vehicle levels, though a few including PI3K, JNK, and PKC showed a very slight increase in EpCAM compared to SS without kinase inhibitor pretreatment (Fig. 3.2B). Then the possibility of SS action on EpCAM through proteasomal degradation pathways was explored with several inhibitors. HCT-116 cells were pretreated with Ada-vinyl sulphone, lactacycine, epoxomicin, MG132, and YU102; however, none of these were able to even partially protect EpCAM from loss by SS treatment (Fig. 3.2C). These results indicate that SS-mediated EpCAM down-regulation is not mediated by transcription regulation, kinase pathways, or proteasomal degradation pathways.

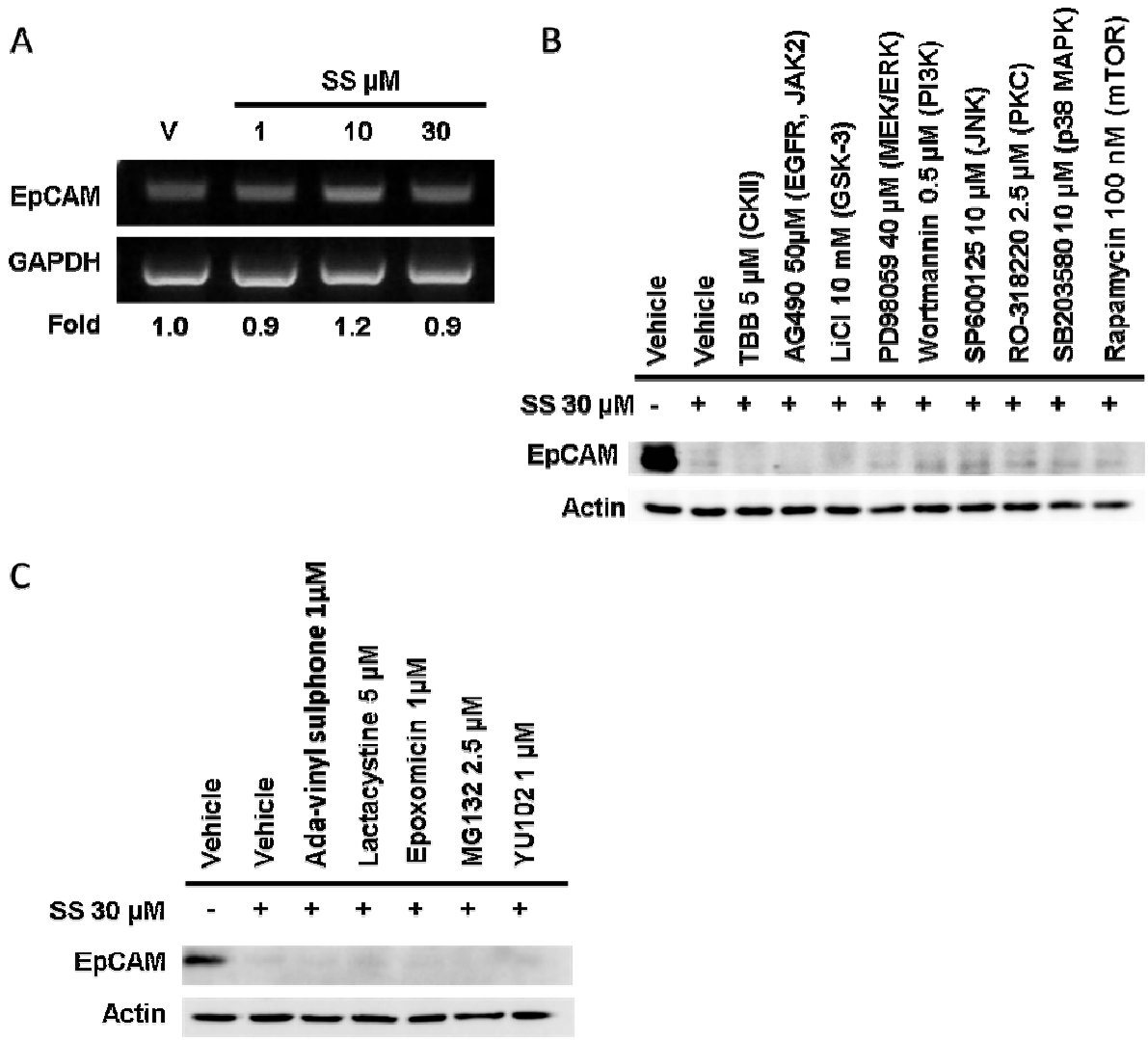

Figure 3.2 SS effects EpCAM protein expression in a manor independent of transcriptional regulation, kinase activity, or proteasomal degradation.

(A) Sulindac sulfide's effect on EpCAM mRNA expression visualized by reverse transcriptase polymerase chain reaction in HCT-116 cells. Densitometric fold change relative to vehicle is shown below the gel pictures. (B) Western blot screen of various kinase inhibitors for rescue of EpCAM protein expression under 30 µM sulindac sulfide treatment (4,5,6,7-tetrabromobenzotriazol 5 µ, AG490 50 µM, lithium chloride 10 mM, PD98059 40 µM, Wortmannin 0.5 µM, SP600125 10 µM, RP-318220 2.5 µM, SB203580 10 µM). (C) Western blot screen of proteasomal degradation inhibitors for rescue of EpCAM protein expression under 30 µM sulindac sulfide treatment (adavinyl sulphone 1 µM, lactacystine 5 µM, Epoxomicin 1 µM, MG132 2.5 µ, and YU102 1 µM).

3.4.3 SS facilitates a specific cleavage of EpCAM at the N-terminal region.

In order to investigate how SS reduces EpCAM expression, full-length EpCAM was cloned into pcDNA3.1 V5/His/TOPO/TA vector. This provided C-terminal V5 and polyhistidine tags. Subsequently, we used site-directed mutagenesis to insert FLAG tag at the N-terminal region of EpCAM, right after the signal peptide to prevent the tag from being cleaved with the signal peptide during processing (Fig. 3.3A). After transfecting into HCT-116 cells, the FLAG tag expression pattern under SS treatment is similar to what we observed with the endogenous EpCAM. Interestingly, when we probed with V5 tag, we observed a specific extra EpCAM band that is smaller than full size and not visible with either FLAG antibody or endogenous EpCAM antibody (Fig. 3.3B). This band will be referred to as a truncated EpCAM (EpTCAM). EpTCAM is induced by SS treatment while full length EpCAM is reduced by SS treatment and total EpCAM expression (full length EpCAM and EpTCAM together) is fairly constant under SS treatment (Fig. 3.3B).

To further investigate the role of EpCAM in cancer cells a stable EpCAM-iFLAG-V5/His cell line was developed in HCT-116 cells. Immunofluorescence staining was performed to test this cell line for proper membrane localization. The data exhibited a strong overlap of FLAG and V5 signal along the cell membrane, suggesting that full length tagged EpCAM is expressed in cell membrane where the majority of it should be (Fig. 3.3C). There are portions of the cytoplasm where V5 staining (red) can be seen in the absence of FLAG (green) staining; this could indicate the presence of the small cleaved EpICD previously reported [155].

Next, we further analyzed these EpCAM over-expression cells. The conversion of full length EpCAM to EpTCAM by SS occurs in a dose and time dependent manner (Fig. 3.3D & Fig. 3.3E). Proteasomal degradation inhibitors were tested again; this time to observe the SS's effect on EpTCAM. As shown in Fig. 3.3F, EpTCAM expression is affected by SS and further stabilized EpTCAM in the presence of proteasomal inhibitors. Finally we confirmed that EpTCAM is affected by proteasomal degradation pathways, as evidence that cycloheximide treatment increases EpTCAM expression in the presence of SS (Fig. 3.3G).

Figure 3.3 Exploring SS/EpCAM interaction through generation of a multi-tagged expression vector.

(A) Diagram showing locations of tags on the EpCAM-iFLAG/V5-His expression vector relative to previously reported EpCAM protein features. Location of EpCAM (VU-1D9) antibody is marked on the diagram. (B) Western blot data showing FLAG, V5, and actin antibodies blotted against HCT-116 cells transiently transfected with LacZ control vector or EpCAM-iFLAG/V5-His vector. A protein ladder is included on the left and arrows indicated various protein forms present. (C) Immunofluorescence staining of HCT-116 cells stable transfected with EpCAM-iFLAG-V5/His construct. The nuclei are stained blue in the DAPI panel, EpCAM is green in the FLAG panel, and EpCAM is red in the V5 panel. Merged panel shows overlapping FLAG and V5 as yellow. (D-G) Western blots of HCT-116 cells stable transfected with EpCAM-iFLAG-V5/His. (D) Cells treated with incrementally increasing doses of SS for 24 hours and blotted for V5 tagged EpCAM. (E) Time course of cells treated with 30 µM SS for increasing amounts of time and blotted for V5 tagged EpCAM. (F) Cells pretreated with proteasomal degradation inhibitors 5 µM lactacystin, 2.5 µM MG132, and 1 µM YU-102, than treated with 30 µM SS for 24 hours. Cells pretreated with 20 µM SS for 9 hours than co-treated with a cycloheximide time course and stained for FLAG tagged EpCAM, V5 tagged EpCAM, β-catenin, and cyclin D1.

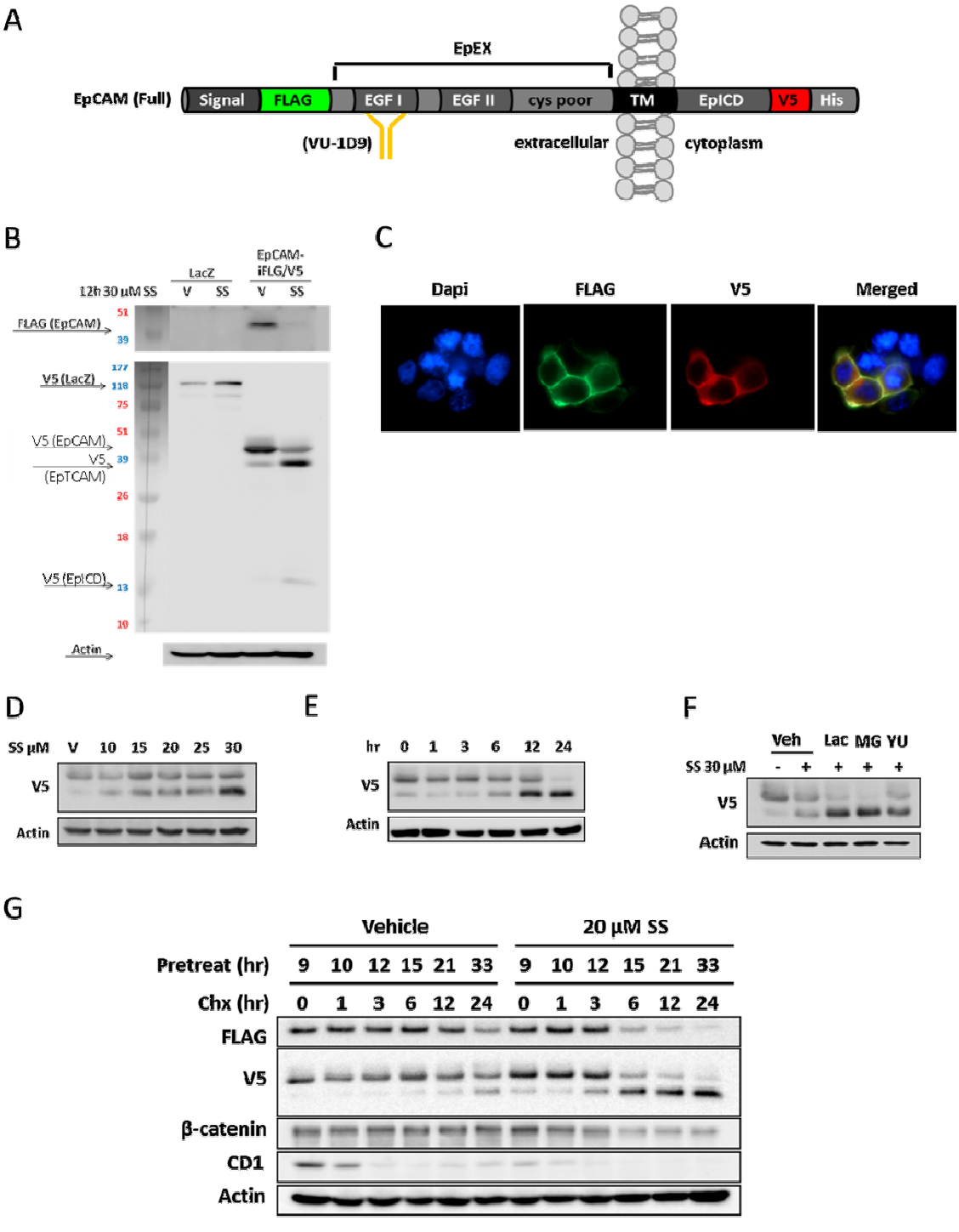

Figure 3.3 Continued.

3.4.4 Determination of SS cleavage site in the EpCAM protein

To examine which region of EpCAM is affected by SS, we generated several deletion constructs based on our full-length FLAG and V5 tagged EpCAM clone (Fig. 3.4A). First, we deleted the region ranging from amino acids 55 to 81. Then we divided this region up into four smaller segments of 6-8 amino acids and made a deletion construct for each of these (Fig. 3.4A). All of these constructs were transfected into HCT-116 cells and the production of EpTCAM in the presence of SS was examined. As shown in Fig. 3.4B, none of the deletion clones produced truncated forms, indicating the importance of this entire region (55 to 81) in the production of the truncated form.

Next, we examined EpCAM expression by SDS-PAGE gel under non-reducing conditions. As shown in Fig. 3.4C, we could not find the truncated EpCAM form with V5 antibody under non-reducing conditions. These results along with previously reported structural data indicate that EpCAM has a well-developed tertiary structure including six highly conserved di-sulfide bonds in the extracellular domain [157]. A diagram showing this structure can be seen in Fig. 3.4C.

3.4.5 Mutation of the suspected EpCAM cleavage site influenced by SS.

Recently a study by Schnell et al. observed many truncated forms of EpCAM including one which appears to be the same size as our SS-induced truncation [156]. Therefore, we made point mutations changing this Arg80/Arg81 cleavage site to Ala80/Ala81. This construct does not produce truncated EpCAM when transfected into HCT-116 cells with or without SS treatment (Fig. 3.5A). In addition, this mutant clone

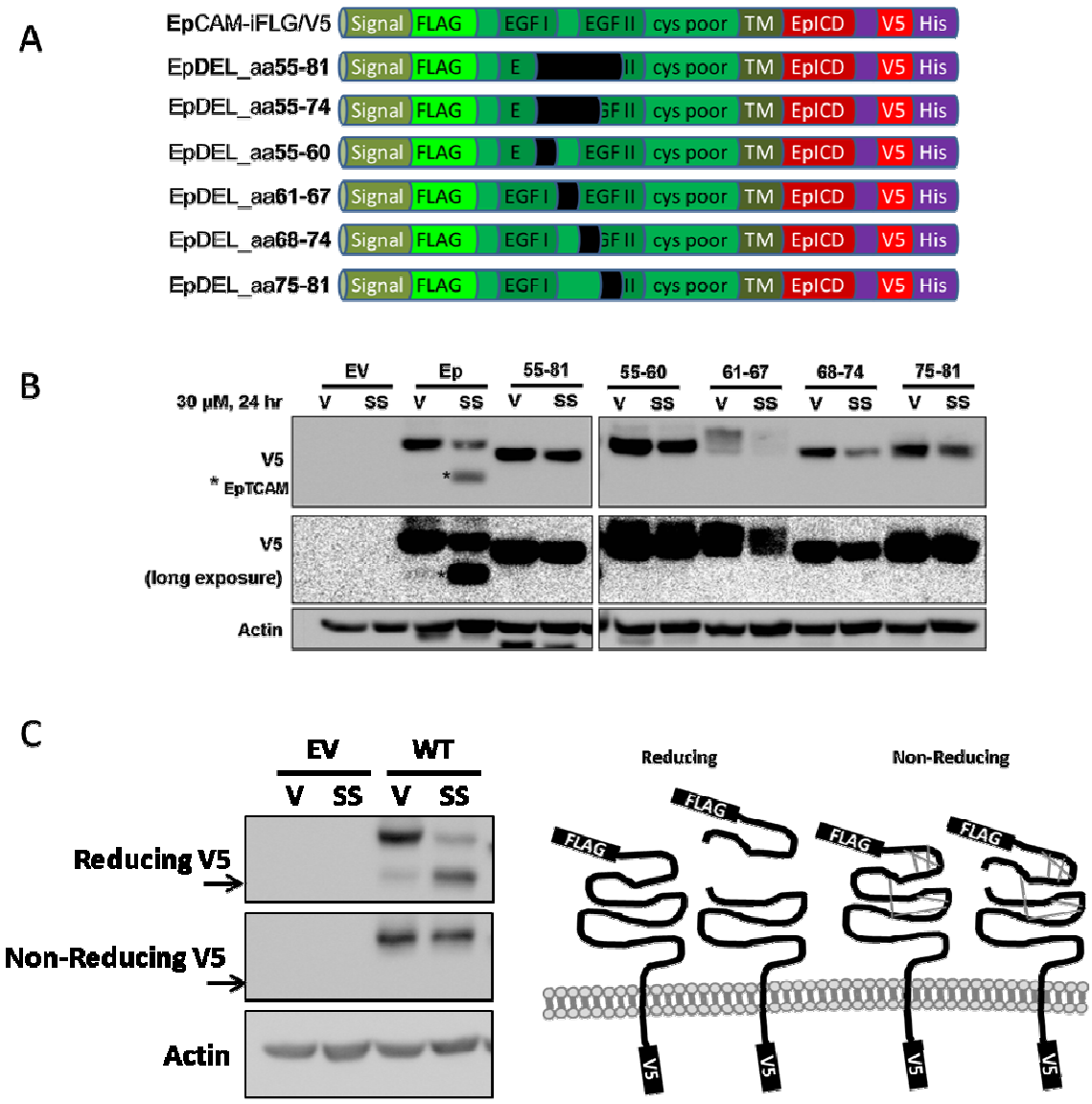

Figure 3.4 Deletions to explore potential SS related cleavage sites on EpCAM.

(A) Diagram showing the regions of EpCAM-iFLAG-V5/His construct deleted in black. (B) Western blot of HCT-116 cells transiently transfected with EpCAM deletion constructs, treated with 30 µM SS and blotted for V5 tagged EpCAM. (C) Reducing conditions shows EpCAM without disulfide bonds while the non-reducing conditions shows the disulfide bonds intact. Western blot of HCT-116 cells stable transfected with empty vector and EpCAM-iFLAG-V5/His treated with 30 µM SS and ran under reducing (normal) or non-reducing conditions. Arrows indicate the correct size for EpTCAM.

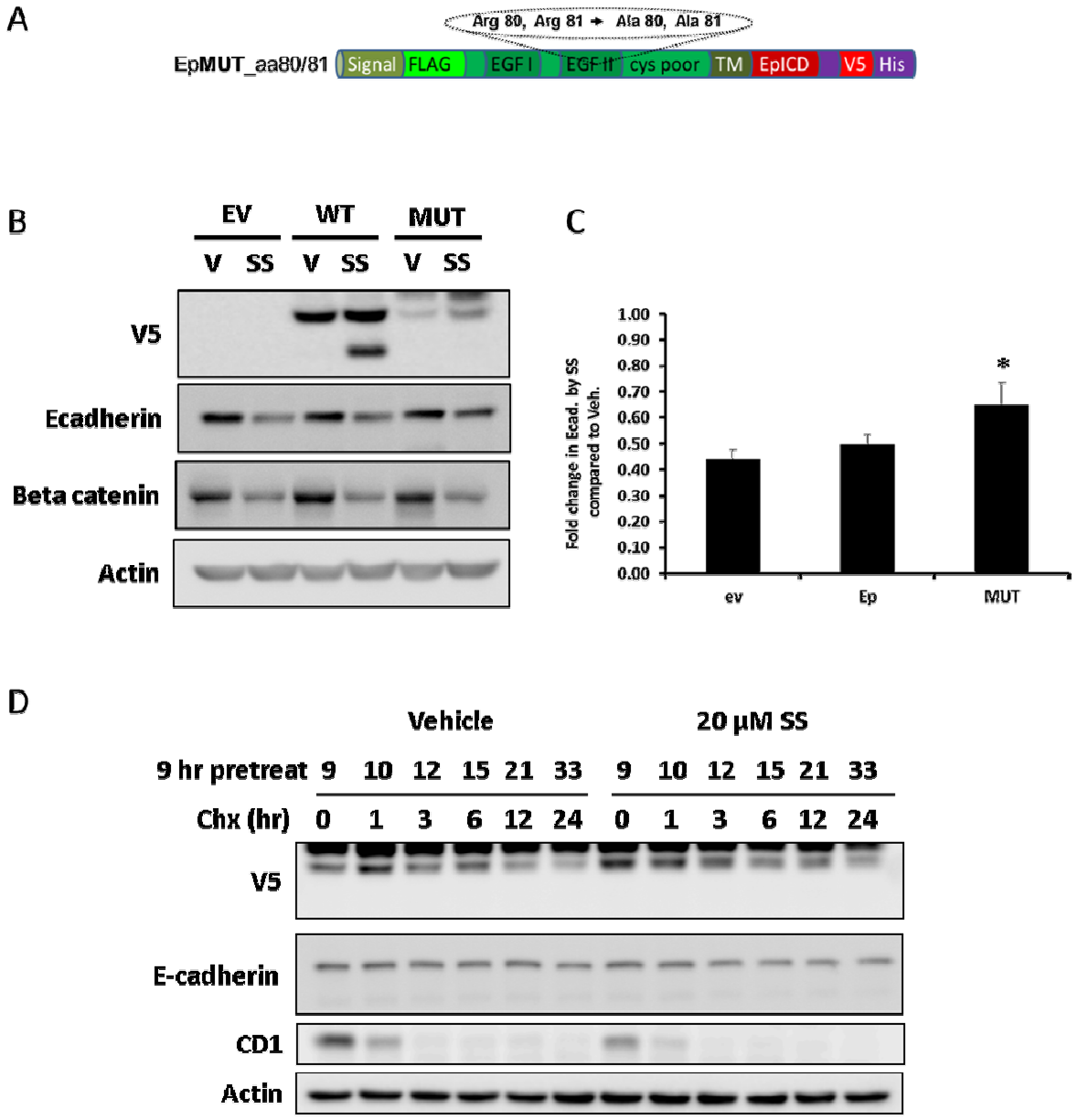

Figure 3.5 Mutation of the suspected EpCAM cleavage site influenced by SS.

(A) Diagram of EpCAM protein structure showing cleave site between arginine residues at amino acids 80/81 (shown by doted circle). (B) Western blot of HCT-116 cells transiently transfected with empty vector, EpCAM-iFLAG-V5/His, or EpMUT-A80A81 and treated with 30 µM SS for 24 hours. (C) Chart shows fold change in E-cadherin by SS compared to vehicle for three experiments. (D) Western blot of wild-type EpCAM stable HCT-116 cells pre-treated with SS prior to cycloheximide time course.

seems to slightly protect E-cadherin protein expression from down-regulation in the presence of SS. This result suggests that EpCAM plays a role in invasion activity and the cleavage of this site (80/81).

3.4.6 Biological activity of EpCAM-iFLAG/V5-His (WT) and EpMUT-A80A81 under SS treatment.

It has been reported that EpCAM is linked to invasion and proliferation [158]. SS inhibits these biological activities. Therefore, we tested to determine if mutant clone (EpMUT-A80/A81) exhibits less sensitivity to SS. Cell proliferation MTS assay was performed using three stability transfected HCT-116 cell lines expressing empty vector, wild-type EpCAM, or mutated EpMUT-A80/A81 (Fig. 3.6A). The wild-type EpCAM over-expressing cells showed significantly more grow then either empty vector or mutant EpCAM cells (Fig. 3.6A) which is consistent with previous MTS assay data performed previous to developing the mutant cell line (data not shown). The mutant cell line showed significantly more sensitivity to SS treatment than the either wild-type EpCAM or empty vector (Fig. 3.6A).

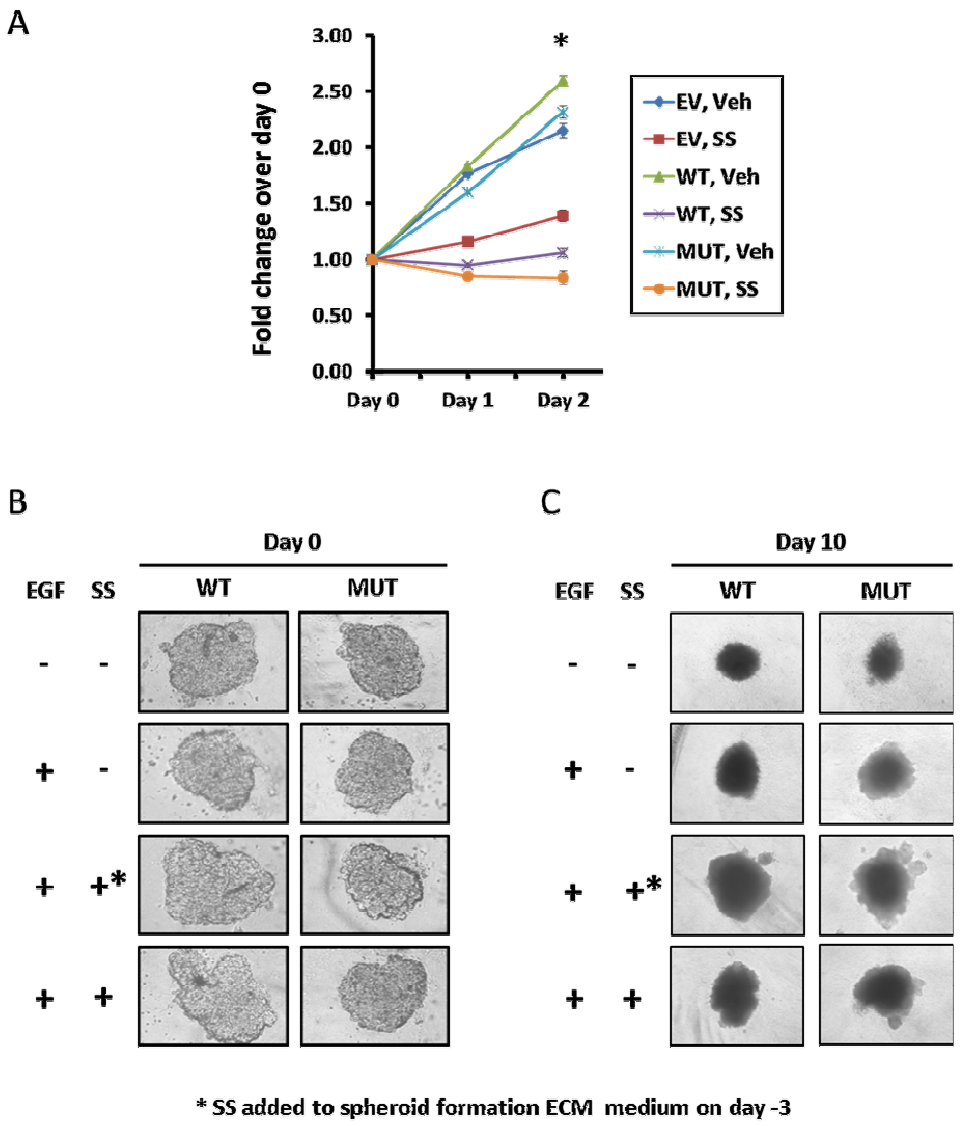

Figure 3.6 Biological activity of EpMUT-A80A81 stable cell line.

Biological activity of HCT-116 cells stable transfected with empty vector (EV), EpCAM-iFLAG/V5-His (WT), or EpMUT-A80A81(MUT) under SS treatment. (A) Cell proliferation assay, 3-(4,5-dimethylthiazol-2-yl)-5-(3-carboxymethoxyphenyl)-2-(4-sulfophenyl)-2H-tetrazolium (MTS), shown as fold change over day 0. The cells were treated with 30 µM SS in medium containing 1% serum. 3-D spherical invasion assay comparing WT cells and MUT cells (B and C). (B) Comparison of spheroids after forming for 72 hours on treatment day 0. (C) SS treatment day 10 after the addition of basement membrane invasion matrix. Please note that different microscopes, cameras, and fields of view were used in (B) and (C) so spheroid size is not comparable between these figures.

We used a 3-D spheroid invasion assay to observe these stabile cell lines under more physiologically relevant conditions. The cells where grown for 72 hours to form the spheroids prior to adding the basement membrane matrix and treatments. The Fig. 3.6B shows that the spheroids were of comparable size and shape 72 hours after plating on treatment day zero. Neither the wild-type EpCAM or the mutant EpCAM cell lines produced spindle-like projections in the invasion matrix with or without epidermal growth factor (EGF) (Fig. 3.6C).

3.5 Discussion

EpCAM is a membrane protein and plays an important role in tumorigenesis [159]. EpCAM contributes to non-canonical β-catenin pathway by releasing ICD bound to β-catenin via FLH2 which can translocate to the nucleus and activate Wnt target genes [154, 155]. This is confirmed by using EpCAM KO mice exhibiting congenital tufting enteropathy, indicating that EpCAM/β-catenin plays a role in the maintenance of intestinal architecture and functionality [160, 161]. Recent data also suggests that EpCAM modulates NF-κB activity, thereby increasing invasion activity in breast cancer [162], and increases cyclin D1 expression to facilitate cell growth activity [144]. Thus, EpCAM plays a pivotal role in tumorigenesis in addition to the role of EpCAM in embryonic stem cells.

NSAIDs have been used for the treatment of inflammation as well as cancer. Among those, SS exhibits a distinctive role in anti-cancer activity. SS is the preferred NSAIDs to suppress polyps in familial adenomatous polyposis (FAP) patients and in animal models. Mechanistically, SS has been shown to suppress TGF-β induced motility of A549 lung adenocarcinoma cells through blocking Akt phosphorylation [163] and increasing tumor suppressor NAG-1 in colorectal cancers [16, 27, 164]. In this study, SS was selected for further study based on its EpCAM down-regulation compared to the other NSAIDs tested and its history in chemotherapy and chemoprevention (Fig. 3.1A). The migraine headache medicine TA was another interesting NSAID which reduced EpCAM protein expression in a dose-dependent manor (data not shown). It has been reported that TA exhibits anti-cancer activity in many ways, including induction of apoptotic genes EGR-1, NAG-1, and ATF3 [165, 166], inhibition of the TGF-β pathway [58] and NF-κB signaling [167], and inhibition of Sp transcription factors [45, 168].

EpCAM mRNA is unaffected by SS treatment (Fig. 3.2A) and inhibition of proteasomal degradation fails to restore full length EpCAM protein expression (Fig. 3.2C). Studying SS's effect on tagged EpCAM allowed us to realize that SS does not actually down-regulate EpCAM protein expression, but instead SS facilitates cleavage of EpCAM (Fig. 3.3). When EpCAM protein is visualized by western blot using either the EpCAM (VU-1D9) antibody or the N-terminal FLAG tag antibody (Fig. 3.3A) it appears that SS decreases total EpCAM protein expression. However, upon examination of the C-terminal V5 tag on EpCAM it becomes clear that EpCAM protein is still present, but

has had a portion of its N-terminal region cleaved leaving the EpTCAM cleavage form (Fig. 3.3B). SS drives a shift in the ratio of EpCAM expression from full length EpCAM to a shorter cleaved form (EpTCAM), but the overall expression level of full length EpCAM and EpTCAM together is not significantly changed.

In order to better understand SS's action on EpCAM we needed to narrow down the cut site. Based on software which can estimate protein sized from western blot data relative to a known standard, we predicted that EpTCAM is 37 kDa. This would put the cleavage site near the region between the two EGF-like domains on the extracellular portion of EpCAM. We generated deletion constructs from our EpCAM-iFLAG-V5/His plasmid to narrow down the region involved. Two large deletions were generated deleting EpCAM amino acids 55-81 and 55-74, as well as four smaller 6-7 amino acid deletions which break the 55-81 amino acid deletion up into four parts (Fig. 3.4A). Each of these deletion clones blocked the generation of EpTCAM (Fig. 3.4B). This region could be structurally important for correctly positioning EpCAM for SS driven cleavage.

The large 55-81 amino acid deletion clone as well as the small 75-81 amino acid deletion clone both remove a known EpCAM cleavage site which is not well studied. EpCAM has been shown to undergo a cleavage event between arginine 80 and arginine 81 [169]. EpCAM has 12 highly conserved cysteine residues forming disulfide bonds on the extracellular region of EpCAM (Fig. 3.4C). It has been previously shown that under non-reducing conditions these disulfide bonds will hold the cleaved 1-80 amino acid portion of EpCAM in place in several cancer cell lines including: colorectal, skin, and liver [169]. This shows that this cleavage form is not unique to HCT-116 cells. Under

normal reducing western blot conditions these disulfide bonds are broken and the cleaved 1-80 amino acid portion of EpCAM is lost. To test whether this 80/81 amino acid site might be the same site cleaved under SS treatment we ran the same EpCAM-iFLAG/V5-His lysates treated with either vehicle or SS in both normal reducing conditions as well as non-reducing conditions to see if non-reducing conditions would eliminate the EpTCAM cleavage form (Fig. 3.4C). Non-reducing conditions showed only the full-length form of EpCAM suggesting that the cleaved region is being held in place by disulfide bonds under non-reducing conditions. To confirm that this is in fact the SS cleavage site, we generated a mutation construct where arginine 80 and arginine 81 are changed to alanine 80 and alanine 81 (Fig. 3.5A, dotted circle). This point mutation did block generation of the cleaved EpCAM form by SS (Fig. 3.5C). This led to our next significant revelation in understanding SS action on EpCAM, that under physiological conditions the portion of EpCAM which SS drives cleavage of is not released from the protein, but remains tethered by a disulfide bond which complicates the study of this system. It would be ideal to overexpress the truncated EpTCAM form to better study its biological activity or lack of activity as the case may be, however, an artificial construct of 80/81 amino acid cleaved EpCAM would lack the 56 amino acid long region of EpCAM anchored by the cysteine bond which could have profound effects on its activity.

While the 3D spheroid invasion assay did not demonstrate the typical spindle-like projections of cells invading from the spheroid into through the basement membrane matrix, there were clear morphological differences between the wild-type EpCAM cell

line and the mutant EpCAM cell line (Fig. 3.6). The mutant cell line showed invasive-like growth out from the spheroids while the wild-type cells stayed in much tighter spheroid shapes. Curiously, these invasive-like features seemed to be more prominent under SS treatment. Observing more invasive properties from the mutant cells than the wild-type cells would have made sence if the wild-type cells had shown invasion with EGF treatment in the absence of SS. It is possible that HCT-116 cells simply are not invasive enough for this assay as they have been previously shown to not be invasive in other 3D spheroid models [170]. Spheroids still represent an improved *in vitro* method of observing treatment effects on cancer cells by mimicking many of the conditions seen *in vivo* such as formation of cell-cell bonds, hypoxic cores, and increased cell survival [171-173].

The Arg80/81 cleavage of EpCAM can be observed in HCT-116 cells without SS treatment and has been observed in several cancer cell lines. In the absence of protein synthesis EpCAM naturally shifts from full-length form to cleaved form over time and this shift is greatly speed up by the addition of SS treatment (Fig. 3.3G). SS driven proteolysis of EpCAM could decrease EpCAM protein stability.

3.6 Conclusion

EpCAM is a complicated protein with many cleavage forms and the potential for many biological outcomes. It has been implicated in both positive and negative roles in many cancer types depending on the stage and context of its expression. Initially this study suggested that SS down-regulated EpCAM protein expression in a manner that is

independent of: COX activity, transcription, de novo protein synthesis, and proteasomal degradation. Further analysis using EpCAM, which carries an N-terminal FLAG tag and a C-terminal V5 tag, revealed that this is not exactly the case. SS is acting on EpCAM in a manner independent of the above mentioned pathways; however, EpCAM protein expression is not down-regulated. Instead SS facilitates a poorly understood cleavage of EpCAM between arginine residues 80 and 81. Mutation of these residues resulted in the loss of EpCAM with a truncation at 80/81. Also, deletion of this site and the neighboring region resulted in a loss of truncated EpCAM. The realization that SS is driving EpCAM arginine 80/81 cleavage also brought the revelation that under physiological conditions the truncated portion of EpCAM is still tethered to the membrane-bound EpCAM by disulfide bonds bridging highly conserved cysteine residues. We have discovered a novel COX-independent mechanism of action for NSAIDs. SS facilitates cleavage of EpCAMs 80/81 amino acid site.

CONCLUSION

NSAIDs interact with many pathways in cancer cells. There are many promising cyclooxygenase-independent mechanisms utilized by NSAIDs which provide potential avenues for developing new and better drugs that minimize or eliminate the undesirable side effects of cyclooxygenase inhibition such as gastric bleeding and cardiovascular risks. NSAIDs up-regulate a number of transcription factors such as the tumor suppressors EGR-1, ATF3, and CHOP, and down-regulate oncogenic transcription factors Sp1 and β-catenin.

This study demonstrates that multiple Nesprin-2 isoforms are down-regulated by SS and Nesprin-α2 is confirmed at the protein level. Knock-down of Nesprin-2 reduced cell-cell and cell-substrate adhesion as well as reducing plasma membrane potential in human CRC cells. Immunostaining of Nesprin-2 in human normal vs tumor tissues showed higher and more frequent staining in tumor tissue compared to normal in many tissue types.

Next we demonstrated that SS modulates the adhesion protein EpCAM at the post-translational level. Mutation of EpCAM amino acids 80 and 81 from arginine to alanine blocks truncation by SS demonstrating that this is the specific cut site. Deletion of the 55-81 amino acid region of EpCAM disrupts the tertiary protein structure and blocks SS-driven cleavage of the EpCAM 80/81 site. Thus, Nesrpin-2 represents a novel NSAID target and potential cancer-associated protein and EpCAM cleavage demonstrates a unique COX-independent NSAID mechanism of action.

REFERENCES

[1] J. Ferlay, H.R. Shin, F. Bray, D. Forman, C. Mathers, D.M. Parkin, Estimates of worldwide burden of cancer in 2008: GLOBOCAN 2008, Int J Cancer, 127 (2010) 2893-2917.
[2] A. Jemal, F. Bray, M.M. Center, J. Ferlay, E. Ward, D. Forman, Global cancer statistics, CA: a cancer journal for clinicians, 61 (2011) 69-90.
[3] W.L. Smith, Localization of enzymes responsible for prostaglandin formation, Handbook of Eicosanoids: Prostaglandins and Related Lipids, (1987) 175-184.
[4] W.L. Smith, D.L. DeWitt, R.M. Garavito, Cyclooxygenases: structural, cellular, and molecular biology, Annual review of biochemistry, 69 (2000) 145-182.
[5] H.R. Herschman, Prostaglandin synthase 2, Biochimica et biophysica acta, 1299 (1996) 125.
[6] T. Tanabe, N. Tohnai, Cyclooxygenase isozymes and their gene structures and expression, Prostaglandins & other lipid mediators, 68 (2002) 95-114.
[7] M. Khan, A. Fraser, Cox-2 inhibitors and the risk of cardiovascular thrombotic events, (2012).
[8] I. Bjarnason, Gastrointestinal safety of NSAIDs and over-the-counter analgesics, International journal of clinical practice. Supplement, (2013) 37-42.
[9] S.D. Solomon, J.J. McMurray, M.A. Pfeffer, J. Wittes, R. Fowler, P. Finn, W.F. Anderson, A. Zauber, E. Hawk, M. Bertagnolli, Cardiovascular risk associated with celecoxib in a clinical trial for colorectal adenoma prevention, New England journal of medicine, 352 (2005) 1071-1080.
[10] S.D. Solomon, J. Wittes, P.V. Finn, R. Fowler, J. Viner, M.M. Bertagnolli, N. Arber, B. Levin, C.L. Meinert, B. Martin, Cardiovascular Risk of Celecoxib in 6 Randomized Placebo-Controlled Trials The Cross Trial Safety Analysis, Circulation, 117 (2008) 2104-2113.
[11] V.P. Sukhatme, X.M. Cao, L.C. Chang, C.H. Tsai-Morris, D. Stamenkovich, P.C. Ferreira, D.R. Cohen, S.A. Edwards, T.B. Shows, T. Curran, et al., A zinc finger-encoding gene coregulated with c-fos during growth and differentiation, and after cellular depolarization, Cell, 53 (1988) 37-43.
[12] E.S. Silverman, T. Collins, Pathways of Egr-1-mediated gene transcription in vascular biology, The American journal of pathology, 154 (1999) 665.
[13] A. Krones-Herzig, S. Mittal, K. Yule, H. Liang, C. English, R. Urcis, T. Soni, E.D. Adamson, D. Mercola, Early growth response 1 acts as a tumor suppressor in vivo and in vitro via regulation of p53, Cancer research, 65 (2005) 5133-5143.
[14] P. Nair, S. Muthukkumar, S.F. Sells, S.-S. Han, V.P. Sukhatme, V.M. Rangnekar, Early growth response-1-dependent apoptosis is mediated by p53, Journal of biological chemistry, 272 (1997) 20131-20138.
[15] S.J. Baek, J.-S. Kim, S.M. Moore, S.-H. Lee, J. Martinez, T.E. Eling, Cyclooxygenase inhibitors induce the expression of the tumor suppressor gene EGR-1, which results in the up-regulation of NAG-1, an antitumorigenic protein, Molecular pharmacology, 67 (2005) 356-364.
[16] S.J. Baek, J.S. Kim, S.M. Moore, S.H. Lee, J. Martinez, T.E. Eling, Cyclooxygenase inhibitors induce the expression of the tumor suppressor gene EGR-1, which results in the up-regulation of NAG-1, an antitumorigenic protein, Molecular pharmacology, 67 (2005) 356-364.
[17] V. Vaish, H. Piplani, C. Rana, K. Vaiphei, S.N. Sanyal, NSAIDs may regulate EGR-1-mediated induction of reactive oxygen species and non-steroidal anti-inflammatory drug-induced gene (NAG)-1 to initiate intrinsic pathway of apoptosis for the chemoprevention of colorectal cancer, Molecular and cellular biochemistry, (2013).

[18] S.H. Lee, J.H. Bahn, C.K. Choi, N.C. Whitlock, A.E. English, S. Safe, S.J. Baek, ESE-1/EGR-1 pathway plays a role in tolfenamic acid-induced apoptosis in colorectal cancer cells, Molecular cancer therapeutics, 7 (2008) 3739-3750.
[19] T. Virolle, E.D. Adamson, V. Baron, D. Birle, D. Mercola, T. Mustelin, I. de Belle, The Egr-1 transcription factor directly activates PTEN during irradiation-induced signalling, Nature Cell Biology, 3 (2001) 1124-1128.
[20] S.H. Liang, W. Zhang, B.C. McGrath, P. Zhang, D.R. Cavener, PERK (eIF2alpha kinase) is required to activate the stress-activated MAPKs and induce the expression of immediate-early genes upon disruption of ER calcium homoeostasis, The Biochemical journal, 393 (2006) 201-209.
[21] B. Xie, C. Wang, Z. Zheng, B. Song, C. Ma, G. Thiel, M. Li, Egr-1 transactivates Bim gene expression to promote neuronal apoptosis, The Journal of Neuroscience, 31 (2011) 5032-5044.
[22] N.C. Whitlock, J.H. Bahn, S.-H. Lee, T.E. Eling, S.J. Baek, Resveratrol-induced apoptosis is mediated by early growth response-1, Krüppel-like factor 4, and activating transcription factor 3, Cancer Prevention Research, 4 (2011) 116-127.
[23] P.L. Kuo, Y.H. Chen, T.C. Chen, K.H. Shen, Y.L. Hsu, CXCL5/ENA78 increased cell migration and epithelial-to-mesenchymal transition of hormone-independent prostate cancer by early growth response-1/snail signaling pathway, Journal of cellular physiology, 226 (2011) 1224-1231.
[24] D.X. Liu, D. Qian, B. Wang, J.-M. Yang, Z. Lu, p300-dependent ATF5 acetylation is essential for Egr-1 gene activation and cell proliferation and survival, Molecular and cellular biology, 31 (2011) 3906-3916.
[25] A.-M. Schjerning Olsen, E.L. Fosbøl, J. Lindhardsen, C. Andersson, F. Folke, M.B. Nielsen, L. Køber, P.R. Hansen, C. Torp-Pedersen, G.H. Gislason, Cause-Specific Cardiovascular Risk Associated with Nonsteroidal Anti-Inflammatory Drugs among Myocardial Infarction Patients - A Nationwide Study, PLoS ONE, 8 (2013) e54309.
[26] F.G. Bottone, Y. Moon, J.S. Kim, B. Alston-Mills, M. Ishibashi, T.E. Eling, The anti-invasive activity of cyclooxygenase inhibitors is regulated by the transcription factor ATF3 (activating transcription factor 3), Molecular cancer therapeutics, 4 (2005) 693-703.
[27] H. Yang, S.H. Park, H.J. Choi, Y. Moon, The integrated stress response-associated signals modulates intestinal tumor cell growth by NSAID-activated gene 1 (NAG-1/MIC-1/PTGF-beta), Carcinogenesis, 31 (2010) 703-711.
[28] S.H. Lee, J.H. Bahn, N.C. Whitlock, S.J. Baek, Activating transcription factor 2 (ATF2) controls tolfenamic acid-induced ATF3 expression via MAP kinase pathways, Oncogene, 29 (2010) 5182-5192.
[29] S.H. Lee, K.W. Min, X. Zhang, S.J. Baek, 3,3'-Diindolylmethane induces activating transcription factor 3 (ATF3) via ATF4 in human colorectal cancer cells, The Journal of nutritional biochemistry, 24 (2013) 664-671.
[30] F. Fan, S. Jin, S.A. Amundson, T. Tong, W. Fan, H. Zhao, X. Zhu, L. Mazzacurati, X. Li, K.L. Petrik, ATF3 induction following DNA damage is regulated by distinct signaling pathways and over-expression of ATF3 protein suppresses cells growth, Oncogene, 21 (2002) 7488-7496.
[31] C. Yan, D.D. Boyd, ATF3 regulates the stability of p53: a link to cancer, Cell Cycle, 5 (2006) 926-929.

[32] K. Yamaguchi, S.-H. Lee, J.-S. Kim, J. Wimalasena, S. Kitajima, S.J. Baek, Activating transcription factor 3 and early growth response 1 are the novel targets of LY294002 in a phosphatidylinositol 3-kinase–independent pathway, Cancer research, 66 (2006) 2376-2384.
[33] D. Lu, C.D. Wolfgang, T. Hai, Activating transcription factor 3, a stress-inducible gene, suppresses Ras-stimulated tumorigenesis, Journal of biological chemistry, 281 (2006) 10473-10481.
[34] X. Huang, X. Li, B. Guo, KLF6 induces apoptosis in prostate cancer cells through up-regulation of ATF3, Journal of biological chemistry, 283 (2008) 29795-29801.
[35] D. Ron, J.F. Habener, CHOP, a novel developmentally regulated nuclear protein that dimerizes with transcription factors C/EBP and LAP and functions as a dominant-negative inhibitor of gene transcription, Genes & development, 6 (1992) 439-453.
[36] M. White, G. Johnson, W. Zhang, J. Hobrath, G. Piazza, M. Grimaldi, Sulindac sulfide inhibits sarcoendoplasmic reticulum Ca2+ ATPase, induces endoplasmic reticulum stress response, and exerts toxicity in glioma cells: Relevant similarities to and important differences from celecoxib, Journal of neuroscience research, 91 (2013) 393-406.
[37] L.L. Haak, M. Grimaldi, S.S. Smaili, J.T. Russell, Mitochondria regulate Ca2+ wave initiation and inositol trisphosphate signal transduction in oligodendrocyte progenitors, Journal of neurochemistry, 80 (2002) 405-415.
[38] G. Suske, The Sp-family of transcription factors, Gene, 238 (1999) 291-300.
[39] S. Scohy, P. Gabant, T. Van Reeth, V. Hertveldt, P.L. Dreze, P. Van Vooren, M. Riviere, J. Szpirer, C. Szpirer, Identification of KLF13 and KLF14 (SP6), novel members of the SP/XKLF transcription factor family, Genomics, 70 (2000) 93-101.
[40] K. Nakashima, X. Zhou, G. Kunkel, Z. Zhang, J.M. Deng, R.R. Behringer, B. de Crombrugghe, The novel zinc finger-containing transcription factor osterix is required for osteoblast differentiation and bone formation, Cell, 108 (2002) 17-29.
[41] M.A. Milona, J.E. Gough, A.J. Edgar, Genomic structure and cloning of two transcript isoforms of human Sp8, BMC genomics, 5 (2004) 86.
[42] J. Turner, M. Crossley, Mammalian Kruppel-like transcription factors: more than just a pretty finger, Trends in biochemical sciences, 24 (1999) 236-240.
[43] S. Safe, M. Abdelrahim, Sp transcription factor family and its role in cancer, European Journal of Cancer, 41 (2005) 2438-2448.
[44] M. Abdelrahim, C.H. Baker, J.L. Abbruzzese, D. Sheikh-Hamad, S. Liu, S.D. Cho, K. Yoon, S. Safe, Regulation of vascular endothelial growth factor receptor-1 expression by specificity proteins 1, 3, and 4 in pancreatic cancer cells, Cancer research, 67 (2007) 3286-3294.
[45] M. Abdelrahim, C.H. Baker, J.L. Abbruzzese, S. Safe, Tolfenamic acid and pancreatic cancer growth, angiogenesis, and Sp protein degradation, Journal of the National Cancer Institute, 98 (2006) 855-868.
[46] G. Chadalapaka, I. Jutooru, S. Sreevalsan, S. Pathi, K. Kim, C. Chen, L. Crose, C. Linardic, S. Safe, Inhibition of rhabdomyosarcoma cell and tumor growth by targeting specificity protein (Sp) transcription factors, Int J Cancer, 132 (2013) 795-806.
[47] J. Colon, M.R. Basha, R. Madero-Visbal, S. Konduri, C.H. Baker, L.J. Herrera, S. Safe, D. Sheikh-Hamad, A. Abudayyeh, B. Alvarado, M. Abdelrahim, Tolfenamic acid decreases c-Met expression through Sp proteins degradation and inhibits lung cancer cells growth and tumor formation in orthotopic mice, Investigational new drugs, 29 (2011) 41-51.

[48] M. Abdelrahim, S. Safe, Cyclooxygenase-2 inhibitors decrease vascular endothelial growth factor expression in colon cancer cells by enhanced degradation of Sp1 and Sp4 proteins, Molecular pharmacology, 68 (2005) 317-329.
[49] S. Pathi, X. Li, S. Safe, Tolfenamic acid inhibits colon cancer cell and tumor growth and induces degradation of specificity protein (Sp) transcription factors, Molecular carcinogenesis, (2013).
[50] S.S. Pathi, I. Jutooru, G. Chadalapaka, S. Sreevalsan, S. Anand, G.R. Thatcher, S. Safe, GT-094, a NO-NSAID, inhibits colon cancer cell growth by activation of a reactive oxygen species-microRNA-27a: ZBTB10-specificity protein pathway, Molecular Cancer Research, 9 (2011) 195-202.
[51] S. Pathi, I. Jutooru, G. Chadalapaka, V. Nair, S.-O. Lee, S. Safe, Aspirin Inhibits Colon Cancer Cell and Tumor Growth and Downregulates Specificity Protein (Sp) Transcription Factors, PLoS ONE, 7 (2012) e48208.
[52] M. Whitman, Smads and early developmental signaling by the TGFβ superfamily, Genes & development, 12 (1998) 2445-2462.
[53] Y. Shi, J. Massague, Mechanisms of TGF-beta signaling from cell membrane to the nucleus, Cell, 113 (2003) 685-700.
[54] Y. Kang, W. He, S. Tulley, G.P. Gupta, I. Serganova, C.-R. Chen, K. Manova-Todorova, R. Blasberg, W.L. Gerald, J. Massagué, Breast cancer bone metastasis mediated by the Smad tumor suppressor pathway, Proceedings of the National Academy of Sciences of the United States of America, 102 (2005) 13909-13914.
[55] M. Adorno, M. Cordenonsi, M. Montagner, S. Dupont, C. Wong, B. Hann, A. Solari, S. Bobisse, M.B. Rondina, V. Guzzardo, A.R. Parenti, A. Rosato, S. Bicciato, A. Balmain, S. Piccolo, A Mutant-p53/Smad complex opposes p63 to empower TGFbeta-induced metastasis, Cell, 137 (2009) 87-98.
[56] P.J. Koelink, L.J. Hawinkels, E. Wiercinska, C.F. Sier, P. ten Dijke, C.B. Lamers, D.W. Hommes, H.W. Verspaget, 5-Aminosalicylic acid inhibits TGF-beta1 signalling in colorectal cancer cells, Cancer letters, 287 (2010) 82-90.
[57] M.L. Slattery, J.S. Herrick, A. Lundgreen, R.K. Wolff, Genetic variation in the TGF-beta signaling pathway and colon and rectal cancer risk, Cancer epidemiology, biomarkers & prevention : a publication of the American Association for Cancer Research, cosponsored by the American Society of Preventive Oncology, 20 (2011) 57-69.
[58] X. Zhang, K.W. Min, J. Liggett, S.J. Baek, Disruption of the transforming growth factor-beta pathway by tolfenamic acid via the ERK MAP kinase pathway, Carcinogenesis, (2013).
[59] H.A. Pangburn, H. Kraus, D.J. Ahnen, P.L. Rice, Sulindac metabolites inhibit epidermal growth factor receptor activation and expression, Journal of carcinogenesis, 4 (2005) 16.
[60] S. Tavolari, A. Munarini, G. Storci, S. Laufer, P. Chieco, T. Guarnieri, The decrease of cell membrane fluidity by the non-steroidal anti-inflammatory drug Licofelone inhibits epidermal growth factor receptor signalling and triggers apoptosis in HCA-7 colon cancer cells, Cancer letters, 321 (2012) 187-194.
[61] S.M. Brouxhon, S. Kyrkanides, X. Teng, M. Athar, S. Ghazizadeh, M. Simon, M.K. O'Banion, L. Ma, Soluble E-cadherin: a critical oncogene modulating receptor tyrosine kinases, MAPK and PI3K/Akt/mTOR signaling, Oncogene, (2013).

[62] E.J. Greenspan, F.C. Nichols, D.W. Rosenberg, Molecular alterations associated with sulindac-resistant colon tumors in ApcMin/+ mice, Cancer prevention research (Philadelphia, Pa.), 3 (2010) 1187-1197.
[63] T. Kato, H. Fujino, S. Oyama, T. Kawashima, T. Murayama, Indomethacin induces cellular morphological change and migration via epithelial-mesenchymal transition in A549 human lung cancer cells: a novel cyclooxygenase-inhibition-independent effect, Biochemical pharmacology, 82 (2011) 1781-1791.
[64] S. Sribenja, S. Wongkham, C. Wongkham, Q. Yao, C. Chen, Roles and mechanisms of beta-thymosins in cell migration and cancer metastasis: an update, Cancer investigation, 31 (2013) 103-110.
[65] H.-L. Hsiao, W.-S. Wang, P.-M. Chen, Y. Su, Overexpression of thymosin β-4 renders SW480 colon carcinoma cells more resistant to apoptosis triggered by FasL and two topoisomerase II inhibitors via downregulating Fas and upregulating Survivin expression, respectively, Carcinogenesis, 27 (2006) 936-944.
[66] A.K. Jain, S.M. Moore, K. Yamaguchi, T.E. Eling, S.J. Baek, Selective nonsteroidal anti-inflammatory drugs induce thymosin β-4 and alter actin cytoskeletal organization in human colorectal cancer cells, Journal of Pharmacology and Experimental Therapeutics, 311 (2004) 885-891.
[67] S. Tojkander, G. Gateva, P. Lappalainen, Actin stress fibers--assembly, dynamics and biological roles, J Cell Sci, 125 (2012) 1855-1864.
[68] S. Pellegrin, H. Mellor, Actin stress fibres, Journal of cell science, 120 (2007) 3491-3499.
[69] T.D. Pollard, J.A. Cooper, Actin, a central player in cell shape and movement, Science (New York, N.Y.), 326 (2009) 1208-1212.
[70] M.J. Weyant, A.M. Carothers, M.E. Bertagnolli, M.M. Bertagnolli, Colon cancer chemopreventive drugs modulate integrin-mediated signaling pathways, Clinical cancer research : an official journal of the American Association for Cancer Research, 6 (2000) 949-956.
[71] R. Pai, I.L. Szabo, A.Q. Giap, H. Kawanaka, A.S. Tarnawski, Nonsteroidal anti-inflammatory drugs inhibit re-epithelialization of wounded gastric monolayers by interfering with actin, Src, FAK, and tensin signaling, Life sciences, 69 (2001) 3055-3071.
[72] X. Wang, S.J. Baek, T. Eling, COX inhibitors directly alter gene expression: role in cancer prevention?, Cancer and Metastasis Reviews, 30 (2011) 641-657.
[73] M.E. Mercado-Pimentel, A.D. Hubbard, R.B. Runyan, Endoglin and Alk5 regulate epithelial–mesenchymal transformation during cardiac valve formation, Developmental biology, 304 (2007) 420-432.
[74] M.A. Kaygusuz, C.C. Turan, N.E. Aydin, I. Temel, S. Firat, T. Bulut, I. Kuku, The effects of G-CSF and naproxen sodium on the serum TGF-beta1 level and fracture healing in rat tibias, Life sciences, 80 (2006) 67-73.
[75] I. Opitz, S. Arni, B. Oberreiter, L.M. Asmis, P. Vogt, V. Rousson, W. Weder, D. Lardinois, Perioperative diclofenac application during video-assisted thoracic surgery pleurodesis modulates early inflammatory and fibrinolytic processes in an experimental model, European surgical research. Europaische chirurgische Forschung. Recherches chirurgicales europeennes, 50 (2013) 14-23.
[76] J.K. Chang, L.Y. Chuang, M.L. Ho, G.J. Wang, Effects of nonsteroidal anti-inflammatory drugs on transforming growth factor-beta expression and bioactivity in rat osteoblast-enriched culture, The Kaohsiung journal of medical sciences, 19 (2003) 278-288.

[77] S.J. Baek, L.C. Wilson, T.E. Eling, Resveratrol enhances the expression of non-steroidal anti-inflammatory drug-activated gene (NAG-1) by increasing the expression of p53, Carcinogenesis, 23 (2002) 425-432.
[78] P.-X. Li, J. Wong, A. Ayed, D. Ngo, A.M. Brade, C. Arrowsmith, R.C. Austin, H.J. Klamut, Placental TGF-β is a downstream mediator of the growth arrest and apoptotic response of tumor cells to DNA damage and p53 overexpression, Journal of biological chemistry, (2000).
[79] S.J. Baek, J.S. Kim, J.B. Nixon, R.P. DiAugustine, T.E. Eling, Expression of NAG-1, a transforming growth factor-beta superfamily member, by troglitazone requires the early growth response gene EGR-1, The Journal of biological chemistry, 279 (2004) 6883-6892.
[80] A. Reddy, W.G. Kaelin, Jr., Using cancer genetics to guide the selection of anticancer drug targets, Curr Opin Pharmacol, 2 (2002) 366-373.
[81] P. Ricchi, S. Pignata, R.V. Iaffaioli, B. Daniele, Cyclo-oxygenase inhibition in colorectal adenomas and cancer, J Clin Gastroenterol, 37 (2003) 281-287.
[82] M.M. Taketo, Cyclooxygenase-2 inhibitors in tumorigenesis (part I), J Natl Cancer Inst, 90 (1998) 1529-1536.
[83] J.A. Baron, Aspirin and NSAIDs for the prevention of colorectal cancer, Recent Results Cancer Res, 181 (2009) 223-229.
[84] T. Iwama, NSAIDs and colorectal cancer prevention, J Gastroenterol, 44 Suppl 19 (2009) 72-76.
[85] G.A. Piazza, A.K. Rahm, T.S. Finn, B.H. Fryer, H. Li, A.L. Stoumen, R. Pamukcu, D.J. Ahnen, Apoptosis primarily accounts for the growth-inhibitory properties of sulindac metabolites and involves a mechanism that is independent of cyclooxygenase inhibition, cell cycle arrest, and p53 induction, Cancer Res, 57 (1997) 2452-2459.
[86] C.H. Chiu, M.F. McEntee, J. Whelan, Sulindac causes rapid regression of preexisting tumors in Min/+ mice independent of prostaglandin biosynthesis, Cancer Res, 57 (1997) 4267-4273.
[87] X. Wang, P.J. Kingsley, L.J. Marnett, T.E. Eling, The role of NAG-1/GDF15 in the inhibition of intestinal polyps in APC/Min mice by sulindac, Cancer Prev Res (Phila), 4 (2011) 150-160.
[88] P.L. Rice, J. Kelloff, H. Sullivan, L.J. Driggers, K.S. Beard, S. Kuwada, G. Piazza, D.J. Ahnen, Sulindac metabolites induce caspase- and proteasome-dependent degradation of beta-catenin protein in human colon cancer cells, Mol Cancer Ther, 2 (2003) 885-892.
[89] S.J. Baek, K.S. Kim, J.B. Nixon, L.C. Wilson, T.E. Eling, Cyclooxygenase inhibitors regulate the expression of a TGF-beta superfamily member that has proapoptotic and antitumorigenic activities, Mol Pharmacol, 59 (2001) 901-908.
[90] S.J. Baek, L.C. Wilson, T.E. Eling, Resveratrol enhances the expression of non-steroidal anti-inflammatory drug-activated gene (NAG-1) by increasing the expression of p53, Carcinogenesis, 23 (2002) 425-432.
[91] S.J. Shiff, M.I. Koutsos, L. Qiao, B. Rigas, Nonsteroidal antiinflammatory drugs inhibit the proliferation of colon adenocarcinoma cells: effects on cell cycle and apoptosis, Exp Cell Res, 222 (1996) 179-188.
[92] Y. Goldberg, Nassif, II, A. Pittas, L.L. Tsai, B.D. Dynlacht, B. Rigas, S.J. Shiff, The anti-proliferative effect of sulindac and sulindac sulfide on HT-29 colon cancer cells: alterations in tumor suppressor and cell cycle- regulatory proteins, Oncogene, 12 (1996) 893-901.

[93] I. Casanova, M. Parreno, L. Farre, S. Guerrero, M.V. Cespedes, M.A. Pavon, F.J. Sancho, E. Marcuello, M. Trias, R. Mangues, Celecoxib induces anoikis in human colon carcinoma cells associated with the deregulation of focal adhesions and nuclear translocation of p130Cas, Int J Cancer, 118 (2006) 2381-2389.
[94] C.A. Weyant MJ, Bertagnolli ME, Bertagnolli MM., Colon cancer chemopreventive drugs modulate integrin-mediated signaling pathways., Clin Cancer Res., 3 (2000) 949-956.
[95] N.N. Mahmoud, R.T. Bilinski, M.R. Churchill, W. Edelmann, R. Kucherlapati, M.M. Bertagnolli, Genotype-phenotype correlation in murine Apc mutation: differences in enterocyte migration and response to sulindac, Cancer Res, 59 (1999) 353-359.
[96] N.N. Mahmoud, S.K. Boolbol, R.T. Bilinski, C. Martucci, A. Chadburn, M.M. Bertagnolli, Apc gene mutation is associated with a dominant-negative effect upon intestinal cell migration, Cancer Res, 57 (1997) 5045-5050.
[97] Y.Y. Zhen, T. Libotte, M. Munck, A.A. Noegel, E. Korenbaum, NUANCE, a giant protein connecting the nucleus and actin cytoskeleton, J Cell Sci, 115 (2002) 3207-3222.
[98] V.C. Padmakumar, S. Abraham, S. Braune, A.A. Noegel, B. Tunggal, I. Karakesisoglou, E. Korenbaum, Enaptin, a giant actin-binding protein, is an element of the nuclear membrane and the actin cytoskeleton, Exp Cell Res, 295 (2004) 330-339.
[99] D.T. Warren, Q. Zhang, P.L. Weissberg, C.M. Shanahan, Nesprins: intracellular scaffolds that maintain cell architecture and coordinate cell function?, Expert Rev Mol Med, 7 (2005) 1-15.
[100] Q. Zhang, C.D. Ragnauth, J.N. Skepper, N.F. Worth, D.T. Warren, R.G. Roberts, P.L. Weissberg, J.A. Ellis, C.M. Shanahan, Nesprin-2 is a multi-isomeric protein that binds lamin and emerin at the nuclear envelope and forms a subcellular network in skeletal muscle, J Cell Sci, 118 (2005) 673-687.
[101] W. Lu, M. Schneider, S. Neumann, V.M. Jaeger, S. Taranum, M. Munck, S. Cartwright, C. Richardson, J. Carthew, K. Noh, M. Goldberg, A.A. Noegel, I. Karakesisoglou, Nesprin interchain associations control nuclear size, Cellular and molecular life sciences : CMLS, (2012).
[102] R.N. Rashmi, B. Eckes, G. Glockner, M. Groth, S. Neumann, J. Gloy, L. Sellin, G. Walz, M. Schneider, I. Karakesisoglou, L. Eichinger, A.A. Noegel, The nuclear envelope protein Nesprin-2 has roles in cell proliferation and differentiation during wound healing, Nucleus (Austin, Tex.), 3 (2012) 172-186.
[103] Z.H. Libotte T, Abraham S, Padmakumar VC, Schneider M, Lu W, Munck M, Hutchison C, Wehnert M, Fahrenkrog B, Sauder U, Aebi U, Noegel AA, Karakesisoglou I., Lamin A/C-dependent localization of Nesprin-2, a giant scaffolder at the nuclear envelope., Mol Biol Cell., 7 (2005) 3411-3424.
[104] D. Rajgor, J.A. Mellad, F. Autore, Q. Zhang, C.M. Shanahan, Multiple novel nesprin-1 and nesprin-2 variants act as versatile tissue-specific intracellular scaffolds, PloS one, 7 (2012) e40098.
[105] S. Arndt, J. Seebach, K. Psathaki, H.J. Galla, J. Wegener, Bioelectrical impedance assay to monitor changes in cell shape during apoptosis, Biosens Bioelectron, 19 (2004) 583-594.
[106] H.W. Yin, Frank Lei. Wang, Angelo Lei. Cheng, Jing. Zhou, Yuxiang. , Bioelectrical Impedance Assay to Monitor Changes in Aspirin-Treated Human Colon Cancer HT-29 Cell Shape during Apoptosis, Analytical Letters, 40 (2007) 85 - 94.
[107] S.J. Baek, T.E. Eling, Changes in gene expression contribute to cancer prevention by COX inhibitors, Prog Lipid Res, 45 (2006) 1-16.

[108] I. Giaever, C.R. Keese, Monitoring Fibroblast Behavior in Tissue Culture With an Applied Electric Field, Proc. Natl. Acad. Sci. USA, 81 (1984) 3761-3764.
[109] I. Giaever, C.R. Keese, Use of Electric Fields to Monitor the Dynamical Aspect of Cell Behavior in Tissue Culture, IEEE Trans. Biomed. Eng., BME-33 (1986) 242-247.
[110] A.R. Burns, R.A. Bowden, S.D. MacDonell, D.C. Walker, T.O. Odebunmi, E.M. Donnachie, S.I. Simon, M.L. Entman, C.W. Smith, Analysis of Tight Junctions During Neutrophil Transendothelial Migration, Journal of Cell Science, 113 (2000) 45-57.
[111] J.P. Gainor, C.A. Morton, J.T. Roberts, P.A. Vincent, F.L. Minnear, Platelet-Conditioned Medium Increases Endothelial Electrical Resistance Independently of cAMP/PKA and cGMP/PKG, Am. J. Physiol. Heart Circ. Physiol., 281 (2001) H1992-H2001.
[112] N. Kataoka, K. Iwaki, K. Hashimoto, S. Mochizuki, Y. Ogasawara, M. Sato, K. Tsujioka, F. Kajiya, Measurements of Endothelial Cell-to-Cell and Cell-to-Substrate Gaps and Micromechanical Properties of Endothelial Cells During Monocyte Adhesion, Proc. Natl. Acad. Sci., 99 (2002) 15638-15643.
[113] C.K. Choi, A.E. English, S.I. Jun, K.D. Kihm, P.D. Rack, An endothelial cell compatible biosensor fabricated using optically thin indium tin oxide silicon nitride electrodes, Biosens Bioelectron, 22 (2007) 2585-2590.
[114] C.K. Choi, C.H. Margraves, A.E. English, K.D. Kihm, Multicontrast microscopy technique to dynamically fingerprint live-cell focal contacts during exposure and replacement of a cytotoxic medium, Journal of biomedical optics, 13 (2008) 054069.
[115] C.K. Choi, A.E. English, K.D. Kihm, C.H. Margraves, Simultaneous dynamic optical and electrical properties of endothelial cell attachment on indium tin oxide bioelectrodes, Journal of biomedical optics, 12 (2007) 064028.
[116] I. Giaever, C.R. Keese, Micromotion of Mammalian Cells Measured Electrically, Proc. Natl. Acad. Sci. USA, 88 (1991) 7896-7900.
[117] I. Giaever, C.R. Keese, Correction: Micromotion of Mammalian Cells Measured Electrically, Proc. Natl. Acad. Sci. USA, 90 (1993) 1634.
[118] A.E. English, C.P. Plaut, A.B. Moy, A Riemannian manifold analysis of endothelial cell monolayer impedance parameter precision, J Math Biol, 55 (2007) 721-743.
[119] A.S. Curtis, The Mechanism of Adhesion of Cells to Glass. A Study by Interference Reflection Microscopy, J Cell Biol, 20 (1964) 199-215.
[120] D. Gingell, I. Todd, Interference reflection microscopy. A quantitative theory for image interpretation and its application to cell-substratum separation measurement, Biophys J, 26 (1979) 507-526.
[121] C.S. Izzard, L.R. Lochner, Cell-to-substrate contacts in living fibroblasts: an interference reflexion study with an evaluation of the technique, J Cell Sci, 21 (1976) 129-159.
[122] H. Strong, N. Warner, A. Renwick, C. George, Sulindac metabolism: the importance of an intact colon, Clinical Pharmacology & Therapeutics, 38 (1985) 387-393.
[123] W.R. Waddell, G.F. Ganser, E.J. Cerise, R.W. Loughry, Sulindac for polyposis of the colon, The American journal of surgery, 157 (1989) 175-179.
[124] B.N. Swanson, V.K. Boppana, P.H. Vlasses, G.I. Holmes, K. Monsell, R.K. Ferguson, Sulindac disposition when given once and twice daily, Clinical Pharmacology & Therapeutics, 32 (1982) 397-403.
[125] D. Duggan, L. Hare, C. Ditzler, B. Lei, K. Kwan, The disposition of sulindac, Clinical pharmacology and therapeutics, 21 (1977) 326.

[126] D. Duggan, K. Hooke, S. Hwang, Kinetics of the tissue distributions of sulindac and metabolites. Relevance to sites and rates of bioactivation, Drug Metabolism and Disposition, 8 (1980) 241-246.
[127] R. Hanif, A. Pittas, Y. Feng, M.I. Koutsos, L. Qiao, L. Staiano-Coico, S.I. Shiff, B. Rigas, Effects of nonsteroidal anti-inflammatory drugs on proliferation and on induction of apoptosis in colon cancer cells by a prostaglandin-independent pathway, Biochemical pharmacology, 52 (1996) 237-245.
[128] D.P. Kunte, R.K. Wali, J.L. Koetsier, H.K. Roy, Antiproliferative effect of sulindac in colonic neoplasia prevention: role of COOH-terminal Src kinase, Molecular cancer therapeutics, 7 (2008) 1797-1806.
[129] Y.S. Tao, R.A. Edwards, B. Tubb, S. Wang, J. Bryan, P.D. McCrea, beta-Catenin associates with the actin-bundling protein fascin in a noncadherin complex, J. Cell Biol., 134 (1996) 1271-1281.
[130] M.J. Thun, M.M. Namboodiri, E.E. Calle, W.D. Flanders, C.W. Heath, Aspirin use and risk of fatal cancer, Cancer research, 53 (1993) 1322-1327.
[131] S.K. Boolbol, A.J. Dannenberg, A. Chadburn, C. Martucci, X. Guo, J.T. Ramonetti, M. Abreu-Goris, H.L. Newmark, M.L. Lipkin, J.J. DeCosse, Cyclooxygenase-2 overexpression and tumor formation are blocked by sulindac in a murine model of familial adenomatous polyposis, Cancer research, 56 (1996) 2556-2560.
[132] M.M. Taketo, Cyclooxygenase-2 inhibitors in tumorigenesis (part I), Journal of the National Cancer Institute, 90 (1998) 1529-1536.
[133] M.M. Taketo, Cyclooxygenase-2 inhibitors in tumorigenesis (Part II), Journal of the National Cancer Institute, 90 (1998) 1609-1620.
[134] S.J. Baek, K.-S. Kim, J.B. Nixon, L.C. Wilson, T.E. Eling, Cyclooxygenase inhibitors regulate the expression of a TGF-β superfamily member that has proapoptotic and antitumorigenic activities, Molecular pharmacology, 59 (2001) 901-908.
[135] A.-L. Hsu, T.-T. Ching, D.-S. Wang, X. Song, V.M. Rangnekar, C.-S. Chen, The cyclooxygenase-2 inhibitor celecoxib induces apoptosis by blocking Akt activation in human prostate cancer cells independently of Bcl-2, Journal of biological chemistry, 275 (2000) 11397-11403.
[136] M. Balzar, I.H. Briaire-de Bruijn, H.A. Rees-Bakker, F.A. Prins, W. Helfrich, L. de Leij, G. Riethmuller, S. Alberti, S.O. Warnaar, G.J. Fleuren, S.V. Litvinov, Epidermal growth factor-like repeats mediate lateral and reciprocal interactions of Ep-CAM molecules in homophilic adhesions, Mol Cell Biol, 21 (2001) 2570-2580.
[137] S.V. Litvinov, M. Balzar, M.J. Winter, H.A. Bakker, I.H. Briaire-de Bruijn, F. Prins, G.J. Fleuren, S.O. Warnaar, Epithelial cell adhesion molecule (Ep-CAM) modulates cell–cell interactions mediated by classic cadherins, The Journal of cell biology, 139 (1997) 1337-1348.
[138] M. Joo, H. Kim, M.K. Kim, H.J. Yu, J.P. Kim, Expression of Ep-CAM in intestinal metaplasia, gastric epithelial dysplasia and gastric adenocarcinoma, Journal of gastroenterology and hepatology, 20 (2005) 1039-1045.
[139] D. Wenqi, W. Li, C. Shanshan, C. Bei, Z. Yafei, B. Feihu, L. Jie, F. Daiming, EpCAM is overexpressed in gastric cancer and its downregulation suppresses proliferation of gastric cancer, Journal of cancer research and clinical oncology, 135 (2009) 1277-1285.
[140] H.S. Shim, B.S. Yoon, N.H. Cho, Prognostic significance of paired epithelial cell adhesion molecule and E-cadherin in ovarian serous carcinoma, Human pathology, 40 (2009) 693-698.

[141] P. Went, M. Vasei, L. Bubendorf, L. Terracciano, L. Tornillo, U. Riede, J. Kononen, R. Simon, G. Sauter, P. Baeuerle, Frequent high-level expression of the immunotherapeutic target Ep-CAM in colon, stomach, prostate and lung cancers, British journal of cancer, 94 (2006) 128-135.
[142] M. Münz, C. Kieu, B. Mack, B. Schmitt, R. Zeidler, O. Gires, The carcinoma-associated antigen EpCAM upregulates c-myc and induces cell proliferation, Oncogene, 23 (2004) 5748-5758.
[143] N.V. Sankpal, M.W. Willman, T.P. Fleming, J.D. Mayfield, W.E. Gillanders, Transcriptional repression of epithelial cell adhesion molecule contributes to p53 control of breast cancer invasion, Cancer research, 69 (2009) 753-757.
[144] A. Chaves-Perez, B. Mack, D. Maetzel, H. Kremling, C. Eggert, U. Harréus, O. Gires, EpCAM regulates cell cycle progression via control of cyclin D1 expression, Oncogene, (2012).
[145] B.A. Frederick, B.A. Helfrich, C.D. Coldren, D. Zheng, D. Chan, P.A. Bunn, D. Raben, Epithelial to mesenchymal transition predicts gefitinib resistance in cell lines of head and neck squamous cell carcinoma and non–small cell lung carcinoma, Molecular cancer therapeutics, 6 (2007) 1683-1691.
[146] M. Santisteban, J.M. Reiman, M.K. Asiedu, M.D. Behrens, A. Nassar, K.R. Kalli, P. Haluska, J.N. Ingle, L.C. Hartmann, M.H. Manjili, Immune-induced epithelial to mesenchymal transition in vivo generates breast cancer stem cells, Cancer research, 69 (2009) 2887-2895.
[147] D.B. Seligson, A.J. Pantuck, X. Liu, Y. Huang, S. Horvath, M.H. Bui, K.-r. Han, A.J. Correa, M. Eeva, S. Tze, Epithelial Cell Adhesion Molecule (KSA) Expression Pathobiology and Its Role as an Independent Predictor of Survival in Renal Cell Carcinoma, Clinical cancer research, 10 (2004) 2659-2669.
[148] T. Klatte, A.J. Pantuck, J.W. Said, D.B. Seligson, N.P. Rao, J.C. LaRochelle, B. Shuch, A. Zisman, F.F. Kabbinavar, A.S. Belldegrun, Cytogenetic and molecular tumor profiling for type 1 and type 2 papillary renal cell carcinoma, Clinical cancer research, 15 (2009) 1162-1169.
[149] C. Ensinger, R. Kremser, R. Prommegger, G. Spizzo, K.W. Schmid, EpCAM overexpression in thyroid carcinomas: a histopathological study of 121 cases, Journal of Immunotherapy, 29 (2006) 569-573.
[150] R. Ralhan, J. Cao, T. Lim, C. MacMillan, J.L. Freeman, P.G. Walfish, EpCAM nuclear localization identifies aggressive thyroid cancer and is a marker for poor prognosis, BMC cancer, 10 (2010) 331.
[151] T. Yamashita, M. Forgues, W. Wang, J.W. Kim, Q. Ye, H. Jia, A. Budhu, K.A. Zanetti, Y. Chen, L.-X. Qin, EpCAM and α-fetoprotein expression defines novel prognostic subtypes of hepatocellular carcinoma, Cancer research, 68 (2008) 1451-1461.
[152] M.M. Heiss, P. Murawa, P. Koralewski, E. Kutarska, O.O. Kolesnik, V.V. Ivanchenko, A.S. Dudnichenko, B. Aleknaviciene, A. Razbadauskas, M. Gore, The trifunctional antibody catumaxomab for the treatment of malignant ascites due to epithelial cancer: results of a prospective randomized phase II/III trial, International Journal of Cancer, 127 (2010) 2209-2221.
[153] M. Schmidt, M. Scheulen, C. Dittrich, P. Obrist, N. Marschner, L. Dirix, D. Rüttinger, M. Schuler, C. Reinhardt, A. Awada, An open-label, randomized phase II study of adecatumumab, a fully human anti-EpCAM antibody, as monotherapy in patients with metastatic breast cancer, Annals of oncology, 21 (2010) 275-282.

[154] C. Labalette, C.-A. Renard, C. Neuveut, M.-A. Buendia, Y. Wei, Interaction and functional cooperation between the LIM protein FHL2, CBP/p300, and β-catenin, Molecular and cellular biology, 24 (2004) 10689-10702.
[155] D. Maetzel, S. Denzel, B. Mack, M. Canis, P. Went, M. Benk, C. Kieu, P. Papior, P.A. Baeuerle, M. Munz, Nuclear signalling by tumour-associated antigen EpCAM, Nature Cell Biology, 11 (2009) 162-171.
[156] U. Schnell, J. Kuipers, B.N. Giepmans, EpCAM proteolysis: new fragments with distinct functions?, Bioscience reports, (2013).
[157] J.M. Chong, D.W. Speicher, Determination of Disulfide Bond Assignments andN-Glycosylation Sites of the Human Gastrointestinal Carcinoma Antigen GA733-2 (CO17-1A, EGP, KS1-4, KSA, and Ep-CAM), Journal of biological chemistry, 276 (2001) 5804-5813.
[158] T. Nübel, J. Preobraschenski, H. Tuncay, T. Weiss, S. Kuhn, M. Ladwein, L. Langbein, M. Zöller, Claudin-7 regulates EpCAM-mediated functions in tumor progression, Molecular Cancer Research, 7 (2009) 285-299.
[159] B.T. van der Gun, L.J. Melchers, M.H. Ruiters, L.F. de Leij, P.M. McLaughlin, M.G. Rots, EpCAM in carcinogenesis: the good, the bad or the ugly, Carcinogenesis, 31 (2010) 1913-1921.
[160] M. Sivagnanam, J.L. Mueller, H. Lee, Z. Chen, S.F. Nelson, D. Turner, S.H. Zlotkin, P.B. Pencharz, B.Y. Ngan, O. Libiger, Identification of EpCAM as the gene for congenital tufting enteropathy, Gastroenterology, 135 (2008) 429-437.
[161] E. Guerra, R. Lattanzio, R. La Sorda, F. Dini, G.M. Tiboni, M. Piantelli, S. Alberti, mTrop1/Epcam knockout mice develop congenital tufting enteropathy through dysregulation of intestinal E-cadherin/β-catenin, PLoS ONE, 7 (2012) e49302.
[162] N.V. Sankpal, T.P. Fleming, W.E. Gillanders, EpCAM modulates NF-kappaB signaling and interleukin-8 expression in breast cancer, Molecular cancer research : MCR, 11 (2013) 418-426.
[163] Y. Shigeoka, T. Igishi, S. Matsumoto, H. Nakanishi, M. Kodani, K. Yasuda, Y. Hitsuda, E. Shimizu, Sulindac sulfide and caffeic acid phenethyl ester suppress the motility of lung adenocarcinoma cells promoted by transforming growth factor-β through Akt inhibition, Journal of cancer research and clinical oncology, 130 (2004) 146-152.
[164] F.G. Bottone, Jr., S.J. Baek, J.B. Nixon, T.E. Eling, Diallyl disulfide (DADS) induces the antitumorigenic NSAID-activated gene (NAG-1) by a p53-dependent mechanism in human colorectal HCT 116 cells, J Nutr, 132 (2002) 773-778.
[165] S.-H. Lee, J.H. Bahn, C.K. Choi, N.C. Whitlock, A.E. English, S. Safe, S.J. Baek, ESE-1/EGR-1 pathway plays a role in tolfenamic acid-induced apoptosis in colorectal cancer cells, Molecular cancer therapeutics, 7 (2008) 3739-3750.
[166] S.-H. Lee, J.H. Bahn, N.C. Whitlock, S.J. Baek, Activating transcription factor 2 (ATF2) controls tolfenamic acid-induced ATF3 expression via MAP kinase pathways, Oncogene, 29 (2010) 5182-5192.
[167] J.B. Jeong, X. Yang, R. Clark, J. Choi, S.J. Baek, S.H. Lee, A mechanistic study of the proapoptotic effect of tolfenamic acid: involvement of NF-kappaB activation, Carcinogenesis, 34 (2013) 2350-2360.
[168] M. Abdelrahim, R. Smith, 3rd, R. Burghardt, S. Safe, Role of Sp proteins in regulation of vascular endothelial growth factor expression and proliferation of pancreatic cancer cells, Cancer Res, 64 (2004) 6740-6749.

[169] U. Schnell, J. Kuipers, B.N. Giepmans, EpCAM proteolysis: new fragments with distinct functions?, Bioscience reports, 33 (2013).
[170] H. Dolznig, C. Rupp, C. Puri, C. Haslinger, N. Schweifer, E. Wieser, D. Kerjaschki, P. Garin-Chesa, Modeling Colon Adenocarcinomas< i> in Vitro</i>: A 3D Co-Culture System Induces Cancer-Relevant Pathways upon Tumor Cell and Stromal Fibroblast Interaction, The American journal of pathology, 179 (2011) 487-501.
[171] M. Vinci, S. Gowan, F. Boxall, L. Patterson, M. Zimmermann, C. Lomas, M. Mendiola, D. Hardisson, S.A. Eccles, Advances in establishment and analysis of three-dimensional tumor spheroid-based functional assays for target validation and drug evaluation, Bmc Biology, 10 (2012) 29.
[172] R. Sutherland, B. Sordat, J. Bamat, H. Gabbert, B. Bourrat, W. Mueller-Klieser, Oxygenation and differentiation in multicellular spheroids of human colon carcinoma, Cancer research, 46 (1986) 5320-5329.
[173] F. Hirschhaeuser, H. Menne, C. Dittfeld, J. West, W. Mueller-Klieser, L.A. Kunz-Schughart, Multicellular tumor spheroids: an underestimated tool is catching up again, Journal of biotechnology, 148 (2010) 3-15.

VITA

Jason L. Liggett was born in Knoxville, TN. He joined the Environmental Carcinogenesis Laboratory at the University of Tennessee Veterinary College as an ungraduated student worker in August 2003. In December of 2005 he graduated from the University of Tennessee, Knoxville with a bachelor's degree in Medical Technology. Then he spent 2006 working as a Medical Technologist for LabCorp of America at the University of Tennessee Medical Center, Knoxville in the Core Lab. In 2007 he returned to the Environmental Carcinogenesis Lab as a graduate student assistant. He completed his dissertation in the fall of 2013.